University of Siena

Department of Molecular Medicine and Development

Doctoral Research in Molecular Medicine

Ciclo XXXIII

Coordinator: Prof. Vincenzo Sorrentino

MOLECULAR MECHANISMS OF ANGIOGENESIS-RELATED OCULAR DISEASES IN PRECLINICAL MODELS

SETTORE SCIENTIFICO-DISCIPLINARE:BIO/09

PhD student

Noemi Anna Pesce

NOEMI ANNA PESCE Signed
28/06/2021

Tutor

Massimo Dal Monte

Helder André

Academic year 2019/2020

ABSTRACT

Neovascularization in the eye contributes to visual loss in several ocular diseases, including proliferative diabetic retinopathy (PDR), neovascular glaucoma (NVG) and retinopathy of prematurity (ROP). In these diseases, the neovascular mechanisms originate from the retina, but some advanced stages of PDR or nG can lead to the development of rubeosis iridis (RI), a clinical manifestation characterized by iris angiogenesis. Vascular endothelial growth factors (VEGFs) and their receptor (VEGFRs) are the key promoters of angiogenesis, playing a crucial role in both physiological and pathological angiogenesis. For this reason, anti-VEGF therapies have represented a great step forward in the treatment of ocular neovascular diseases, but the effects can be somewhat limited. In addition, beyond the vascular alterations, degenerative changes might occur in the neuroretina, including inflammation and neurodegeneration, which further compromise visual function in people affected by ocular diseases. Consequently, a pharmacologic strategy aimed at inhibiting several pathways might be a more suitable therapeutic approach.

A first suitable target may be represented by the pathway triggered by the urokinase plasminogen activator (uPA) and its receptor (uPAR), which play a pivotal role in extracellular matrix remodeling during angiogenesis, where uPAR, a glycosylphosphatidylinositol-anchored protein, regulates cell migration and proliferation through the assembly with transmembrane receptors. An additional pathway that may represent an interesting target is autophagy, as an expanding body of literature suggests that mechanisms of autophagy are involved in neurodegeneration in ocular disease. Autophagy is an essential process in maintaining the normal cellular homeostasis and energy balance. In retinal diseases, autophagy contributes to retinal cells protecting themselves against harmful stress stimuli; however, dysregulated autophagy may result in retinal deterioration.

Here, we investigate the effects of the uPAR antagonist—UPARANT—on the angiogenic and inflammatory processes, in a context of hypoxia-induced angiogenesis, using a novel *ex vivo* human iris angiogenesis assay and, an *in vivo* mouse model of RI-associated with proliferative retinopathy (PR).

A rat model of oxygen-induced retinopathy (OIR), an acknowledged model of ROP, was used to evaluate neuroretinal changes in the expression of key mediators of autophagy, induced by disease. First, we investigated the autophagic profile in newborn rats and, subsequently determined a correlation between autophagy and mechanisms of cell death in the OIR rat retina. In addition, an

inhibitor of autophagy was valuated to analyze the possible effects of in mitigating autophagy-associated cell death and retinal function in the OIR rat model.

LIST OF SCIENTIFIC PAPERS

I. **Noemi A. Pesce**, Filippo Locri, Vincenzo Pavone, Anders Kvanta, Massimo Dal Monte, Helder André "UPARANT mitigates human iris angiogenesis through uPAR/LRP-1 interaction in an organotypic *ex vivo* model" *In Review (FASEB Journal).*

II. Filippo Locri*, **Noemi A. Pesce***, Monica Aronsson, Maurizio Cammalleri, Mario De Rosa, Vincenzo Pavone, Paola Bagnoli, Anders Kvanta, Massimo Dal Monte, Helder André "Gaining insight on mitigation of rubeosis iridis by UPARANT in a mouse model associated with proliferative retinopathy" *J Mol Med.* 2020 Nov;98(11):1629-1638. (doi:10.1007/s00109-020-01979-8). * First co-authors

III. **Noemi A. Pesce**, Alessio Canovai, Emma Lardner, Maurizio Cammalleri, Anders Kvanta, Helder André, Massimo Dal Monte "Autophagy involvement in the postnatal development of the rat retina" *Cells.* 2021 Jan 17;10(1):177. (doi: 10.3390/cells10010177).

IV. **Noemi A. Pesce**, Alessio Canovai, Flavia Plastino, Emma Lardner, Maurizio Cammalleri, Anders Kvanta, Helder André, Massimo Dal Monte "An imbalance in the autophagy flux contributes to retinal dysfunction in the OIR rat model" *In Review (J Mol Med.).*

SCIENTIFIC PAPERS NOT INCLUDED IN THE THESIS

I. Flavia Plastino, Álvaro Santana-Garrido, **Noemi A. Pesce**, Monica Aronsson, Emma Lardner, Alfonso Mate, Anders Kvanta, Carmen M. Vázquez, Helder André. "Echinomycin mitigates ocular angiogenesis by transcriptional inhibition of the hypoxia-inducible factor-1". Exp Eye Res. 2021 Feb 24; 108518. (doi: 10.1016/j.exer.2021.108518).

II. Flavia Plastino, **Noemi A. Pesce**, Helder André. MicroRNAs and the HIF/VEGF axis in ocular neovascular diseases. Acta Ophthalmol. 2021 Mar 17. Epub ahead of print. (doi: 10.1111/aos.14845).

CONTENTS

LIST OF ABBREVIATIONS

3-MA	3-Methyladenine
4E-BP1	Eukaryotic translation initiation factor-4E binding protein 1
AKT	Protein kinase B
AMP	Adenosine monophosphate
ATG	Autophagy-related protein
ATP	Adenosine triphosphate
Casp-8	Caspase-8
CCL2	Chemokine ligand 2
CRA	Central Retinal Artery
CREB	cAMP response element-binding protein
CRV	Central Retinal Vein
CXCR4	C-X-C Motif Chemokine Receptor 4
ECM	Extracellular Matrix
ECs	Endothelial Cells
EGFR	Epidermal growth factor receptor
ER	Endoplasmic reticulum
ERG	Electroretinogram
ERK	Extracellular signal-regulated kinase
FAK	Focal Adhesion Kinase
fMLF	Formyl-methionyl-leucyl-phenylalanine
FPRs	Formyl peptide receptors
GCL	Ganglion Cell Layer
GPI	Glycosylphosphatidylinositol
hIECs	Human Iris epithelial cells
HIF	Hypoxia-Induced Factor
HRE	Hypoxia-Response Element
hRECs	Human retinal endothelial cells
IB4	Isolectin B4
iBRB	Inner Blood Retinal Barrier

IL6	Interleukin 6
ILβ	Interleukin β
IPL	Inner plexiform layer
JAK	Janus Kinase
LC3 AB	Microtubule-associated protein A/1B-light chain 3
LRP-1	Low density lipoprotein receptor-related protein-1
MAPK	Mitogen-activated protein kinase
MMP	Matrix Metallo Proteinases
mTOR	mammalian Target of Rapamycin
NF-kB	Nuclear Factor kappa-light-chain-enhancer of activated B cells
NVG	Neovascular Glaucoma
O_2	Oxygen
oBRB	Outer Blood Retinal Barrier
OIR	Oxygen-induced Retinopathy
OPL	Outer plexiform layer
OS	Outer Segment
P	Postnatal
p62	Sequestosome-1
PAI	Serine protease inhibitor
PDGFRs	Platelet Derived Growth Factor Receptor
PDR	Proliferative Diabetic Retinopathy
PECAM	Platelet endothelial cell adhesion molecule
PHD	Prolyl Hydroxylase Domain
PI	Phosphatidylinositol
PIIII-K	PhosphatidylinositolIII-Kinase
PI3P	Phosphatidylinositol 3-phosphate
PR	Proliferative Retinopathy
RA	Room Air
RI	Rubeosis Iridis
RIPKs	Receptor interacting protein kinases
ROP	Retinopathy of Prematurity
RPE	Retinal pigment epithelium

S6	Ribosomal protein
STAT	Signal Transducer and Activator of Transcription
TGFα	Transforming Growth Factor alpha
Ulk	Unc-51 like autophagy activating kinase
uPA	Urokinase-Type Plasminogen Activator
uPAR	Urokinase-Type Plasminogen Activator Receptor
VEGFRs	Vascular Endothelial Growth Factor Receptors
VEGFs	Vascular Endothelial Growth Factors
Vsp	Vesicular protein sorting
WNK	Lysine deficient protein kinase

1. INTRODUCTION

The visual system is a part of the central nervous system required for processing and interpreting visual information to build a representation of the surrounding world [1].

1.1 STRUCTURE OF THE EYE

The eye is the organ sense responsible for absorbing and converting light into nerve impulses. Anatomically, the eyeball can be divided into three different layers, each characterized by several structures with specific functions (Figure 1A):

1. the *fibrous tunic* represents the outermost layer of the eye, constituted of connective tissue. It consists of the **cornea,** responsible for focusing most of the light that enters the eye, and the **sclera**, essential to maintain the excess pressure within the eyeball and its shape [2];

2. the *vascular tunic* or *uvea* forms the middle layer, which includes the **choroid**, a vascular layer that supplies nutrients and oxygen to the eye; the **ciliary body**, which controls the shape of the lens and produces the *aqueous humour* to provide nutrition for the avascular ocular tissue; and the **iris**, a diaphragm constituted by endothelial and epithelial cells, which regulates the amount of light that crosses a circular opening, the **pupil** [3].

3. the *inner layer* is formed by the **retina**, which consists of an outer pigmented layer, **retinal pigment epithelium (RPE)**, and an inner neural layer, **neuroretina**. RPE is a single layer of cells attached to the choroid (Figure 1B), responsible for absorbing scatter light and supplying nutrients to the sensory retina. Tight junctions between RPE cells constitute the outer retina blood barrier (oBRB), which controls ion and metabolite homeostasis. The neuroretina consists of three neuron layers interconnected by synapses —the outer layer of photoreceptors (cones and rods), a middle layer of bipolar neurons, and an inner layer of ganglion cells that collect and carry visual signals to the optic nerve for the perception of images (Figure 1B) [4].

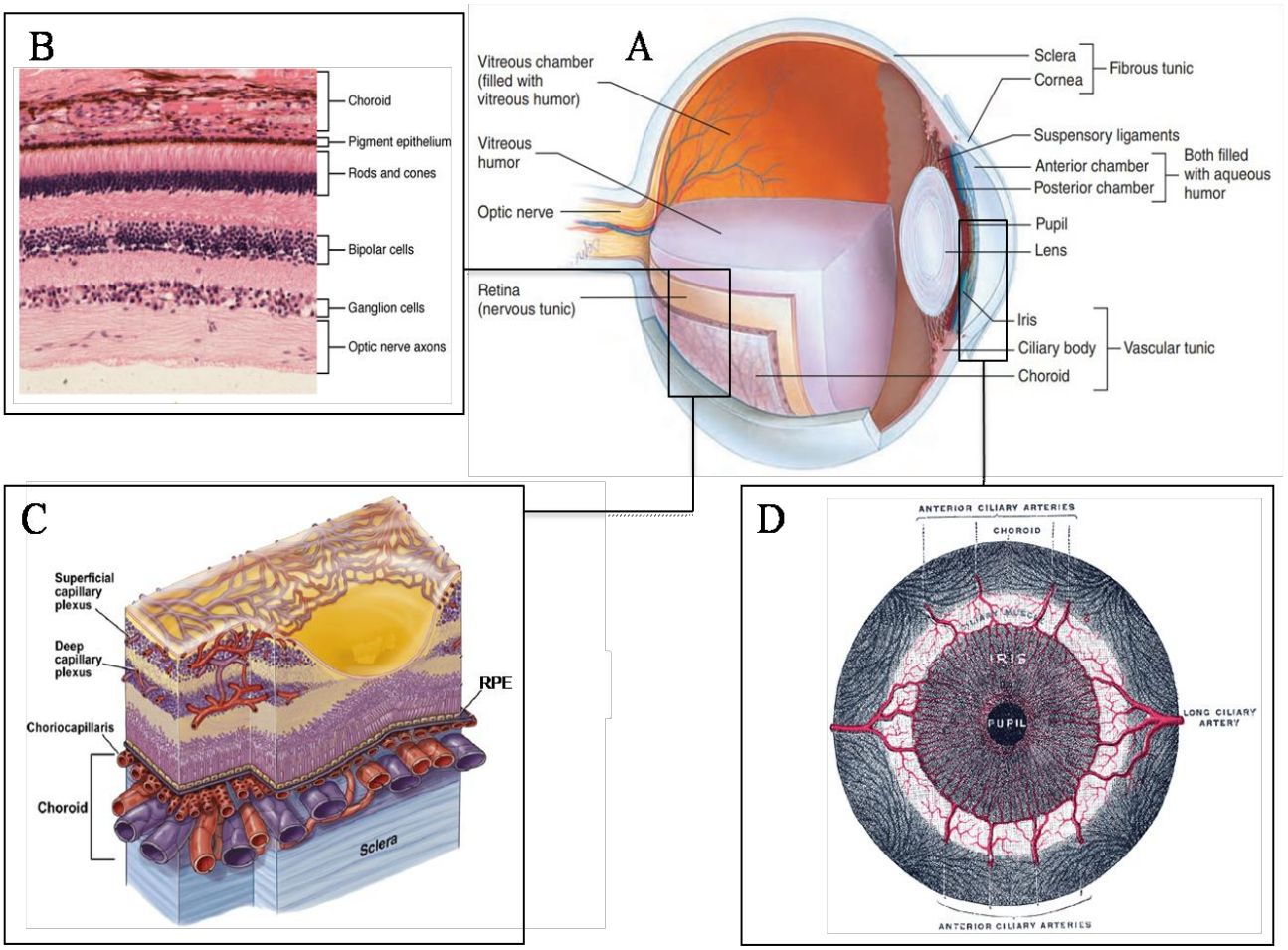

Figure 1. Schematic representation of human eye with vasculature. (A) Structure of the human eye. The sclera and the cornea constitute the eye outer layer. The pupil is between the cornea and the eye's clear lens. The middle layer is occupied by the uvea, which is composed by iris, ciliary body and choroidal, while the inner layer constitutes the retina. The vitreous is a gelatinous mass located between the back surface of the crystalline and the retina. The optic nerve is formed by the ganglion cells, axons of the retina and transmits visual information from the retina to the brain. **(B) Retinal neuronal layers.** Retina consists of three layers of neurons: photoreceptors (rods and cones), bipolar cells and ganglion cells. The pigment epithelial monolayer (RPE), attached to the choroid, separates the neuroretina from the choroid. Choroid provides oxygen and nutrients to outer retina. **(C) Vascular supply of the retina.** The retinal and choroidal vasculature, with choriocapillaris, RPE and the superficial and deep capillary layers. **(D)Vascular supply of the iris.** The vascular supply to the iris originates in the anterior and long posterior ciliary branches of the ophthalmic artery. These branches merge at the ciliary body to form the major arterial circle before entering radially into the iris.

1.2 VASCULAR BEDS WITHIN THE EYE

Ocular blood flow is a vital component for providing oxygen and nutrients to the eye [5]. The mature eye is supplied by two separate vascular beds: the **ciliary vessels (uvea)** (Figure 1D), which furnish diffusible nutrients directly to the iris, and indirectly to the outer layer of the retina, sclera and lens; and the **retinal vessels**, including the central retinal artery (CRA), the central retinal vein (CRV) and branches (Figure 1D), which supply the inner layer of the retina [6]. Both ciliary and retinal vessels emerge from the ophthalmic artery, a branch of the internal carotid artery [7].

1.2.1 Uvea

The uvea represents the most vascularized ocular tissue. During development, the uveal vasculature develops with the formation of a large plexus of primitive vessels, located posterior to the RPE layer, and supplies the more superficial part of the developing eye (Figure 1A) [8,9]. In adulthood, the uvea becomes a highly complex network that interconnects the anterior, the long posterior and the short posterior ciliary arterial systems [10]. The anterior ciliary arteries supply the conjunctiva and the sclera [11]; the long posterior ciliary arteries supply the choroid and the ciliary muscle; and the short posterior ciliary arteries supply the choroid [12]. The iris receives vascular contributions from the long and anterior ciliary arteries, which are subdivided into an upper and a lower branch. The two branches are anastomized with corresponding contralateral arteries and front ciliary arteries, forming the circulus arteriosus major of the iris at its base. From this circle, the vessels converge towards the iris free margin where they communicate and form a second circle, the circulus arteriosus minor (Figure 1D) [13].

1.2.2 Retinal vasculature

The mature retina is considered one of the highest oxygen-demanding tissues in the body, with a considerable metabolic activity [14]. The retinal circulation supplies the inner retina, while the outer retina, consisting primarily of photoreceptors, and receives oxygen and nutrients from the choroidal circulation [15]. During development, the retinal vasculature goes through considerable changes and reorganization [16]. In the early stages of embryogenesis, the interior of the optic cup is metabolically supplied by a transient embryonic circulatory network in the vitreous, referred to as the hyaloid system [17]; in the later stages of gestation, the hyaloid vasculature regresses and concurrently is replaced by the retinal vasculature. The retinal vessels progress along the inferior margin of the

optic nerve, enter the eye through the optic disk, and form branches. Consequently, the mature retinal vasculature network results composed of three capillary layers: superficial, intermediate and deep layers [15,18] (Figure 1C). In human, retinal vascularization is completed just before birth, approximately at 40 gestational weeks [15], while in rodents it develops postnatally [17,19].

Mature retinal vascular endothelial cells present highly specialized tight junctions, forming the inner blood retinal barrier (iBRB), which controls the diffusion of certain substances between the circulating blood and the neural retina [20].

1.3 MECHANISMS INVOLVED IN BLOOD VESSELS GROWTH

During development, in the eye blood vessels are initially formed by mechanism of vasculogenesis, where the precursors of endothelial cells differentiate into endothelial cells (ECs) and, generate a primitive network of vessels, known as the primary capillary plexus, [21]. At this stage, mechanisms of vasculogenesis ceases and all further developments of the vascular network proceed through angiogenesis mechanisms, where new blood vessels are formed from existing ones. In this manner, the primary vascular plexus significantly expands due to capillary branching and is transformed into the highly organized vascular network [22,23]. Albeit, vasculogenesis mechanisms are pronominally limited to development, angiogenesis has a pivotal role during both embryonic development and adult life [24].

1.3.1 Angiogenesis mechanisms

In adulthood, blood vessels remain mostly in a quiescent state, yet ECs maintain the capability of rapid proliferation in response to microenvironmental changes or physiological stimuli, which may result in activation of angiogenesis [25]. This process is strictly regulated, and activated only under defined conditions, including wound healing and uterine cycling; and its imbalance might result in excessive formation of blood vessels, which can lead to serious diseases [26–28].

During both development and in adulthood, angiogenesis can occur by two different mechanisms: intussusceptive angiogenesis, where new blood vessels form by a process of splitting vessels; and sprouting angiogenesis, where ECs branch out from the existing vessels [29,30].

Sprouting angiogenesis is a dynamic process in which oxygen acts as the main molecular signal that coordinates blood vessel growth with the metabolic demands of growing tissues [31]. At the cellular level, in response to a hypoxic environment (lack of oxygen), ECs secrete several proangiogenic growth factors that lead to degradation of vascular basement membrane, and vascular sprouting within the interstitial matrix. At this stage, ECs adopt highly proliferative phenotypes, known as tip or stalk cells [32,33], characterized by their long and dynamic filopodia, which extends from the cell surface. Thus, filopodia establish adherent and tight junctions to ensure the stability of the new sprout, and generate a functional vascular network [34]. Vascular endothelial growth factors (VEGFs) and their receptors (VEGFRs) are the main involved in the regulation of vasculogenesis and angiogenesis, regulating all these multiple aspects of endothelial behavior, in both physiological and pathological condition [35]. The VEGF family consists of seven members (VEGF-A, VEGF-B, VEGF-C, VEGF-D, VEGF-E, VEGF-F and Placental Growth Factor) that bind three different receptors (VEGFR-1, VEGFR-2 and VEGFR-3). Among the different ligands, VEGF-A is most prominently involved in the angiogenic process, by binding to either VEGFR-1 and VEGFR-2. VEGFR-1 is expressed in different cells, including endothelial cells, and its expression is upregulated during angiogenesis and hypoxic condition; while VEGFR-2 is crucial for vasodilatation, endothelial cell migration and proliferation processes, and it is considered the be a major mediator of physiological and pathological effects of VEGF-A on endothelial cells [36,37].

1.3.1.1 Hypoxia-Induced Angiogenesis

In the cells, molecular oxygen participates in numerous intracellular biochemical reactions and is essential to produce energy for metabolic activities. For this reason, the regulation and preservation of O_2 homeostasis is crucial for cell activity and survival [38]. In the eye, oxygen deprivation generates a significant cellular stress that results in the activation of complex adaptive responses, which can damage permanently the cells [39]. However, in certain circumstances hypoxic condition plays an important and beneficial role. During development, for instance, the physiological hypoxia drives the proliferation of retinal blood vessels, thus inducing the formation of the retinal vasculature [40].

In both cases, hypoxia response consists of the activation of specific genes, which coordinate different biological processes, including angiogenesis and cell proliferation [41]. The main regulators of oxygen levels are the hypoxia-inducible factors (HIFs), a family of heterodimeric transcription

factors composed of an oxygen-sensitive α-subunit (HIF-α) and, a constitutively expressed β-subunit (HIF-β) [42]. Under normoxic condition, the HIF-α isoforms are rapidly hydroxylated at one of two proline sites by prolyl hydroxylases domain (PHDs) and degraded into the preteasome. In hypoxia, PHDs are inhibited, consequently HIF-α accumulates, translocates into the nucleus and heterodimerizes with the stable HIF-β subunit. At this stage, the HIF transcriptional complex binds to the hypoxia-response elements (HREs) and induce the transcription of several genes, including VEGF and their receptors, which promote angiogenesis mechanisms (Figure 2) [43] amongst others, such as energetic adaptation to anaerobic metabolic pathways and cell survival.

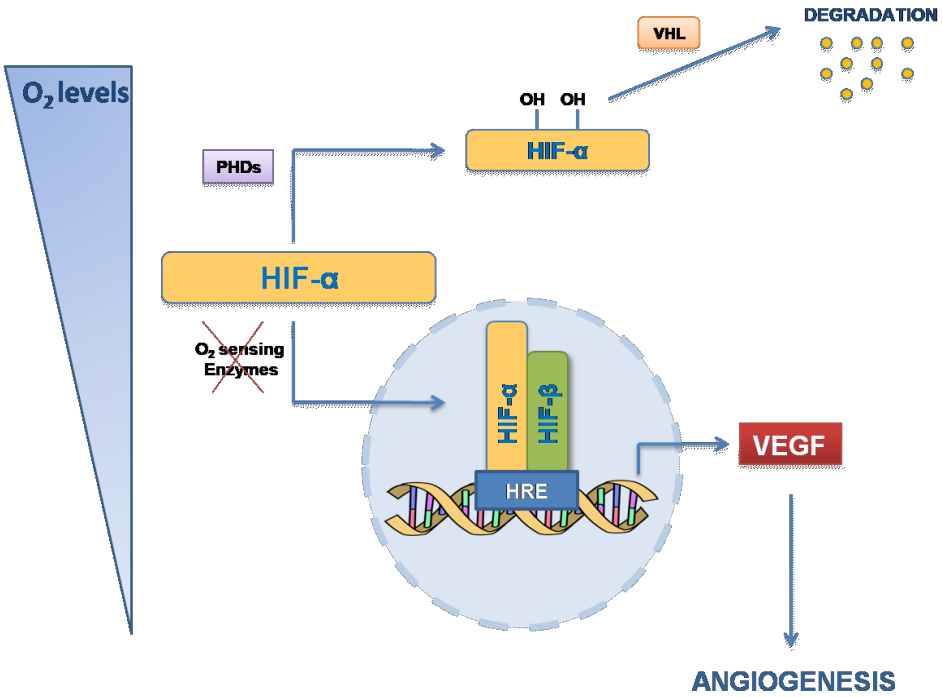

Figure 2 Schematic representation of Hypoxia-induced factor (HIF)α pathway. Physiologic oxygen levels maintain the hydroxylation of HIF-α, through the prolyn-hydroxylases (PHDs) activity. HIF-a hydroxylated is recognized by VHL E3 ubiquitin ligase (VHL) and subsequently degraded. In contrast, low oxygen levels lead to an inactivation of PHDs and an accumulation of HIF-α, which goes into nucleus, binds HIF-β and promotes the transcription of several genes, including vascular endothelial growth factor (VEGF), which promotes angiogenesis mechanism. HRE: Hypoxia-response Element. O_2: oxygen.

1.4 OCULAR NEOVASCULARIZATION

In the eye, a state of equilibrium between cells and environment is essential to maintain the proper function of the tissues; a lack of homeostasis can result from an imbalance of cellular factors, which can compromise the function of the eye. The vast majority of diseases that cause vision loss are a result of ocular neovascularization [44]. In these diseases, a common denominator is the molecular imbalance between angiogenic inducers and inhibitors, which results in an excessive growth of blood vessels that compromises the two vascular beds in the eye: uveal and retinal vessels [45].

In many cases, the neovascularization is located in the retina, such as in retinopathy of prematurity (ROP) and proliferative diabetic retinopathy (PDR), where an ischemic condition in the retina leads to an increase of proangiogenic factors with consequent formation of aberrant neoangiogenesis, neuronal cell death and, in the worst scenario, retinal detachment [46]. Furthermore, some advanced stages of PDR can culminate in pathologic rubeosis iridis (RI), characterized by iris neoangiogenesis. Little is known about iris neoangiogenesis, yet during PDR it is assumed to be a result of increased vitreal proangiogenic factors, originating from the proliferating retina vasculature [47]. The proliferation of new blood vessels, along the surface of the iris, can lead to obstruction of the aqueous humor flow, increased intraocular pressure, and finally leading to neovascular glaucoma (NVG) [48].

In these pathological angiogenesis events, VEGF is the most canonical angiogenic mediator, yet other angiogenic factors play an essential role in neoangiogenesis.

1.4.1 uPA-uPAR system

During angiogenesis, extracellular matrix (ECM) remodeling is fundamental to grant endothelial cells' migration and proliferation. The cellular receptor (uPAR) for the urokinase-type plasminogen activator (uPA) plays a key role in the plasminogen activation system, a well characterized system of serine-proteases involved in thrombolysis, inflammation, cell migration, tissue remodeling, cancer invasion and vascularization [49]. uPA and uPAR are expressed by a variety of cells, including monocytes, macrophages, fibroblasts, and endothelial and smooth muscle cells [50]. uPAR is synthesized as a single polypeptide chain, and following post-translational modifications, the mature receptor results in a multi-domain glycoprotein tethered to the cell membrane through a glycosyl-phosphatidyl-inositol (GPI) anchor, formed by 3 domains, connected by short linker regions: D1 is the N-terminal domain that interacts with uPA, D2 connects D1 and D3, and D3 is

the C-terminal domain that anchors the molecule to the membrane through the GPI tail [51]. Various proteases, including trypsin, elastase, chymotrypsin, plasmin, and uPA can cleavage uPAR in the linker region that connects D1 and D2 domains, promoting the release of domain D1 and leaving a truncated form of uPAR constituted by domains D2 and D3, on the surface of the cell (Figure 3). In addition, the truncated uPAR can be released from the plasma membrane by the cleave of either its GPI tail or different sites of its globular domains to produce a soluble form (suPAR) [52], which plays a role in numerous physiological pathways, mainly involving immune activation, including plasminogen-activating pathway, migration, proliferation and cell adhesion, and systemic inflammation [53].

1.4.1.1. uPAR extracellular ligands

The extracellular ligand uPA, a serine protease, regulates the activity of the plasminogen activation system. uPA is negatively regulated by activator inhibitor (PAI)-1 and -2, serine protease that can bind uPA/uPAR complex, exposing a binding site for low-density lipoprotein receptor-related protein (LRP-1), which promotes uPAR/uPA/PAI-1/LPR-1 internalization. uPA and PAI-1 are eventually degraded in the lysozome, and uPAR and LRP-1 are recycled back from the endocytic compartment to the plasma membrane [54]. Vitronectin, an ECM glycoprotein, is also a uPAR ligand and is involved in uPAR signaling. Both vitronectin and uPA can bind uPAR simultaneously, coordinating different signal transductions, such as cell motility, invasion, proliferation and survival [55]. Moreover, it has been demonstrated that uPA binding can stimulate uPAR dimerization, enhancing the binding capacity to vitronectin, and enhance uPAR signal transduction [56].

1.4.1.2 uPAR co-receptors

Considering uPAR is linked to the cell surface solemnly by the GPI anchor, its signals are a part of a multiprotein signaling-receptor complex [56]. In support of this theory, it has been shown that multiple signaling receptors have been co-localized with cell surface uPAR, among which integrins [57], heterodimeric transmembrane receptors constituted by two subunits, α and β [58]. Integrins facilitate ECM adhesion and bind ECM proteins, including fibronectin, vitronectin, laminins and collagens. The interactions with integrins and vitronectin are positively regulated by uPA and both

uPA and vitronectin can induce uPAR-mediated cytoskeletal reorganization and cell migration [59,60]. In addition, other studies have previously demonstrated that uPAR activates intracellular signaling cascades by other lateral interactions with neighboring receptors, such as epidermal growth factor receptor (EGFR), platelet-derived growth factor receptors (PDGFRs) and formyl peptide receptors (FPRs) [61,62], all also implicated in angiogenesis through signaling cascades involving focal adhesion kinase (FAK), Src, Rac, Extracellular-signal Regulated Kinases (ERK)/ Mitogen-activated protein kinases (MAPK) and Janus Kinase (JAK)/ Signal Transducers and Activators of Transcription (STAT) [50]. Moreover, FPRs G protein-coupled receptors have the ability to bind N-formyl-methionyl-leucyl-phenylalanine (fMLF), a potent chemotactic peptide released by tissue bacteria to stimulates a variety of intracellular signaling cascades, including both neutrophils and macrophages chemotaxis, ROS production, cytokine expression, phagocytosis, and changes in cell surface marker expression [63].

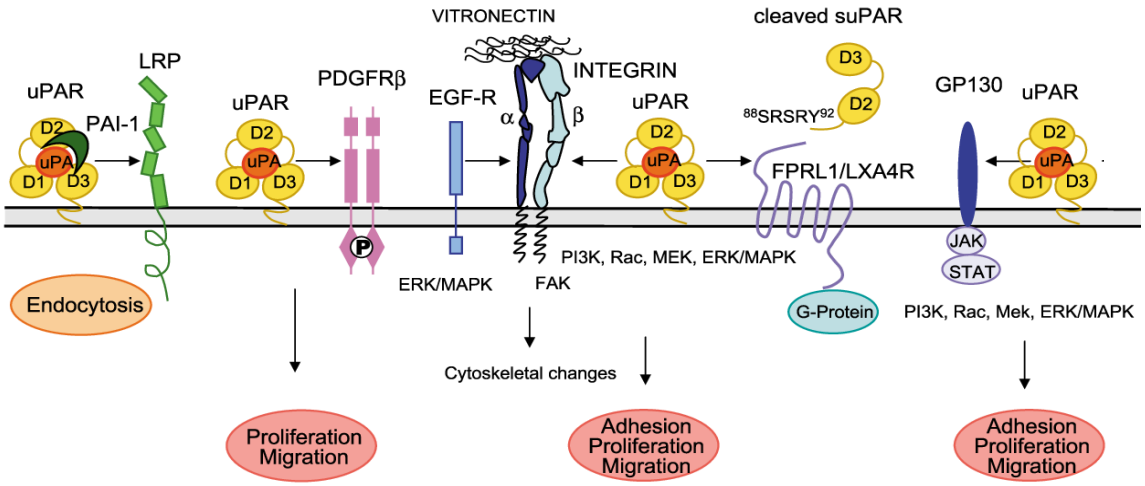

Figure 3. Schematic representation of uPAR interactome with intracellular pathways. Several ligands bind uPAR and co-receptors to promote different intracellular mechanisms. uPAR: urokinase-type plasminogen activator receptor; uPA: urokinase-type plasminogen activator; *PAI-1*: plasminogen activator inhibitor 1; *LRP*: low-density lipoprotein receptor-related protein; *PDGFR-β*: platelet-derived growth factor receptor beta; *EGF-R*: epidermal growth factor receptor; *FAK:* focal adhesion kinase; *FRPL1/LXA4R:* Formyl peptide receptor 2; *GP130*: Glycoprotein 130; *PI3K*: phosphatidylinositol-4,5-bisphosphate 3-kinase; *RAC, Mek*: subfamily of small rho GTPases; *ERK*: extracellular-signal regulated kinases; *MAPK:* mitogen-activated protein kinases.

1.5 MECHANISMS LINKING OCULAR NEOVASCULARIZATION

Pathologic angiogenesis and microvascular changes are not the only events that cause ocular damage. Metabolic and oxidative stress, neuroinflammation and subsequent cell death are also important contributors to the eye diseases [64,65].

In the retina, the neurons are very susceptible to insufficient supply of nutrients and oxygen; for this reason, an inadequate support from the vasculature can result in disruption of retinal cells homeostasis [14,66]. In retinopathies, such as PDR and ROP, the abnormal retinal vasculature is further accompanied by a breakdown of iBRB, which causes an increase of vascular permeability and a possible leakage of macromolecules and other potentially harmful agents into the retina [67,68]. Altogether, these pathological events occur with the microvascular abnormalities, causing chronic retinal neurodegeneration with an increased mechanism of cell death and a gradual loss of neurons, and thus contributing to a decrease in the electric response and visual acuity [69–71].

1.5.1 Autophagic mechanisms

In pathological conditions, retinal changes generate a significant activation of several complex adaptive responses, by promoting rapid induction of specific molecules involved in several pathways, among which autophagy [72].

Autophagy is a self-degradative evolutionary conserved mechanism that is essential for maintaining the normal cellular homeostasis and energy balance [73]. Due to its high metabolic demand, the retina is characterized by a strong expression of autophagy proteins [74]. During development, when the cells are preparing to undergo structural remodeling, autophagic mechanisms are critical to balance bioenergetic dynamic mechanisms of both endothelial and retinal cells [75,76]. In adulthood, at low basal levels, autophagy plays an important role in the turnover of damaged organelles, such as peroxisomes and endoplasmic reticulum, as well as in removing toxic aggregated or misfolded proteins [77]. Autophagy is rapidly upregulated when cells need nutrients and energy, e.g. during starvation or high bioenergetic demands [73]. However, in pathological circumstances, a deregulated autophagy might be damaging and promote autophagic-associated cell death [74,75,78–83], which has been associated with various disorders, including retinal diseases [84–86].

Autophagy is categorized by three different mechanisms: *chaperone-mediated autophagy*, a specific lysosomal-dependent protein degradation pathway; *microautophagy*, where cytoplasmic contents enter the lysosome through an invagination of the lysosomal membrane; and *macroautophagy*, the

canonical mode of autophagy and mostly known as “autophagy”, where the delivery of cytoplasmic cargo is sequestered inside the double-membrane vesicles – autophagosomes – to the lysosome. Despite morphologically distinct, all three mechanisms culminate in the same manner: cargo to the lysosome for degradation and recycling [87].

1.5.1.1 Macroautophagy

Among different variants of autophagic mechanisms, macroautophagy (here forth referred to as autophagy), is the most studied lysosomal pathway. The mechanism of autophagy is coordinated by different stages, which are regulated by several molecules and multiple signaling pathways (Figure 4). Autophagy-related genes (Atg) are paramount required for autophagy. *Atg* genes encode proteins that assemble into functional complexes, which are mandatory to promote autophagic mechanisms [88]. The induction of autophagy is promoted by the activity of the Unc-51 Like Autophagy Activating Kinase (Ulk)1 (mammalian homologue of *Atg1*), in a complex with Atg13 and Atg17 [89,90], with other two complexes: the phosphoinositide 3-kinase (PIIII-K) complex, constituted by Vesicular protein sorting (Vps)34 complexed to Atgs /Beclin-1; and the phosphatidyl inositol triphosphate (PI3P)-binding complex, formed by different Atg complexed proteins.

Autophagy begins with the nucleation and elongation of an isolation membrane, known as phagophore, derived from lipid bilayer contributed by the endoplasmic reticulum (ER) and/or the trans-Golgi and endosomes [91]. Vps34 is a PI3 kinase that uses phosphatidylinositol (PI) as substrate to produce PI3P, which is essential for phagophore elongation and recruitment of other Atg proteins to the phagophore [92]. The process continues with the fusion of the edges of the phagophore to form the autophagosome, a vesicle constituted by a double membrane that sequesters cytoplastic contents. Autophagosome elongation and maturation involves two ubiquitin-like conjugation systems: the microtubule-associated protein I light chain 3B (LC3B-I) system; and the Atg12 system. LC3B-I, the mammalian homologue of Atg8, is conjugated to phosphatidylethanolamine, converted in LC3B-II and inserted into the autophagosomal membrane, by the action of Atg5 and Atg7 enzymes [93]. This step is crucial for autophagosome formation and will continue until the end of this stage. The synthesis and processing of LC3-II is increased during autophagy, making it a key marker of levels of autophagy in cells [94].

The cargos presented to the autophagosome are selected by targeted ubiquitination, which is recognized by ubiquitin-interacting domains of autophagic cargo receptor proteins, such as

sequestosome-1, also known as the ubiquitin-binding protein p62, and carrying through the binding of LC3-II interacting regions [95,96]. The p62 is itself degraded by autophagy and is used as a marker to investigate autophagic flux. When autophagy is inhibited p62 accumulates, while when autophagy is induced p62 levels decrease [97].

Autophagy terminates when the autophagosome fuses with the lysosome to create the autolysosome where the inner material is degraded by lysosomal hydrolase (Figure 4). Once degradation ended, the resulting biomolecules, such as amino acids or lipids, can be recycled back to the cytoplasm and reused by the cell to synthesize new biomolecules [98].

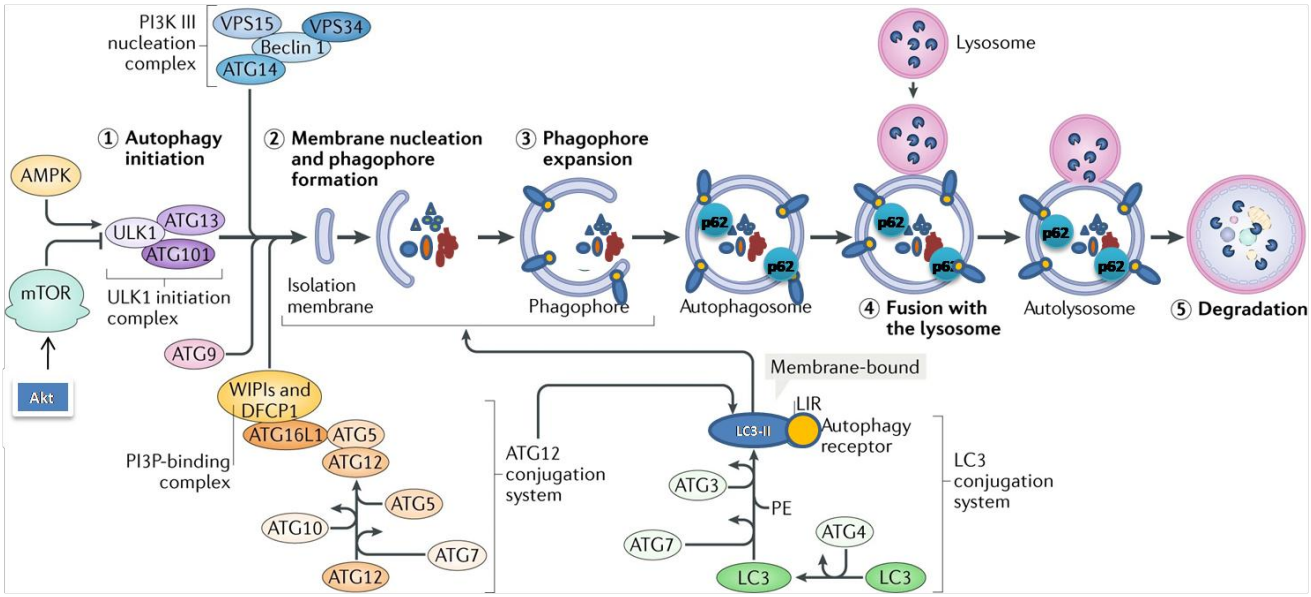

Figure 4 Schematic representation of autophagic mechanism. Autophagy is induced by AMPKα, which leads to autophagy initiation, through the phosphorylation of Ulk1. The mechanism continues with the formation and expansion of phagophore and ultimates with the fusion of autophagosome and lysosome to promote degradation.
AKT: protein kinase B; mTOR: mammalian target of rapamycin; *AMPKα*: Adenosine monophosphate-activated protein kinase alpha; *Ulk*: Unc-51 Like Autophagy Activating Kinase; ATG: Autophagy-related genes; *PI3KIII*: Phosphoinositide 3-kinase; *VPS 15/34*: Vesicular protein sorting; *WIPIs-DFCP1*: WIPIs-double FYVE-containing protein 1; *PI3P*: Phosphatidyl inositol triphosphate; LC3 I/II: microtubule-associated protein I light chain 3 I/II; *PE:* Phosphatidylethanolamine; LIR: LC3-interacting region.

1.5.1.2 Regulation of autophagy

Among the numerous components involved in the regulation of the autophagic machinery, the mammalian target of rapamycin (mTOR) kinase is the major negative regulators of autophagy, in response to cellular physiological conditions and environmental stress [99,100]. mTOR is regulated by the availability of nutrients and integrates upstream activating signals that inhibit autophagy through the protein kinase B (Akt) pathway (Figure 4) [77,101]. At the molecular level, in presence of nutrients and/or growth factors, the kinase Akt phosphorylates and activates mTOR, inhibiting autophagy by phosphorylation of Ulk1 on the Ser^{777} site, which could not further activate the essential inductor Beclin-1/Vs34 complex [102]. Upon activation, p-mTOR phosphorylates other translational regulators, including initiation factor 4E-binding protein (4E-BP1) and the ribosomal S6 protein (S6), which have a crucial role to regulate the initiation of translation of distinct mRNAs [103–105]. On the other hand, in response to energy stress, such us nutrient starvation but also reduced growth factor signaling, the adenosine monophosphate-activated AMPKα acts as a positive regulator of autophagy. AMPKα is activated by a decrease of ATP/AMP ratio through phosphorylation, and inhibits mTOR activity. AMPKα then phosphorylates Ulk1 on Ser^{555}, activates Ulk1 kinase and induces autophagy [102,106]. Despite the mTOR1 and AMPKα antagonistic roles, their activities are molecularly connected; the inhibition of mTOR1 activity is one of the main mechanisms by which AMPKα increases autophagic degradation and conversely [107].

1.5.1.3 Autophagy flux and mechanisms of cell death

By responding to nutrient availability, cells modulate the autophagic flux in order to meet the metabolic demands and to guarantee cellular viability. The autophagic flux is defined as a measure of autophagic degradation activity, which is intrinsically dependent on lysosomal function [108]. The transport of autophagosomes to lysosomes, followed by the process of autophagosomal lysosomal fusion, is indispensable for autophagic function. Hence, a dysfunction in either intracellular autophagosomal trafficking or fusion will negatively affect autophagic flux, and may lead to pathologic events and mechanisms of cell death [109,110].

In literature, autophagy mechanisms have been associated also with autophagy-dependent cell death, when mechanistically the cellular death depends on the autophagic machinery; and as autophagy-mediated cell death, when autophagy may precede and trigger a different programmed

cell death, such as apoptosis and necroptosis [81,111–114]. In pathological conditions, both apoptosis and necroptosis, if induced, can compromise cell viability. Apoptosis is characterized by loss of cell-cell contact, detachment, nuclear condensation and fragmentation, and occur by the activation of the Caspase family of proteases. Contrarily, necroptosis is identified by cell swelling and, involves the receptor-interacting protein kinases (RIPKs)-dependent pathway [115,116]. Several mechanistic links between autophagy, apoptosis and necroptosis have been proposed, although the fundamental molecular mechanisms are not fully elucidated [117,118]. Studies have suggested that in stress conditions, the autophagy machinery might promote either apoptosis or necroptosis, based on the energetic state of the cells and ATP availability. Importantly, a high level of intracellular ATP often promotes apoptosis, whereas a rapid drop in ATP intracellular concentration, which occurs during mitochondrial injury, is implicated in necrotic cell death [119–122]. In line with the specific role of autophagy in responding to metabolic activity, it is clear that the efficacy of the autophagic flux further determines the extent of metabolite contribution.

In ocular neovascular diseases, oxidative and nutrients stress have been implicated in impairment of the autophagic flux [123,124]. In such conditions, autophagy activity is not compatible with cellular metabolism, thus the efflux rate does not match the metabolic demands, leading to drastic loss in ATP. In this manner, and dependent on specific intracellular ATP levels, apoptotic or necrotic mechanisms of cell death can be induced, leading to several pathologic events in the eye [120,122].

1.6 TREATMENT OF OCULAR NEOVASCULAR DISEASES

Currently, targeting VEGF signaling is the most utilized strategy in the pharmacological treatment of ocular neovascularization [125]. Moreover, surgical methods, such as laser photocoagulation, are also a standard treatment for ablating aberrant blood vessels to reduce further tissue damage [126,127]. However these procedures have been target of criticism due to different disadvantages. Laser photocoagulation has been shown to have several side effects, such as peripheral visual fields loss, reduction in night vision and reduction in contrast sensitivity; in addition, in many cases little or no improvement of the visual function has been reported [128,129].

Despite anti-VEGF strategy has represented a great step forward in the treatment of ocular neovascular diseases, its effects can be somewhat limited [130]. Frequent intravitreal injections can lead to complications, including infectious endophthalmitis, intraocular inflammation, acute rise of

intraocular pressure and, in rare cases, haematogenous retinal detachment [131]. Moreover, anti-VEGF drugs, even if injected locally, can lead to a significant reduction in systemic plasma free-VEGF levels and this suppression may have implications [132,133]. It is interesting to note that VEGF is an important growth factor, not only for the induction of vascular responses but also for retinal neuroprotection. VEGF has been shown to be expressed and released to protect retinal neurons. In an *in vivo* rat model, repeated intravitreal administrations of an anti-VEGF drug have been shown to induce neuronal loss in the retina [134]. Moreover, in a 'knock-out mouse model with the HRE in the VEGF promoter deleted, has demonstrated a correlation between the critical reduction of VEGF and the development of neuropathology, suggesting that neurons are extremely sensitive to depletions in the levels of VEGF [135].

Consequently to all these disadvantages and limitations, new molecular pathways and therapeutic strategies should be investigated to address ocular neovascular pathologies.

2. AIMS

Ocular neovascularization is characterized by an excessive growth of blood vessels, which can compromise the two vascular beds in the eye: uvea and retinal vessels. In these pathologies, the microvascular abnormalities can lead also to a form of metabolic stress, resulting in an insufficient supply of nutrients to the respective target tissues. Consequently, hemorrhages and extravasation of plasma might be accompanied by other pathological events, such as neuroinflammation and cell death, which dramatically affect the neurons of the retina [65,136].

In the recent years of therapeutics' ophthalmology, anti-VEGF drugs have represented a great step forward in the treatment of ocular neovascular diseases, but the effects are exclusively at angiogenic levels and can be associated with potential risks [130]. Consequently, a pharmacologic strategy aimed at inhibiting several pathways could be a more suitable therapeutic approach.

The aim of the thesis was to investigate:

- non-canonical angiogenesis mechanisms associated with a vascular bed of the eye, **UVEA**, in a model of iris neovascularization characterized by pathologic angiogenesis, associated to pro-inflammatory and extracellular matrix driven mechanisms;
- mechanisms of autophagy in the **NEURORETINA** of newborn rats and in a rat model of oxygen induced retinopathy (OIR), an acknowledged model of ROP, characterized by retinal neovascularization and retinal dysfunction.

Pharmacologically, targeting the uPAR/uPA system, by using the inhibitor UPARANT, was evaluated as a possible strategy to mitigate angiogenic and inflammatory process in models of iris neovascularization; an inhibitor of the autophagy mechanism, 3-Methyladenine, was tested to preserve retinal neuronal damage, in a model of retinal neurodegeneration consequent to neovascularization.

2.1 SPECIFIC AIMS OF THE PAPERS

2.1.1 <u>Project 1- uPAR/uPA system in iris neovascularization</u>

Paper I: To analyze the angiogenic effects of UPARANT, in a context of hypoxia-induced angiogenesis, using a novel *ex vivo* human iris angiogenesis assay.

Paper II: To investigate the effects of UPARANT on angiogenic and inflammatory processes, using an *in vivo* non-invasive iris imaging and standard molecular and cellular methodologies.

2.1.2 Project 2- Autophagic mechanism in the rat retina

Paper III: To evaluate the expression profile of autophagy markers in the rat retina during development.

Paper IV: To evaluate the autophagic flux and mechanisms of cell death in the retina of rat pups exposed to OIR protocol; and concomitantly to analyze whether modulating autophagy through the inhibitor 3-Methyladenine, may reduce retinal neuronal damage and restore retinal function.

3. OVERVIEW

All the experiments performed during my PhD are presented in two collated projects.

3.1 PROJECT 1- uPAR/uPA system in iris neovascularization

PAPER I

The first paper "*UPARANT mitigates human iris angiogenesis through uPAR/LRP-1 interaction in an organotypic ex vivo model*" demonstrates the angiogenic effect of UPARANT on an *ex vivo* human iris angiogenesis assay, showing an effect on endothelial cells and not on iris epithelial cells. Moreover, for the first time, we show an unidentified antagonism of UPARANT in the interaction of uPAR with the LPR-1, resulting in inhibition of β-catenin–mediated angiogenesis.

PAPER II

The second paper "*Gaining insight on mitigation of rubeosis iridis by UPARANT in a mouse model associated with proliferative retinopathy*" elaborates that UPARANT is effective to decrease iris vasculature *in vivo,* acting predominantly by reducing the upregulated inflammatory and ECM degradation responses. In this study, we suggested that UPARANT, systemically administered, could open to novel improved therapies for proliferative ocular diseases.

3.2 PROJECT 2- Autophagic mechanism in the rat retina

PAPER III

In this paper titled "*Autophagy involvement in the postnatal development of the rat retina*" we characterize an intrinsically association of autophagic mechanisms with the hypoxic phase of the first stages of retinal rat development. This is the first study to illustrate the autophagic flux in the rat developing retina and characterize the hypoxia implications in developmental autophagy mechanisms.

PAPER IV

This paper *"An imbalance in the autophagy flux contributes to retinal dysfunction in the OIR rat model"* demonstrates a dysregulation of autophagic mechanisms in the neuroretina of OIR rats and

a correlation link between autophagy and necroptosis in this model. Here, we suggest that autophagy could be considered as a molecular target for ROP neuroprotective treatment strategies.

4. RESULTS AND DISCUSSION

4.1 PROJECT 1- uPAR/uPA system in iris neovascularization

4.1.1 PAPER I

During angiogenesis, uPA and its receptor uPAR play a pivotal role in ECM remodeling, where uPAR regulates endothelial cell migration and proliferation through assembly with transmembrane receptors [61]. Within the uPAR interactome, FPRs have been shown to have a prevalent crosstalk in VEGF regulation [137], although through indirect mechanisms.

In this first paper, in the context of hypoxia-induced angiogenic stimulus, we investigated UPARANT effects in an *ex vivo* human iris angiogenesis assay, and compared to the clinically used anti-VEGF, Aflibercept. Additionally, to further elucidate UPARANT's mechanisms of action, we performed an *in vitro* assays on human iris epithelial versus human retinal endothelial cells, corroborated by colocalization of immunofluorescence signals *ex vivo*. The mechanisms of VEGF-independent iris neovascularization were elaborated by analysis of uPAR co-receptor interactome.

4.1.1.1 MAJOR FINDINGS

UPARANT does not affect human iris epithelium yet reduces sprouting angiogenesis in human retinal endothelial spheroids

The macrostructure of the iris includes epithelial and endothelial structures that both can contribute to the neovascular mechanisms[138]. To assess the effects of UPARANT in either epithelium or endothelium, we performed *in vitro* assays. Precisely, using antagonism of both UPARANT and Aflibercept on hypoxia-stimulated hIEC migration was indiscernible from vehicle-treated controls, while hREC 3D culture's sprouting was mitigated by Aflibercept and even further by UPARANT (Paper I, Figure 1A-B).

Subsequently, to further elaborate on UPARANT's ineffectiveness on human iris epithelial cells, we performed expression analysis of FPR genes in both hIEC and hREC. We demonstrated that uPAR and its ligands, uPA and PAI-1, were expressed in both hIEC and hREC, yet the canonical uPAR co-receptors FPR2 and -3 were only detectable in hREC (Paper I, Figure 1C). Combined these data suggested that UPARANT does not influence iris epithelial cells but affects ocular endothelial cells. The current observation that UPARANT exerts a considerable antagonistic effect in hREC is in agreement with previous data, where UPARANT has been demonstrated to inhibit

both FPR- and VEGFR-mediated uPAR signaling in endothelial cells [139]. On the contrary, the absence of expression of FPRs in hIEC is confounding, since expression of uPAR and FPR signaling has been shown in other epithelial cells [11,27]. Albeit, the expression of uPAR on epithelial cells has been performed in tumorigenic cell lines where the uPAR/FPR system has been demonstrated to be upregulated[142] and antagonism of uPAR binding to FPRs could interfere with lipid-raft partitioning, thus impairing epithelial cell migration [143]. The present data is limited to the *in vitro* nature of the study, where isolated iris epithelial cells lack their tissue cues and context, and also by the unavailability of iris endothelial cells, thus the use of retinal endothelium as an ocular model of vascular endothelial cells. Consequently, we analyzed protein expression of FPRs and uPAR in human iris with colocalization to the vasculature. Confocal imaging displayed expression of uPAR predominantly in human iris blood vessels, with colocalization of FPR1 and -2 expression (Paper I, Figure 2), a result substantiated with previous mouse iris analysis [144]. Collectively, the present data demonstrated that canonical FPR/uPAR signaling is focal to human iris vasculature, and may be associated with iris neovascular responses to angiogenic stimuli.

UPARANT potently inhibits hypoxia-induced *ex vivo* iris angiogenesis

Iris neovascularization during RI has been associated with an increase in pro-angiogenic factors, particularly VEGF in PDR patients, as a result of an hypoxic stimulus to the diabetic retina [3,7,29]. Thus, we established iris organotypic cultures, a novel model of human *ex vivo* neoangiogenesis, to analyze their ability to create angiogenic sprouts when embedded in ECM. Under hypoxia stimulated angiogenic conditions, human iris explants formed *ex vivo* capillary sprouts expressing both VEGFR2 and PECAM-1 endothelial markers (Paper I, Figure 3A), which confirmed sprouting angiogenesis [147]. In this context, human iris *ex vivo* organotypic cultures treated with UPARANT demonstrated a reduction of angiogenic sprouts' area (Paper I, Figure 3B).

UPARANT reduces phospho-transcription factors associated with angiogenesis in human iris

As discusses previously, hypoxia and inflammation responses play a central role in ocular neovascular diseases [25,26]. In this context, we performed a western blot analysis to determine the effect of UPARANT on transcriptional activators mediating hypoxia and pro-inflammatory responses in human iris (Paper I, Figure 4). In agreement with canonical uPAR/FPRs mediated mechanisms [7–9,17,27], here we demonstrated that UPARANT leads to a decrease of HIF-1α protein levels compared to both vehicle and Aflibercept treated irises, concomitantly with a decrease in

phosphorylation levels of pro-inflammatory proteins (Paper I, Figure 4). With these results, we further confirmed the role of uPAR and its interactome in regulating neoangiogenic processes in human iris vasculature.

Animal models of RI have demonstrated both VEGF-dependent and -independent neovascularization mechanisms in the iris [16,19,20]. Consequently, to further elaborate on the mechanistic aspects of UPARANT-mediated uPAR antagonism in human iris, we used a phospho-proteome array to determine the phosphorylation status of factors involved in angiogenesis, cell survival, migration and chemotaxis, as well as auto-phosphorylation of EGFR, in human iris *ex vivo* organotypic cultures (Paper I, Figure 5). Studies have suggested that uPAR activates directly EGFR, through lateral interaction with integrin α5β1, initiating an intracellular signaling that leads to tube formation and motility of cells [20,38,39]. Moreover, inflammation and migration regulating pathways, including several factors downstream responses of activation of EGFR [156–158]. The interference of UPARANT with the uPAR/uPA system decreased phosphorylation levels of downstream proteins, which leads to the observed inhibition of migration and sprout formation in human iris *ex vivo* neovascularization. Interestingly, UPARANT decreased β-catenin phosphorylation levels in human iris (Paper I, Figure 5). Considering that uPAR is linked to the cell surface solemnly by a glycosylphosphatidylinositol anchor, its signal is dependent on lateral interaction with neighboring receptors, such as integrins, EGFR and LRP-1, all implicated in β-catenin–mediated angiogenesis [38,43–46].

UPARANT interferes with the binding of uPAR to LRP-1

Previous studies have demonstrated that PAI-1 interacts with LRP-1, inducing cellular migration [159,160]. PAI-1 has been described generically as a physiological inhibitor of uPA that can inhibit cell migration and adhesion [161]. Yet, protease cleaved PAI-1 can bind both uPA and LRP-1, and induce cell motility through the activation of β-catenin intracellular pathways [162] and the modulation of LRP-1 binding to the lipid-rafts [50,51]. Elaborating on the observation of β-catenin modulation in the presence of UPARANT, we determined the expression of both uPAR and LRP-1 in *ex vivo* hypoxia-stimulated human irises. Protein levels of either uPAR and LRP-1 were unaffected by UPARANT or Aflibercept treatment (Paper I, Figure 6A). Albeit, immunoprecipitation of the uPAR/LRP-1 complex demonstrated an interaction between LRP-1 and uPAR in human iris (Paper I, Figure 6B), which could be impaired in the presence of UPARANT, but Aflibercept. In addition, we observed that both uPAR and LRP-1 protein colocalized in human iris, with focal expression to

the vascular structures; and we detected an expression of the ligands uPA and PAI-1 in iris epithelial cells (Paper I, Figure 6C). In this manner, UPARANT interferes with uPAR/LRP-1 complex and inhibits cell motility induced by β-catenin (Paper I, Figure 7).

4.1.1.2 CONCLUDING REMARKS

The present data provide a better understanding of the molecular mechanisms of action of UPARANT in the iris, using a novel *ex vivo* human angiogenesis model. The study has the novelty of determining expression of FPR and uPAR in human iris vasculature. Moreover, we have established a new human *ex vivo* iris angiogenesis model using organotypic cultures addresses molecular and cellular queries in a whole-tissue context, which heightens the molecular relevance of UPARANT antagonism of angiogenesis at a multicellular level. In line with the multileveled complexity of the organotypic cultures, the current study illustrated a yet uncharacterized mechanism of action of UPARANT, through inhibition of uPAR/LRP-1 interactome and its β-catenin downstream signaling.

4.1.2 PAPER II

Advanced stages of proliferative retinopathies (PR) have been associated with the development of pathological RI, due to an increase of a myriad of pro-angiogenic factors, including VEGF, originating from the retinal tissue [48,165]. An increase of similar angiogenic factors has been identified in hypoxia-exposed RPE cell media [153,166]. In the present study, we have established a murine model of puncture-induced RI [167] in association with PR (RI-PR) by co-injection of pro-angiogenic factors derived from hypoxia-exposed RPE culture media. The purpose was to mimic the increase in proangiogenic pressure from the posterior compartment of the eye. Moreover, to assess the effectiveness of intravitreal administration of UPARANT and anti-VEGF drugs in the RI-PR model, we compared the effects of UPARANT with those of the VEGFR1 chimera protein.

4.1.2.1 MAJOR FINDINGS

UPARANT reduces neovascularization in RI associated with PR

Before assessing the effects of UPARANT on RI-PR mice, we first analyzed their iris vasculature. In the eyes of RI-PR mice, we observed an increase of approximately 35% of iris vasculature when compared to untreated controls (Paper II, Figure 2). Subsequently, we executed intravitreal UPARANT or VEGFR1 chimera injections (Paper II, Figure 1).

Intravitreal administration of UPARANT promptly reduced RI-PR macrovasculature, as determined by noninvasive analysis of iris vasculature. Despite a considerable slower effect, anti-VEGF treatment produced similar outcomes within the study protocol (Paper II, Figure 2).

The mouse iris neovasculature develops through anastomosis[153], characterized by formation of vascular sprouts and branching. Thus, we analyzed the iris microvascular beds of the various experimental group by immunofluorescence assay. The analysis of irises microvasculature with PECAM-1 demonstrated that UPARANT-treated RI-PR eyes were indistinguishable from controls regarding number of blood vessels, sprouting, and branching, with a stronger reduction when compared with anti-VEGF. Overall, UPARANT demonstrated a faster mitigation and broader efficacy in decreasing microvascular events compared with anti- VEGF strategies in the RI-PR murine model. These obtained data are in agreement with previous studies demonstrating inflammation and ECM degradation as primary mechanisms of iris neovascularization in the mouse model [144,153] even in the presence of increased hypoxia-mediated proangiogenic factors, including VEGF and many other factors as we demonstrated here. Our results corroborate that UPARANT acts on several angiogenic pathways, while anti-VEGF strategies are limited to VEGFR-driven angiogenesis. In fact, UPARANT reduces all analyzed iris microvascular parameters in the murine model of RI-PR to levels undistinguishable from untreated controls, while anti-VEGF treatment only significantly reduced vascular branching in RI-PR—a mechanism dependent on gradients of angiogenic factors, particularly VEGF [34].

UPARANT counteracts inflammation and ECM remodeling in the RI-PR model

UPARANT has been reported to antagonize uPAR/FPR signaling [151,168–171]. In the iris, it has been demonstrated FPR1 expression is localized on endothelial cells, and activation of FPR1 mediated hypoxia and inflammation cascades [171]. Thus, we performed western blotting to analyze the expression of the pivotal transcription factors for the hypoxia and pro-inflammatory signaling. (Paper II, Fig. 4). We demonstrated that UPARANT antagonism of FPR1 in the mouse model of RI-PR downregulates inflammation-mediated transcription and is independent of the hypoxia pathways. In agreement with previous findings [171], transcripts and proteins mediated by canonical

hypoxia and angiogenesis were not modulated in the RI-PR model. Our data suggests that even in the presence of increased hypoxia-driven pro-angiogenic factors, the ECM and inflammation mechanisms of iris neovascularization appear predominant in the mouse models of induced RI.

Regulation of NFκB phosphorylation (pNFκB) by the plasminogen-activator and inflammation pathways is fundamental in angiogenesis [172–174]. We demonstrate reduced p-NF-κB levels in UPARANT-treated irises with concomitant downregulation of transcripts involved in ECM degradation and inflammation in the murine model of RI-PR, to levels comparable with untreated controls. Noticeable, a discreet non-significant increase in VEGF transcript levels was determined in the RI-PR model, which could be the result of a crosstalk between the VEGFR- and FPR-mediated signaling, as previously suggested [139,147].

Despite the fact, regulation of ECM degradation and inflammation transcripts in the RI-PR murine model was not affected by anti-VEGF treatment, which suggests a major role for FPR-mediated mechanisms over VEGFR-dependent pathways in iris neovascularization.

Systemic efficacy of UPARANT in mitigating RI associated with PR

Systemic administration of UPARANT has been shown to distribute to the eye at pharmacological levels in multiple animal models [168–170], including models of iris neovascularization [171]. Thus, we further assessed the effectiveness of UPARANT subcutaneous route of delivery in mitigating RI-PR. We induced RI-PR on one eye, with the contralateral eye left as untreated control, and subcutaneously treated the mice with UPARANT (Paper II, Fig.1). In the RI-PR model, mouse pups responded rapidly to the induction stimuli by increasing the anastomotic vessels of the iris. However, the stimuli must be repeated routinely to maintain the pathological stress, and warrant maturation of the anastomoses [153].We determined an increase of more than 135% in blood vessel density in RI-PR eyes, respective to untreated controls (Paper II, Fig. 6a).

In the RI-PR model, subcutaneous administration of UPARANT mitigated neovascularization and reduced upregulated markers of extracellular matrix remodeling and inflammation transcripts to control levels, much paralleled to the finding with local administration of UPARANT. As before, we observed that canonical VEGF pathway was not upregulated in RI-PR mice, and the upregulation of FPR1 transcription was significantly decreased to the untreated group in UPARANT-treated animals.

4.1.2.2 CONCLUDING REMARKS

The study in Paper II demonstrates that UPARANT treatment of RI-PR eyes has a protective effect on iris endothelial cell remodeling, thus sustaining the iris vasculature at control levels through the study period. On the contrary, anti-VEGF regimen can protect only endothelia from VEGF-specific signaling, resulting in the observed delay of iris vascular recovery. Furthermore, the effectiveness of subcutaneous UPARANT administration is in line with systemic treatments of proliferative ocular pathologies, which could improve the treatment of patient afflicted by PDR and CRVO, or even NVG.

4.1.4 FUTURE PROSPECTIVES

Currently, treatment of iris angiogenesis associated with PR diseases relies on anti-VEGF intravitreal regimens [175]. Whereas anti-VEGF strategies focus exclusively on VEGF-driven signals, here we demonstrate that UPARANT modulates the upstream molecular mechanisms, leading to angiogenesis and inflammation, and simultaneously downregulates multiple growth factors and cytokines involved in iris neovascularization. These findings both deepen and corroborate the role of UPARANT as a bonafide multifactor inhibitor of ocular vascular endothelial cells, which could benefit the treatment of RI in patients afflicted with PDR or NVG, as well as multiple other ocular neovascular diseases.

4.2 PROJECT 2- Autophagic mechanism in the rat retina

4.2.1 PAPER III

During retinal development, the physiologic hypoxia stimulates endothelial cell proliferation and warrants retina vascularization. Concomitantly, autophagy has been reported to contribute to cellular adaptation to a variety of environmental changes and stresses, including development. Thus, in this paper, we performed a study to further understand the role of autophagy in developing rat retina. In rats, the retinal vascularization is completed postnatally, at around postnatal day (P) 13-P16 [176]. Hence, we conducted our study at different time points: birth, P7, P14 and P18.

4.2.1.1 MAJOR FINDINGS

The rat retina is partially avascular at birth and immature until P7

At the beginning of this study, we assessed the progress of retinal vascularization in the rat, by performing a whole-mount staining and molecular analysis. At birth, the retina surface was partially avascular and still covered by the hyaloid vessels (Paper III, Figure 1A). As reported in literature, the hyaloid network persists until P7 [177,178] by which time the rat retinas displayed nearly full to vascularization (Paper III, Figure 1A). At this time point, the developing retina vascular network is still immature and the BRB is not formed [179]. To form the BRB, endothelial cells require tight junctions, essential to regulate the movement of solutes and nutrients from the outer to the inner retinal layers [180]. In newborn rats, we observed low levels of barrier genes (Paper III, Figure 2A,B), which were increased at P14 and P18, when the retinal vasculature displayed to cover the total surface of retina. This suggests that form birth to P7 the developing retina vascular network is still immature and the BRB is not formed [179]. The retina vascularization is completed and mature around P14-P18, in alignment with the presence of tight junctions in retinal endothelial cells.

At P7 the rat retina is hypoxic

During the early postpartum retinal developmental stage in rats, the involution of the hyaloid vasculature to the retinal vascular network results in a partially avascular and ischemic retina, correlating to increased oxygen demand and resulting in a hypoxic stimulus [40]. In the present study, we observed a peak of HIF-1α and VEGF-A expression at P7, which decreases at P14 and P18 when the retina was fully vascularized (Paper III, Figure 1B). From embryonic stages to birth, the

physiological hypoxia is paramount to drive retinal neovascularization, through the upregulation of HIF-1α and subsequently VEGF-A [181,182].

Autophagic mechanisms increased during the hypoxic phase

During development, autophagic mechanisms have been reported to support cells to adapt and respond to several processes, including proliferation, differentiation and migration [183]. The developing retina requires autophagy to adjust its bioenergetic and biosynthetic demands [75,184]. In this respect, both hypoxia and energy deprivation have been reported to promote AMPK activation, a known inducer of autophagy [185,186]. Here, we observed a clear variation of autophagy during retinal development, indicating an increase of autophagic protein levels at P7, with a decrease at P14 and P18 (Paper III, Figure 4B). We observed a predominant expression of an autophagic marker at P7 in both IPL and OPL, while at birth and on P14 and P18, the autophagic marker was predominantly expressed in the IPL and almost undetectable in the OPL. Moreover, heightened colocalized expression of the autophagy and vascular markers was observed at P7, as compared to birth, P14 and P18, which could be related to the hypoxia associated with the involution of the hyaloid blood vessels.

4.2.1.2 CONCLUDING REMARKS

During the early postpartum developmental stage, the rat retinal cells are affected by ischemia, which is correlated to the peak of expression of HIF-1α and VEGF-A, concomitantly with autophagic markers. Moreover, an expression of autophagy is observed in endothelial cells at P7, suggesting that autophagy may contribute directly to the formation of the retinal vascular network. These findings indicate that during the physiologic hypoxia in the rat retina, HIF-mediated signaling induces the increase in VEGF-A to promote endothelial cell proliferation, and an upregulation of autophagy markers to sustain cellular homeostasis and cellular quality control in retinal cells.

4.2. PAPER IV

In pathological conditions, an impairment of autophagy flux might be damaging and promote autophagy-associated cell death, which is a result of an accumulation of autophagosomes in the cell [80]. Thus, autophagy can mediate mechanisms of programmed cell death, including necroptosis and apoptosis [111,114]. In this paper, we used the rat model of OIR developed by Penn [187] to mimic

pathological events of ROP disease, characterized by an alteration of both endothelial and retinal cells [188], to investigate changes in the expression of key mediators of autophagy and markers of cell death in the rat retina. Here, the newborn rats were exposed to alternating daily cycles of oxygen (50% and 10% O_2 every other day) for the first 14 days and returned to room air until P18. As consequent, the retina presents a delaying of the development of retinal vessels, generating the appearance of an avascular periphery; and, an aberrant retinal vessels growth that leads to the formation of neovascular tufts [189]. In addition, the OIR rats are further characterized by a profound retinal dysfunction. For this study, we analyzed 2 time points: P14 and P18.

4.2.2.1 MAJOR FINDINGS

Increased VEGF modulates retinal vasculature in OIR rat

Here, before studying the autophagy flux in the OIR rat retina, we confirmed the vascular phenotype by whole-retina vasculature analysis, which was characterized by peripheral retinal avascularity at P14, and the presence of neovascular tufts at P18 (Paper IV, Fig. 1a). Subsequently, we monitored protein levels of HIF-1α and VEGF-A, the main factors involved in neovascularization both in the OIR animal models and in ROP afflicted babies [190]. In the rat model, a previous study has reported a significant increase in VEGF levels in pup rats exposed to the OIR protocol, when compared with rats kept in RA [191]. Similarly, we observed a peak of VEGF in OIR rats at both P14 and P18 (Paper IV, Fig. 1c). As demonstrated, the increase of VEGF-A levels is due to an adaption to supplements deficiency, which can be developed by the hypoxic stimulus from retinal cells [192]. In fact, as a consequence of the oxygen fluctuations induced in this model, the retinal blood vessels are fragile, structurally deficient and poorly organized; thus, they are not able to fully nourish oxygen and nutrients to retinal cells [193]. Nevertheless, we detected no significant difference in HIF-1α levels in OIR retinas at P14 and P18. This data would suggest that VEGF-mediated angiogenesis in our OIR rat model might be induced also through HIF-1–independent signaling pathways, as previously demonstrated in human retinal pigment epithelial cells [194,195]. A known sensor of energy status, AMPKα, has been reported to contribute to VEGF upregulation [196,197]. It is putative that the oxygen fluctuations in the rat OIR model could result to a low-grade, HIF-independent cellular hypoxia with elevated intracellular reactive oxygen species [136,198]that lead to starvation signals and AMPKα-mediated VEGF-A expression.

OIR modulates autophagy in the rat retina and compromises the autophagic flux

Energy deprivation promoted AMPKα activation induces autophagic mechanisms by inhibition of mTOR and a direct phosphorylation of autophagy modulators [106]. Interestingly, here in OIR rats we observed an increase of p-AMPKα and autophagic markers, including LC3-II protein, on both P14 and P18 retinas, with a critical reduction on mTOR pathway protein levels. These findings indicated that the 50/10 OIR protocol leads to an overall increased autophagy in the retina.

Subsequently, to monitor the autophagic flux, we further investigated on p62 protein levels. Upon an induction of the autophagic mechanism, autophagosomes fuse with the lysosomes and p62 protein is degraded [199]. Here, we did not observed a decrease of p62 protein levels in the OIR retina. Collectively, these results would suggest that in OIR rat retinas autophagy is induced, through AMPKα pathway, and proceeds with the elongation and nucleation of autophagosomes, as demonstrated by high LC3 protein levels. Albeit, in this model the autophagolysosome formation is limited by the availability of the terminal lysosomal system, ultimately resulting in an autophagic flux blockade. This hypothesis was confirmed by recent findings, which reported that prolonged stresses induce an increase in autophagosome synthesis and a compromised autolysosomal activity. The increase in autophagophore nucleation into autophagosomes with limited fusion with the lysosomes might be a futile process for autophagy, and thus contribute to cell damage and autophagy-associated cell death mechanisms [200].

Autophagic flux and mechanisms of cell death in the OIR rat retina

An accumulation of autophagosomes has been related with several cell death mechanisms, including necroptotic RIPK-1-mediated mechanism, which can be induced directly by the autophagy machinery [201]. Necroptotic mechanisms have been reported to promote neuronal cell death in neurodegeneration and eye disease [202]. The crosstalk between autophagy and necroptosis has been the focus of multiple studies, although the mechanism is not fully elucidated. Necroptotic mechanisms can be induced upon a block of autophagy flux, through a crosstalk between p62, LC3-II and necroptosis markers, such as RIPK-1 [203]. Moreover, autophagy may occur in association with necroptosis when triggered by apoptotic caspase-mediated inhibition. At a molecular level, upon the activation of apoptosis, the RIPK-1 activity is subject to a tight repression, through Casp-8-mediated cleavage [204].

To better understand a possible correlation between autophagy and mechanisms of cells death, we immunostained rat retina sections for LC3 as an autophagic marker, Casp-8 as an apoptotic marker,

and RIPK-1 as a necroptotic marker. Immunohistofluorescence signals demonstrated an increase of expression of both LC3 and RIPK-1 in GCL, IPL, OPL and OS retinal layers of the OIR retina (Paper IV, Fig.4), in agreement with previous studies in rodent retinas [205]. These findings were accompanied by a predominant expression of Casp-8 in retinal endothelial cells. Unlike to RIPK-1, which was only detected in OIR retinas, the expression of Casp-8 was detected also in retinal endothelial cells of RA rats. It is important to highlight that at these time points the retinal vasculature in rat pups is still developing [206]. The expression of Casp-8 has been reported essential for the proper postnatal retinal vascularization, contributing to the physiological vascular remodeling process, as demonstrated in developing rodent retinas [207].

3-methyladenine reduces autophagic and necroptosis markers in the OIR rat retina

In a rat model of retinal ischemia, an inhibition of autophagy-associated with retinal cell death has been shown to prevent neuronal death following injury [208]. Following the observation that LC3 and RIPK-1 co-expressed in the same retinal layers, we evaluated if inhibition of autophagosomes nucleation with 3-MA [209], could decrease necroptosis in OIR retinas. Interestingly, we observed a notable decrease of both autophagic and necroptotic markers in GCL, IPL, OPL and OS retinal layers in OIR retinas treated with 3-MA, yet no reduction of apoptotic marker was observed in retinal endothelial cells. Taken together, these results suggest that the OIR protocol in rats leads to an induction of autophagy-dependent necroptotic mechanisms in retinal neurons, concomitantly with an increase of apoptotic-autophagy-independent mechanisms in retinal endothelial cells.

3-Methyladenine does not affect retinal function

In retinal diseases, mechanisms of retinal cell death have been correlated with retinal dysfunction and visual loss [210]. Concomitantly with reducing retinal cell death, the inhibition of autophagy has been shown to have a neuroprotective effect and result in a partial recovery of visual impairment [211]. By recording ERG responses to full-field light flashed retinas, we measured retinal function at P18 in order to determine whether the effects of 3-MA on autophagy were accompanied by recovered visual function. Although the treatment with 3-MA reduced necroptosis in retinal cells, visual function was not ameliorated in OIR rats treated with autophagy inhibitor (Paper IV, Fig. 5a –b -c). This controversial result could be associated with the fact that, in OIR retinas, the retinal endothelial cells are still branded by a strong activation of apoptosis. On the other hand, alterative

mechanisms of autophagy-independent cell death might be affecting the neurons' functions, as demonstrated in the neuroretina of diabetic rats [212].Therefore, despite a reduction of necroptosis in retinal cells, retinal function still remains compromised due, for instance, to a dysfunction of retinal neurons involved in the generation of ERG traces.

4.2.2.2 CONCLUDING REMARKS

Collectively, the present study demonstrates an activation of the autophagic pathway correlated with necroptosis in retinal cells of OIR rat pups. In this model, the stress induced by oxygen fluctuations from birth to P14, leads to a retinal energetic starvation, which results in the induction of the autophagic flux, through an activation of the AMPKα pathway. Thus, the autophagy induction initially may act as a survival attempt to restore cellular energy in the retina, yet fails due to a putative impairment of the lysosomal system. This failure leads to an accumulation of autophagosomes, which culminate in the activation of mechanisms of cell death, such as necroptosis, that further affect the retina of OIR rats.

4.2.3 FUTURE PROSPECTIVES

Together, Papers III and IV contribute to deepen the understanding of the role of autophagic processes in the vascular and the neuroretina, both during development and in association with pathology of the rat's retina, such as the OIR protocol. In rats, autophagic mechanisms critically contribute to the physiologic development of the different cell layers of the retina. Nevertheless, in pathological condition, autophagy dysregulation can be related to mechanisms of cell death present in retinal neurons of OIR rats. Thus, the present study supports the concept that negative pharmacological regulation of the autophagy flux may contribute to reduce the mechanisms of cells death that occur in retinal cells exposed to prolonged stress, a condition paralleled in ROP-afflicted preterm babies.

5.CONCLUSION

Nowadays, 2.2 billion people have a vision impairment, among which 3.9 millions are affected by ocular neovascularization diseases (World Health Organization, Feb. 2021). Using blockers of the angiogenic protein VEGF are occurring as a benefit to mitigate ocular vascular disorders, but its limited efficacy remain an outstanding problem. Behind ocular visible manifestations, insidious degenerative changes that consist of cell death of neural cells, have become abundant. The relationship between vascular disorders and neuronal cell death is not fully elucidated and the underlying mechanisms of cell death in the eye are still vastly uncharacterized. Consequently, a deeper understanding of molecular events of vascular disorders with new pharmacologic approaches need to be investigated.

Here, in a contest of pathological angiogenesis, our present studies suggest a rational for UPARANT increased effectiveness when compared with anti-VEGF treatment in various models of iris angiogenesis, indicating a gain of insight in the role of UPARANT in mitigating RI. Furthermore, we demonstrate that the effectiveness of subcutaneous UPARANT administration is in line with systemic treatments of proliferative ocular pathologies, which could improve the treatment of patient afflicted by PDR and NVG.

Lastly, in a contest of mechanisms linked ocular vascular diseases, we suggest the possibility that a pharmacological regulation of the autophagy flux may contribute to reduce neurodegeneration mechanisms that affect the neuroretina of OIR rats exposed to prolonged stress, a condition paralleled in ocular neovascularization diseases.

6. CLINICAL RELEVANCE

As summarized in this thesis, it is evident that ocular diseases have a significant impact on the quality life of a large and increasing number of patients. A study conducted in 2012 reported that people affected of vision impairment are at a high risk to develop depression, anxiety, and other psychological problems [213]. The vision is crucial for health and social well-being. Complete loss or even an impairment in vision can feel frightening and timorous to the ability to maintain independence and employment. Moreover, the costs of ophthalmic medical care are exponential and the risks related to routine treatments can aggravate the visual status.

For all these reasons, population health approaches to improve eye and vision health need to withstand a solid focus on medical care and treatments, that can improve directly and indirectly the quality of a person's life. In the presented works, this thesis proposes arguments for better understanding the molecular and cellular events mediating ocular pathologies and multifactorial treatments as an enhanced strategy to treatment of eye diseases, and ultimately contribute to patients' improved quality of life.

7. ACKNOWLEDGMENTS

First of all, I would like to thank my main supervisor Prof. **Massimo Dal Monte**. You accepted me into your laboratory, giving the opportunity to learn and grow. Thanks for introducing me to the world of the Research. I have found my greatest passion that I heavily hope to keep it!

I would like to thank my co-supervisor Dr. **Helder Andrè**. You accepted me when I was a "baby student" and from that time I learned how to stay in a laboratory. The first years were super challenging and, sometime, very hard; but I never felt alone. You knew when to be my friend or my boss.
From you, I learned that there is always a solution, even if you don't see immediately. Your passion for science really motivated me and got me the strength to never give up. Thanks for your teaching, your constant presence and for the great advice during these years. I will be eternally grateful!

From Pisa, I would like to thank my colleagues. **Alessio Canovai**: your constant work and collaboration were essential for my project in Pisa. The adventure in the "autophagy world" (even if sometimes it has driven us to despair :D) wouldn't have been the same if you weren't there. Thanks for your strong contribution and patience!
Maria Grazia Rossino: when I came in Pisa, I met a colleague but I immediately found a friend. We always have been together when we needed to find a solution, a little comfort and a good word. Thanks for your company, friendship and love.
I would like to thank: **Valeria Pecci**, a friend with whom I shared big laughs and lightless moments. Thanks for making "soft" some heavy day in Pisa!
Also, I would like to thank: **Maurizio Cammalleri**, **Rosario Amato** and Prof. **Giovanni Casini**. Everyone of you have contributed to rich my personal and professional experience.

From Stockholm, I would like to thank my colleague and best friend **Flavia Plastino**. They have been some very intense years and you always have been by my side. With you I spent the best moments during the dark days in Stockholm. Our complicity has been our sun. Thanks for making me feel special and super loved! (I miss you).
I would like to thank all other precious colleagues from Stockholm. **Garik Galustjan, Filippo Locri, Mooud Kavei, Joanna Karayanni** and **Jonathan Bernd**, with whom I shared work, ideas, parties and much food. You all made this year very special. Everyone left me some strong value, which improved my personality and opened my view. Thanks guys for everything!

Alla fine, ma non di importanza, voglio ringraziare la mia **famiglia**. Voglio ringraziare mia madre, la quale è stata sempre presente durante il mio percorso. Le tue preoccupazioni mi hanno sempre fatta sentire al sicuro. Voglio ringraziare mio padre, il quale non smette mai di ricordarmi quanto sia orgoglioso di me. Il tuo orgoglio mi ha fatto superare tante paure e preoccupazioni, regalandomi un briciolo di sicurezza ogni tanto. Grazie a entrambi per avermi sostenuta e dato tanta forza, non basterebbe una vita intera per ringraziarvi!
Voglio ringraziare i miei fratelli che nonostante la lontananza mi hanno sempre fatta sentire una sorella speciale. Il vostro amore mi ha riempito le giornate.
Voglio ringraziare il **mio ragazzo**, il mio compagno di vita e di avventure. Grazie per avermi fatto capire quali sono le cose essenziali della vita. Grazie per avermi regalato tanta motivazione nei momenti più

sconfortanti e tanta forza nei momenti più deboli. Con la tua costante presenza mi sono sentita protetta e invincibile. Mi hai spronata, supportato in tutte le mie scelte, e hai avuto sempre una parola giusta per qualsiasi mio momento. Grazie per quello che hai fatto e continui a fare ogni giorno per me!

Infine, voglio ringraziare **Aurora** e **Luigi**, i miei due fantastici nipoti che in questi anni mi hanno reso la zia più orgogliosa e felice al mondo. Vi amo!

8. REFERENCES

1. Prasad, S. & Galetta, S. L. Anatomy and physiology of the afferent visual system. *Handbook of Clinical Neurology* **102**, 3–19 (2011).

2. Kaplan, H. J. Anatomy and function of the eye. *Chemical Immunology and Allergy* **92**, 4–10 (2007).

3. Aronson, S. B. The uvea. *Archives of ophthalmology* **79**, 490–501 (1968).

4. Boll, P. F. On the anatomy and physiology of the retina. *Vision Research* **17**, 1249–1265 (1977).

5. Luo, X., Shen, Y. M., Jiang, M. N., Lou, X. F. & Shen, Y. Ocular Blood Flow Autoregulation Mechanisms and Methods. *Journal of Ophthalmology* **2015**, 864871 (2015).

6. Weigelin, E. The blood circulation of the retina and the uvea. *Advances in ophthalmology = Fortschritte der Augenheilkunde = Progres en ophtalmologie* **25**, 2–27 (1972).

7. Hayreh, S. S. Orbital vascular anatomy. *Eye* **20**, 1130–1144 (2006).

8. Lutty, G. A. & McLeod, D. S. Development of the hyaloid, choroidal and retinal vasculatures in the fetal human eye. *Progress in Retinal and Eye Research* **62**, 58–76 (2018).

9. Miller, P. E. Uvea. *Slatter's Fundamentals of Veterinary Ophthalmology* 203–229 (2008) doi:10.1016/B978-072160561-6.50014-9.

10. Morrison, J. C. & Michael Van Buskirk, E. Anterior Collateral Circulation in the Primate Eye. *Ophthalmology* **90**, 707–715 (1983).

11. Ormerod, L. D., Fariza, E. & Webb, R. H. Dynamics of external ocular blood flow studied by scanning angiographic microscopy. *Eye (Basingstoke)* **9**, 605–614 (1995).

12. Hayreh, S. S. Posterior ciliary artery circulation in health and disease: The Weisenfeld lecture. *Investigative Ophthalmology and Visual Science* **45**, 749–757 (2004).

13. Song, Y., Song, Y. J. & Ko, M. K. A study of the vascular network of the iris using flat preparation. *Korean journal of ophthalmology : KJO* **23**, 296–300 (2009).

14. Wong-Riley, M. Energy metabolism of the visual system. *Eye and Brain* **2**, 99 (2010).

15. Sun, Y. & Smith, L. E. H. Retinal vasculature in development and diseases. *Annual Review of Vision Science* **4**, 101–122 (2018).

16. Davis, G. E. & Senger, D. R. Endothelial extracellular matrix: Biosynthesis, remodeling, and functions during vascular morphogenesis and neovessel stabilization. *Circulation Research* **97**, 1093–1107 (2005).

17. Fruttiger, M. Development of the retinal vasculature. *Angiogenesis* **10**, 77–88 (2007).

18. Campbell, J. P. *et al.* Detailed Vascular Anatomy of the Human Retina by Projection-Resolved Optical Coherence Tomography Angiography. *Scientific Reports* **7**, 1–11 (2017).

19. Engerman, R. L. & Meyer, R. K. Development of retinal vasculature in rats. *American Journal of Ophthalmology* **60**, 628–641 (1965).

20. Hosoya, K. I. & Tachikawa, M. The inner blood-retinal barrier molecular structure and transport

biology. *Advances in Experimental Medicine and Biology* **763**, 85–104 (2013).

21. McLeod, D. S., Hasegawa, T., Prow, T., Merges, C. & Lutty, G. The initial fetal human retinal vasculature develops by vasculogenesis. *Developmental Dynamics* **235**, 3336–3347 (2006).

22. Hughes, S., Yang, H. & Chan-Ling, T. Vascularization of the human fetal retina: Roles of vasculogenesis and angiogenesis. *Investigative Ophthalmology and Visual Science* **41**, 1217–1228 (2000).

23. Provis, J. M. Development of the primate retinal vasculature. *Progress in Retinal and Eye Research* **20**, 799–821 (2001).

24. Ferguson, J. E., Kelley, R. W. & Patterson, C. Mechanisms of endothelial differentiation in embryonic vasculogenesis. *Arteriosclerosis, Thrombosis, and Vascular Biology* **25**, 2246–2254 (2005).

25. Karamysheva, A. F. Mechanisms of angiogenesis. *Biochemistry (Moscow)* **73**, 751–762 (2008).

26. Chung, A. S. & Ferrara, N. Developmental and Pathological Angiogenesis. *Annual Review of Cell and Developmental Biology* **27**, 563–584 (2011).

27. Matkar, P. N., Ariyagunarajah, R., Leong-Poi, H. & Singh, K. K. Friends turned foes: Angiogenic growth factors beyond angiogenesis. *Biomolecules* **7**, 74 (2017).

28. Carmeliet, P. & Jain, R. K. Molecular mechanisms and clinical applications of angiogenesis. *Nature* **473**, 298–307 (2011).

29. Mentzer, S. J. & Konerding, M. A. Intussusceptive angiogenesis: Expansion and remodeling of microvascular networks. *Angiogenesis* **17**, 499–509 (2014).

30. Burri, P. H., Hlushchuk, R. & Djonov, V. Intussusceptive angiogenesis: Its emergence, its characteristics, and its significance. *Developmental Dynamics* vol. 231 474–488 (2004).

31. Krock, B. L., Skuli, N. & Simon, M. C. Hypoxia-Induced Angiogenesis: Good and Evil. *Genes and Cancer* **2**, 1117–1133 (2011).

32. Faller, D. V. Endothelial cell responses to hypoxic stress. *Clinical and Experimental Pharmacology and Physiology* **26**, 74–84 (1999).

33. Michiels, C., Arnould, T. & Remacle, J. Endothelial cell responses to hypoxia: Initiation of a cascade of cellular interactions. *Biochimica et Biophysica Acta - Molecular Cell Research* **1497**, 1–10 (2000).

34. Gerhardt, H. *et al.* VEGF guides angiogenic sprouting utilizing endothelial tip cell filopodia. *Journal of Cell Biology* **161**, 1163–1177 (2003).

35. Shibuya, M. Vascular Endothelial Growth Factor (VEGF) and Its Receptor (VEGFR) Signaling in Angiogenesis: A Crucial Target for Anti- and Pro-Angiogenic Therapies. *Genes and Cancer* **2**, 1097–1105 (2011).

36. Matsumoto, T. & Claesson-Welsh, L. VEGF receptor signal transduction. *Science's STKE : signal transduction knowledge environment* **2001**, (2001).

37. Roy, H., Bhardwaj, S. & Ylä-Herttuala, S. Biology of vascular endothelial growth factors. *FEBS Letters* **580**, 2879–2887 (2006).

38. Nakazawa, M. S., Keith, B. & Simon, M. C. Oxygen availability and metabolic adaptations. *Nature Reviews Cancer* **16**, 663–673 (2016).

39. Ramakrishnan, S., Anand, V. & Roy, S. Vascular endothelial growth factor signaling in hypoxia and inflammation. *Journal of Neuroimmune Pharmacology* **9**, 142–160 (2014).

40. Stone, J. *et al.* Development of retinal vasculature is mediated by hypoxia-induced vascular endothelial growth factor (VEGF) expression by neuroglia. *Journal of Neuroscience* **15**, 4738–4747 (1995).

41. Corrado, C. & Fontana, S. Hypoxia and HIF signaling: One axis with divergent effects. *International Journal of Molecular Sciences* **21**, 1–17 (2020).

42. Forsythe, J. A. *et al.* Activation of vascular endothelial growth factor gene transcription by hypoxia-inducible factor 1. *Molecular and Cellular Biology* **16**, 4604–4613 (1996).

43. Zimna, A. & Kurpisz, M. Hypoxia-Inducible factor-1 in physiological and pathophysiological angiogenesis: Applications and therapies. *BioMed Research International* **2015**, 549412 (2015).

44. Campochiaro, P. A. Ocular neovascularization. *Journal of molecular medicine (Berlin, Germany)* **91**, 311–321 (2013).

45. Campochiaro, P. A. Ocular neovascularization. *Journal of molecular medicine (Berlin, Germany)* **91**, 311–321 (2013).

46. Campochiaro, P. A. & Hackett, S. F. Ocular neovascularization: A valuable model system. *Oncogene* **22**, 6537–6548 (2003).

47. Jeong, Y. C. & Hwang, Y. H. Etiology and features of eyes with rubeosis iridis among Korean patients: A population-based single center study. *PLoS ONE* **11**, (2016).

48. Gartner, S. & Henkind, P. Neovascularization of the iris (rubeosis iridis). *Survey of Ophthalmology* **22**, 291–312 (1978).

49. Montuori, N. & Ragno, P. Role of uPA/uPAR in the modulation of angiogenesis. *Chemical Immunology and Allergy* **99**, 105–122 (2014).

50. Breuss, J. M. & Uhrin, P. VEGF-initiated angiogenesis and the uPA/uPAR system. *Cell Adhesion and Migration* **6**, 535–540 (2012).

51. de Paulis, A. *et al.* Urokinase Induces Basophil Chemotaxis through a Urokinase Receptor Epitope That Is an Endogenous Ligand for Formyl Peptide Receptor-Like 1 and -Like 2. *The Journal of Immunology* **173**, 5739–5748 (2004).

52. Van Veen, M. *et al.* Negative regulation of uPAR activity by a GPI-specific phospholipase C. doi:10.1101/091272.

53. Montuori, N. & Ragno, P. Multiple activities of a multifaceted receptor: Roles of cleaved and soluble upar. *Frontiers in Bioscience* **14**, 2494–2503 (2009).

54. Cortese, K., Sahores, M., Madsen, C. D., Tacchetti, C. & Blasi, F. Clathrin and LRP-1-independent constitutive endocytosis and recycling of uPAR. *PLoS ONE* **3**, (2008).

55. Ferraris, G. M. S. *et al.* The interaction between uPAR and vitronectin triggers ligand-independent adhesion signalling by integrins . *The EMBO Journal* **33**, 2458–2472 (2014).

56. Smith, H. W. & Marshall, C. J. Regulation of cell signalling by uPAR. *Nature Reviews Molecular Cell Biology* **11**, 23–36 (2010).

57. Jo, M. *et al.* Urokinase receptor primes cells to proliferate in response to epidermal growth factor. *Oncogene* **26**, 2585–2594 (2007).

58. Campbell, I. D. & Humphries, M. J. Integrin structure, activation, and interactions. *Cold Spring Harbor Perspectives in Biology* **3**, 1–14 (2011).

59. Kjøller, L. & Hall, A. Rac mediates cytoskeletal rearrangements and increased cell motility induced by urokinase-type plasminogen activator receptor binding to vitronectin. *Journal of Cell Biology* **152**, 1145–1157 (2001).

60. Madsen, C. D., Ferraris, G. M. S., Andolfo, A., Cunningham, O. & Sidenius, N. uPAR-induced cell adhesion and migration: Vitronectin provides the key. *Journal of Cell Biology* **177**, 927–939 (2007).

61. Gorrasi, A. *et al.* The urokinase receptor takes control of cell migration by recruiting integrins and FPR1 on the cell surface. *PLoS ONE* **9**, 86352 (2014).

62. Eden, G., Archinti, M., Furlan, F., Murphy, R. & Degryse, B. The Urokinase Receptor Interactome. *Current Pharmaceutical Design* **17**, 1874–1889 (2011).

63. Dorward, D. A. *et al.* The role of formylated peptides and formyl peptide receptor 1 in governing neutrophil function during acute inflammation. *American Journal of Pathology* **185**, 1172–1184 (2015).

64. Latini, A., Pereira, P. J. S., Couture, R., Campos, M. M. & Talbot, S. Oxidative Stress: Neuropathy, Excitability, and Neurodegeneration. *Oxidative Medicine and Cellular Longevity* **2019**, (2019).

65. Rivera, J. C. *et al.* Retinopathy of prematurity: Inflammation, choroidal degeneration, and novel promising therapeutic strategies. *Journal of Neuroinflammation* **14**, 1–14 (2017).

66. Yap, T. E., Balendra, S. I., Almonte, M. T. & Cordeiro, M. F. Retinal correlates of neurological disorders. *Therapeutic Advances in Chronic Disease* **10**, 2040622319882205 (2019).

67. Klaassen, I., Van Noorden, C. J. F. & Schlingemann, R. O. Molecular basis of the inner blood-retinal barrier and its breakdown in diabetic macular edema and other pathological conditions. *Progress in Retinal and Eye Research* **34**, 19–48 (2013).

68. Vinores, S. A. Breakdown of the blood-retinal barrier. *Encyclopedia of the Eye* 216–222 (2010) doi:10.1016/B978-0-12-374203-2.00137-8.

69. Fulton, A. B. *et al.* Retinal degenerative and hypoxic ischemic disease. *Documenta Ophthalmologica* **118**, 55–61 (2009).

70. Liu, K., Akula, J. D., Falk, C., Hansen, R. M. & Fulton, A. B. The retinal vasculature and function of the neural retina in a rat model of retinopathy of prematurity. *Investigative Ophthalmology and Visual Science* **47**, 2639–2647 (2006).

71. Zafar, S., Sachdeva, M., Frankfort, B. J. & Channa, R. Retinal Neurodegeneration as an Early Manifestation of Diabetic Eye Disease and Potential Neuroprotective Therapies. *Current Diabetes Reports* **19**, (2019).

72. Trachsel-Moncho, L. *et al.* Oxidative stress and autophagy-related changes during retinal

degeneration and development. *Cell Death and Disease* **9**, 812 (2018).

73. Glick, D., Barth, S. & Macleod, K. F. Autophagy: Cellular and molecular mechanisms. *Journal of Pathology* **221**, 3–12 (2010).

74. Lin, W. & Xu, G. Autophagy: A Role in the Apoptosis, Survival, Inflammation, and Development of the Retina. *Ophthalmic Research* **61**, 65–72 (2019).

75. Schaaf, M. B., Houbaert, D., Meçe, O. & Agostinis, P. Autophagy in endothelial cells and tumor angiogenesis. *Cell Death and Differentiation* **26**, 665–679 (2019).

76. Di Bartolomeo, S., Nazio, F. & Cecconi, F. The Role of Autophagy During Development in Higher Eukaryotes. *Traffic* **11**, 1280–1289 (2010).

77. Levine, B. & Kroemer, G. Autophagy in the Pathogenesis of Disease. *Cell* **132**, 27–42 (2008).

78. Ryter, S. W., Mizumura, K. & Choi, A. M. K. The impact of autophagy on cell death modalities. *International Journal of Cell Biology* **2014**, 502676 (2014).

79. Yonekawa, T. & Thorburn, A. Autophagy and cell death. *Essays in Biochemistry* **55**, 105–117 (2013).

80. Denton, D., Nicolson, S. & Kumar, S. Cell death by autophagy: Facts and apparent artefacts. *Cell Death and Differentiation* **19**, 87–95 (2012).

81. Button, R. W., Roberts, S. L., Willis, T. L., Oliver Hanemann, C. & Luo, S. Accumulation of autophagosomes confers cytotoxicity. *Journal of Biological Chemistry* **292**, 13599–13614 (2017).

82. Kroemer, G. & Levine, B. Autophagic cell death: The story of a misnomer. *Nature Reviews Molecular Cell Biology* **9**, 1004–1010 (2008).

83. Frost, L. S., Mitchell, C. H. & Boesze-Battaglia, K. Autophagy in the eye: Implications for ocular cell health. *Experimental Eye Research* **124**, 56–66 (2014).

84. Fraiberg, M. & Elazar, Z. Genetic defects of autophagy linked to disease. *Progress in Molecular Biology and Translational Science* **172**, 293–323 (2020).

85. Khandia, R. *et al.* A Comprehensive Review of Autophagy and Its Various Roles in Infectious, Non-Infectious, and Lifestyle Diseases: Current Knowledge and Prospects for Disease Prevention, Novel Drug Design, and Therapy. *Cells* **8**, 674 (2019).

86. Yang, X. *et al.* Autophagy and Age-Related Eye Diseases. *BioMed Research International* **2019**, 5763658 (2019).

87. Parzych, K. R. & Klionsky, D. J. An overview of autophagy: Morphology, mechanism, and regulation. *Antioxidants and Redox Signaling* **20**, 460–473 (2014).

88. Wesselborg, S. & Stork, B. Autophagy signal transduction by ATG proteins: From hierarchies to networks. *Cellular and Molecular Life Sciences* **72**, 4721–4757 (2015).

89. Wong, P. M., Puente, C., Ganley, I. G. & Jiang, X. The ULK1 complex sensing nutrient signals for autophagy activation. *Autophagy* **9**, 124–137 (2013).

90. Kabeya, Y. *et al.* Atg17 functions in cooperation with Atg1 and Atg13 in yeast autophagy. *Molecular Biology of the Cell* **16**, 2544–2553 (2005).

91. Pyo, J. O., Nah, J. & Jung, Y. K. Molecules and their functions in autophagy. *Experimental and Molecular Medicine* **44**, 73–80 (2012).

92. Simonsen, A. & Tooze, S. A. Coordination of membrane events during autophagy by multiple class III PI3-kinase complexes. *Journal of Cell Biology* **186**, 773–782 (2009).

93. Metlagel, Z., Otomo, C., Takaesu, G. & Otomo, T. Structural basis of ATG3 recognition by the autophagic ubiquitin-like protein ATG12. **110**, 18844–18849 (2013).

94. Tanida, I., Ueno, T. & Kominami, E. LC3 and autophagy. *Methods in Molecular Biology* **445**, 77–88 (2008).

95. Itakura, E. & Mizushima, N. p62 targeting to the autophagosome formation site requires self-oligomerization but not LC3 binding. *Journal of Cell Biology* **192**, 17–27 (2011).

96. Wurzer, B. *et al.* Oligomerization of p62 allows for selection of ubiquitinated cargo and isolation membrane during selective autophagy. *eLife* **4**, (2015).

97. Yoshii, S. R. & Mizushima, N. Monitoring and measuring autophagy. *International Journal of Molecular Sciences* **18**, 1865 (2017).

98. Fader, C. M. & Colombo, M. I. Autophagy and multivesicular bodies: Two closely related partners. *Cell Death and Differentiation* **16**, 70–78 (2009).

99. Jung, C. H., Ro, S. H., Cao, J., Otto, N. M. & Kim, D. H. MTOR regulation of autophagy. *FEBS Letters* **584**, 1287–1295 (2010).

100. Dunlop, E. A. & Tee, A. R. MTOR and autophagy: A dynamic relationship governed by nutrients and energy. *Seminars in Cell and Developmental Biology* **36**, 121–129 (2014).

101. Vadlakonda, L., Dash, A., Pasupuleti, M., Kumar, K. A. & Reddanna, P. The paradox of Akt-mTOR interactions. *Frontiers in Oncology* **3 JUN**, 165 (2013).

102. Bach, M., Larance, M., James, D. E. & Ramm, G. The serine/threonine kinase ULK1 is a target of multiple phosphorylation events. *Biochemical Journal* **440**, 283–291 (2011).

103. Showkat, M., Beigh, M. A. & Andrabi, K. I. mTOR Signaling in Protein Translation Regulation: Implications in Cancer Genesis and Therapeutic Interventions. *Molecular Biology International* **2014**, 1–14 (2014).

104. Jin, B., Shi, H., Zhu, J., Wu, B. & Geshang, Q. Up-regulating autophagy by targeting the mTOR-4EBP1 pathway: A possible mechanism for improving cardiac function in mice with experimental dilated cardiomyopathy. *BMC Cardiovascular Disorders* **20**, 1–7 (2020).

105. Blommaart, E. F. C., Luiken, J. J. F. P., Blommaart, P. J. E., Van Woerkom, G. M. & Meijer, A. J. Phosphorylation of ribosomal protein S6 is inhibitory for autophagy in isolated rat hepatocytes. *Journal of Biological Chemistry* **270**, 2320–2326 (1995).

106. Kim, J., Kundu, M., Viollet, B. & Guan, K. L. AMPK and mTOR regulate autophagy through direct phosphorylation of Ulk1. *Nature Cell Biology* **13**, 132–141 (2011).

107. Alers, S., Loffler, A. S., Wesselborg, S. & Stork, B. Role of AMPK-mTOR-Ulk1/2 in the Regulation of Autophagy: Cross Talk, Shortcuts, and Feedbacks. *Molecular and Cellular Biology* **32**, 2–11 (2012).

108. Loos, B., Hofmeyr, J. H. S., Müller-Nedebock, K., Boonzaaier, L. & Kinnear, C. Autophagic

Flux, Fusion Dynamics, and Cell Death. *Autophagy: Cancer, Other Pathologies, Inflammation, Immunity, Infection, and Aging* **3**, 39–56 (2014).

109. Galluzzi, L. *et al.* Life, death and burial: Multifaceted impact of autophagy. *Biochemical Society Transactions* **36**, 786–790 (2008).

110. Maiuri, M. *et al.* To Die or Not to Die: That is the Autophagic Question. *Current Molecular Medicine* **8**, 78–91 (2008).

111. Jung, S., Jeong, H. & Yu, S. W. Autophagy as a decisive process for cell death. *Experimental and Molecular Medicine* **52**, 921–930 (2020).

112. Bialik, S., Dasari, S. K. & Kimchi, A. Autophagy-dependent cell death - where, how and why a cell eats itself to death. *Journal of Cell Science* **131**, 215152 (2018).

113. Oberst, A. Autophagic cell death RIPs into tumors. *Cell Death and Differentiation* **20**, 1131–1132 (2013).

114. Galluzzi, L. *et al.* Molecular mechanisms of cell death: Recommendations of the Nomenclature Committee on Cell Death 2018. *Cell Death and Differentiation* **25**, 486–541 (2018).

115. Reed, J. C. Warner-Lambert/Parke Davis award lecture: Mechanisms of apoptosis. *American Journal of Pathology* **157**, 1415–1430 (2000).

116. Zhou, W. & Yuan, J. Necroptosis in health and diseases. *Seminars in Cell and Developmental Biology* **35**, 14–23 (2014).

117. Mathew, R., Karantza-Wadsworth, V. & White, E. Role of autophagy in cancer. *Nature Reviews Cancer* **7**, 961–967 (2007).

118. Thorburn, A. Apoptosis and autophagy: Regulatory connections between two supposedly different processes. *Apoptosis* **13**, 1–9 (2008).

119. Goodall, M. L. *et al.* The Autophagy Machinery Controls Cell Death Switching between Apoptosis and Necroptosis. *Developmental Cell* **37**, 337–349 (2016).

120. Loos, B., Engelbrecht, A. M., Lockshin, R. A., Klionsky, D. J. & Zakeri, Z. The variability of autophagy and cell death susceptibility: Unanswered questions. *Autophagy* **9**, 1270–1285 (2013).

121. Nikoletopoulou, V., Markaki, M., Palikaras, K. & Tavernarakis, N. Crosstalk between apoptosis, necrosis and autophagy. *Biochimica et biophysica acta* **1833**, 3448–3459 (2013).

122. Chen, Q., Kang, J. & Fu, C. The independence of and associations among apoptosis, autophagy, and necrosis. *Signal Transduction and Targeted Therapy* **3**, (2018).

123. Trachsel-Moncho, L. *et al.* Oxidative stress and autophagy-related changes during retinal degeneration and development. *Cell Death and Disease* **9**, 812 (2018).

124. Park, H. Y. L., Kim, J. H. & Park, C. K. Activation of autophagy induces retinal ganglion cell death in a chronic hypertensive glaucoma model. *Cell Death and Disease* **3**, e290 (2012).

125. Fogli, S. *et al.* Clinical pharmacology of intravitreal anti-VEGF drugs. *Eye (Basingstoke)* **32**, 1010–1020 (2018).

126. Muqit, M. M. K. *et al.* Study of clinical applications and safety for Pascal® laser photocoagulation in retinal vascular disorders. *Acta Ophthalmologica* **90**, 155–161 (2012).

127. Kapany, N. S., Peppers, N. A., Zweng, H. C. & Flocks, M. Retinal photocoagulation by lasers. *Nature* **199**, 146–149 (1963).

128. Deschler, E. K., Sun, J. K. & Silva, P. S. Side-effects and complications of laser treatment in diabetic retinal disease. *Seminars in Ophthalmology* **29**, 290–300 (2014).

129. Fong, D. S., Girach, A. & Boney, A. Visual side effects of successful scatter laser photocoagulation surgery for proliferative diabetic retinopathy: A literature review. *Retina* **27**, 816–824 (2007).

130. Reibaldi, M. *et al.* Risk of Death Associated with Intravitreal Anti-Vascular Endothelial Growth Factor Therapy: A Systematic Review and Meta-analysis. *JAMA Ophthalmology* **138**, 50–57 (2020).

131. Falavarjani, K. G. & Nguyen, Q. D. Adverse events and complications associated with intravitreal injection of anti-VEGF agents: A review of literature. *Eye (Basingstoke)* **27**, 787–794 (2013).

132. Avery, R. L. *et al.* Systemic pharmacokinetics and pharmacodynamics of intravitreal aflibercept, bevacizumab, and ranibizumab. *Retina* **37**, 1847–1858 (2017).

133. Hirano, T., Toriyama, Y., Iesato, Y., Imai, A. & Murata, T. Changes in plasma vascular endothelial growth factor level after intravitreal injection of bevacizumab, aflibercept, or ranibizumab for diabetic macular edema. *Retina* **38**, 1801–1808 (2018).

134. Romano, M. R. *et al.* Effects of bevacizumab on neuronal viability of retinal ganglion cells in rats. *Brain Research* **1478**, 55–63 (2012).

135. Azzouz, M. *et al.* VEGF delivery with retrogradely transported lentivector prolongs survival in a mouse ALS model. *Nature* **429**, 413–417 (2004).

136. Chinskey, N. D., Besirli, C. G. & Zacks, D. N. Retinal cell death and current strategies in retinal neuroprotection. *Current Opinion in Ophthalmology* **25**, 228–233 (2014).

137. Breuss, J. M. & Uhrin, P. VEGF-initiated angiogenesis and the uPA/uPAR system. *Cell Adhesion and Migration* **6**, 535–540 (2012).

138. Yang, H., Yu, P. K., Cringle, S. J., Sun, X. & Yu, D.-Y. Iridal vasculature and the vital roles of the iris. *Journal of Nature and Science* **1**, 157 (2015).

139. Motta, C. *et al.* Molecular mechanisms mediating antiangiogenic action of the urokinase receptor-derived peptide UPARANT in human retinal endothelial cells. *Investigative Ophthalmology and Visual Science* **57**, 5723–5735 (2016).

140. Bifulco, K. *et al.* An urokinase receptor antagonist that inhibits cell migration by blocking the formyl peptide receptor. *FEBS Letters* **582**, 1141–1146 (2008).

141. Carriero, M. V. *et al.* Structure-based design of an urokinase-type plasminogen activator receptor-derived peptide inhibiting cell migration and lung metastasis. *Molecular Cancer Therapeutics* **8**, 2708–2717 (2009).

142. Noh, H., Hong, S. & Huang, S. Role of urokinase receptor in tumor progression and development. *Theranostics* **3**, 487–495 (2013).

143. Gorrasi, A. *et al.* New Pieces in the Puzzle of uPAR Role in Cell Migration Mechanisms. *Cells* **9**, 2531 (2020).

144. Locri, F. *et al.* UPARANT is an effective antiangiogenic agent in a mouse model of rubeosis iridis. *Journal of Molecular Medicine* **97**, 1273–1283 (2019).

145. Mohan, N., Monickaraj, F., Balasubramanyam, M., Rema, M. & Mohan, V. Imbalanced levels of angiogenic and angiostatic factors in vitreous, plasma and postmortem retinal tissue of patients with proliferative diabetic retinopathy. *Journal of Diabetes and its Complications* **26**, 435–441 (2012).

146. Kovacs, K. *et al.* Angiogenic and inflammatory vitreous biomarkers associated with increasing levels of retinal ischemia. *Investigative Ophthalmology and Visual Science* **56**, 6523–6530 (2015).

147. Domigan, C. K., Ziyad, S. & Luisa Iruela-Arispe, M. Canonical and noncanonical vascular endothelial growth factor pathways: New developments in biology and signal transduction. *Arteriosclerosis, Thrombosis, and Vascular Biology* **35**, 30–39 (2015).

148. Al-Kharashi, A. S. Role of oxidative stress, inflammation, hypoxia and angiogenesis in the development of diabetic retinopathy. *Saudi Journal of Ophthalmology* **32**, 318–323 (2018).

149. Li, Y. & Zhou, Y. Interleukin-17: The role for pathological angiogenesis in ocular neovascular diseases. *Tohoku Journal of Experimental Medicine* **247**, 87–98 (2019).

150. Xu, J. J., Li, Y. M. & Hong, J. X. Progress of anti-vascular endothelial growth factor therapy for ocular neovascular disease: Benefits and challenges. *Chinese Medical Journal* **127**, 1550–1557 (2014).

151. Cammalleri, M. *et al.* The uPAR System as a Potential Therapeutic Target in the Diseased Eye. *Cells* **8**, 925 (2019).

152. Locri, F. *et al.* Gaining insight on mitigation of rubeosis iridis by UPARANT in a mouse model associated with proliferative retinopathy. *Journal of Molecular Medicine* **98**, 1629–1638 (2020).

153. Beaujean, O., Locri, F., Aronsson, M., Kvanta, A. & André, H. A novel in vivo model of puncture-induced iris neovascularization. *PLoS ONE* **12**, e0180235 (2017).

154. Van Cruijsen, H., Giaccone, G. & Hoekman, K. Epidermal growth factor receptor and angiogenesis: Opportunities for combined anticancer strategies. *International Journal of Cancer* **117**, 883–888 (2005).

155. Aguirre Ghiso, J. A. Inhibition of FAK signaling activated by urokinase receptor induces dormancy in human carcinoma cells in vivo. *Oncogene* **21**, 2513–2524 (2002).

156. Lakka, S. S., Gondi, C. S. & Rao, J. S. Proteases and glioma angiogenesis. *Brain Pathology* **15**, 327–341 (2005).

157. Cuenda, A. & Rousseau, S. p38 MAP-Kinases pathway regulation, function and role in human diseases. *Biochimica et Biophysica Acta - Molecular Cell Research* **1773**, 1358–1375 (2007).

158. Dodeller, F. & Schulze-Koops, H. The p38 mitogen-activated protein kinase signaling cascade in CD4 T cells. *Arthritis Research and Therapy* **8**, 205 (2006).

159. Kozlova, N., Jensen, J. K., Chi, T. F., Samoylenko, A. & Kietzmann, T. PAI-1 modulates cell migration in a LRP1-dependent manner via β-catenin and ERK1/2. *Thrombosis and Haemostasis* **113**, 988–998 (2015).

160. Palmieri, D., Lee, J. W., Juliano, R. L. & Church, F. C. Plasminogen activator inhibitor-1 and -3 increase cell adhesion and motility of MDA-MB-435 breast cancer cells. *Journal of Biological*

Chemistry **277**, 40950–40957 (2002).

161. Uhrin, P. & Breuss, J. M. uPAR: A modulator of VEGF-induced angiogenesis. *Cell Adhesion and Migration* **7**, 23–26 (2013).

162. Kamikubo, Y., Neels, J. G. & Degryse, B. Vitronectin inhibits plasminogen activator inhibitor-1-induced signalling and chemotaxis by blocking plasminogen activator inhibitor-1 binding to the low-density lipoprotein receptor-related protein. *International Journal of Biochemistry and Cell Biology* **41**, 578–585 (2009).

163. Wu, L. & Gonias, S. L. The low-density lipoprotein receptor-related protein-1 associates transiently with lipid rafts. *Journal of Cellular Biochemistry* **96**, 1021–1033 (2005).

164. L. Gonias, S., Gaultier, A. & Jo, M. Regulation of the Urokinase Receptor (uPAR) by LDL Receptor-related Protein-1 (LRP1). *Current Pharmaceutical Design* **17**, 1962–1969 (2011).

165. Kovacs, K. *et al.* Angiogenic and inflammatory vitreous biomarkers associated with increasing levels of retinal ischemia. *Investigative Ophthalmology and Visual Science* **56**, 6523–6530 (2015).

166. Takei, A. *et al.* Gene Transfer of Prolyl Hydroxylase Domain 2 Inhibits Hypoxia-inducible Angiogenesis in a Model of Choroidal Neovascularization. *Scientific Reports* **7**, 42546 (2017).

167. Locri, F., Aronsson, M., Beaujean, O., Kvanta, A. & André, H. Puncture-induced iris neovascularization as a mouse model of rubeosis iridis. *Journal of Visualized Experiments* **2018**, (2018).

168. Cammalleri, M. *et al.* The urokinase receptor-derived peptide UPARANT mitigates angiogenesis in a mouse model of laser-induced choroidal neovascularization. *Investigative Ophthalmology and Visual Science* **57**, 2600–2611 (2016).

169. Cammalleri, M. *et al.* The urokinase receptor-derived peptide UPARANT recovers dysfunctional electroretinogram and blood-retinal barrier leakage in a rat model of diabetes. *Investigative Ophthalmology and Visual Science* **58**, 3138–3148 (2017).

170. Cammalleri, M. *et al.* Diabetic Retinopathy in the Spontaneously Diabetic Torii Rat: Pathogenetic Mechanisms and Preventive Efficacy of Inhibiting the Urokinase-Type Plasminogen Activator Receptor System. *Journal of Diabetes Research* **2017**, 2904150 (2017).

171. Locri, F. *et al.* UPARANT is an effective antiangiogenic agent in a mouse model of rubeosis iridis. *Journal of Molecular Medicine* **97**, 1273–1283 (2019).

172. Prevete, N., Liotti, F., Marone, G., Melillo, R. M. & De Paulis, A. Formyl peptide receptors at the interface of inflammation, angiogenesis and tumor growth. *Pharmacological Research* **102**, 184–191 (2015).

173. Tilborghs, S. *et al.* The role of Nuclear Factor-kappa B signaling in human cervical cancer. *Critical Reviews in Oncology/Hematology* **120**, 141–150 (2017).

174. Swamynathan, S., Loughner, C. L. & Swamynathan, S. K. Inhibition of HUVEC tube formation via suppression of NFκB suggests an anti-angiogenic role for SLURP1 in the transparent cornea. *Experimental Eye Research* **164**, 118–128 (2017).

175. Gheith, M. E., Siam, G. A., Monteiro De Barros, D. S., Garg, S. J. & Moster, M. R. Role of intravitreal bevacizumab in neovascular glaucoma. *Journal of Ocular Pharmacology and Therapeutics* **23**, 487–491 (2007).

176. Inagaki, K., Koga, H., Inoue, K., Suzuki, K. & Suzuki, H. Spontaneous intraocular hemorrhage in rats during postnatal ocular development. *Comparative Medicine* **64**, 34–43 (2014).

177. Kim, Y. *et al.* In vivo imaging of the hyaloid vascular regression and retinal and choroidal vascular development in rat eyes using optical coherence tomography angiography. *Scientific Reports* **10**, 12901 (2020).

178. Cairns, J. E. Normal development of the hyaloid and retinal vessels in the rat. *British Journal of Ophthalmology* **43**, 385–393 (1959).

179. Díaz-Coránguez, M., Ramos, C. & Antonetti, D. A. The inner blood-retinal barrier: Cellular basis and development. *Vision Research* **139**, 123–137 (2017).

180. Campbell, M. & Humphries, P. The blood-retina barrier tight junctions and barrier modulation. *Advances in Experimental Medicine and Biology* **763**, 70–84 (2013).

181. Krock, B. L., Skuli, N. & Simon, M. C. Hypoxia-Induced Angiogenesis: Good and Evil. *Genes and Cancer* **2**, 1117–1133 (2011).

182. Rattner, A., Williams, J. & Nathans, J. Roles of HIFs and VEGF in angiogenesis in the retina and brain. *Journal of Clinical Investigation* **129**, 3807–3820 (2019).

183. Di Bartolomeo, S., Nazio, F. & Cecconi, F. The Role of Autophagy During Development in Higher Eukaryotes. *Traffic* **11**, 1280–1289 (2010).

184. Nussenzweig, S. C., Verma, S. & Finkel, T. The role of autophagy in vascular biology. *Circulation Research* **116**, 480–488 (2015).

185. Mazure, N. M. & Pouysségur, J. Hypoxia-induced autophagy: Cell death or cell survival? *Current Opinion in Cell Biology* **22**, 177–180 (2010).

186. Dengler, F. Activation of ampk under hypoxia: Many roads leading to rome. *International Journal of Molecular Sciences* **21**, 2428 (2020).

187. Penn, J. S., Henry, M. M., Wall, P. T. & Tolman, B. L. The range of PaO2 variation determines the severity of oxygen-induced retinopathy in newborn rats. *Investigative Ophthalmology and Visual Science* **36**, 2063–2070 (1995).

188. Wilson, A. & Sapieha, P. Neurons and guidance cues in retinal vascular diseases. *Oncotarget* **7**, 9618–9619 (2016).

189. Li, R. *et al.* Effect(s) of Preterm Birth on Normal Retinal Vascular Development and Oxygen-Induced Retinopathy in the Neonatal Rat. *Current Eye Research* **38**, 1266–1273 (2013).

190. Higgins, R. D. Oxygen Saturation and Retinopathy of Prematurity. *Clinics in Perinatology* **46**, 593–599 (2019).

191. Hartmann, J. S. *et al.* Expression of vascular endothelial growth factor and pigment epithelial-derived factor in a rat model of retinopathy of prematurity. *Molecular Vision* **17**, 1577–1587 (2011).

192. Chung, A. S. & Ferrara, N. Developmental and Pathological Angiogenesis. *Annual Review of Cell and Developmental Biology* **27**, 563–584 (2011).

193. Soetikno, B. T. *et al.* Inner retinal oxygen metabolism in the 50/10 oxygen-induced retinopathy model. *Scientific Reports* **5**, (2015).

194. Kuroki, M. *et al.* Reactive Oxygen Intermediates Increase VEGF Expression Reactive Oxygen Intermediates Increase Vascular Endothelial Growth Factor Expression In Vitro and In Vivo. *J. Clin. Invest* **98**, 1667–1675 (1996).

195. Berra, E., Pagès, G. & Pouysségur, J. MAP kinases and hypoxia in the control of VEGF expression. *Cancer and Metastasis Reviews* **19**, 139–145 (2000).

196. Nagata, D., Mogi, M. & Walsh, K. AMP-activated protein kinase (AMPK) signaling in endothelial cells is essential for angiogenesis in response to hypoxic stress. *Journal of Biological Chemistry* **278**, 31000–31006 (2003).

197. Reihill, J. A., Ewart, M. A. & Salt, I. P. The role of AMP-activated protein kinase in the functional effects of vascular endothelial growth factor-A and -B in human aortic endothelial cells. *Vascular Cell* **3**, 9 (2011).

198. Moreno, M.-L., Mérida, S., Bosch-Morell, F., Miranda, M. & Villar, V. M. Autophagy Dysfunction and Oxidative Stress, Two Related Mechanisms Implicated in Retinitis Pigmentosa. *Frontiers in Physiology* **9**, 1008 (2018).

199. Liu, W. J. *et al.* p62 links the autophagy pathway and the ubiqutin-proteasome system upon ubiquitinated protein degradation. *Cellular and Molecular Biology Letters* **21**, 29 (2016).

200. Settembre, C. *et al.* A block of autophagy in lysosomal storage disorders. *Human Molecular Genetics* **17**, 119–129 (2008).

201. Chaabane, W. *et al.* Autophagy, apoptosis, mitoptosis and necrosis: Interdependence between those pathways and effects on cancer. *Archivum Immunologiae et Therapiae Experimentalis* **61**, 43–58 (2013).

202. Zhang, S., Tang, M. B., Luo, H. Y., Shi, C. H. & Xu, Y. M. Necroptosis in neurodegenerative diseases: a potential therapeutic target. *Cell death & disease* **8**, e2905 (2017).

203. Sanz, L., Sanchez, P., Lallena, M. J., Diaz-Meco, M. T. & Moscat, J. The interaction of p62 with RIP links the atypical PKCs to NF-κB activation. *EMBO Journal* **18**, 3044–3053 (1999).

204. Liccardi, G. *et al.* RIPK1 and Caspase-8 Ensure Chromosome Stability Independently of Their Role in Cell Death and Inflammation. *Molecular Cell* **73**, 413-428.e7 (2019).

205. Pesce, N. A. *et al.* Autophagy Involvement in the Postnatal Development of the Rat Retina. *Cells* **10**, 177 (2021).

206. Engerman, R. L. & Meyer, R. K. Development of retinal vasculature in rats. *American Journal of Ophthalmology* **60**, 628–641 (1965).

207. Tisch, N. *et al.* Caspase-8 modulates physiological and pathological angiogenesis during retina development. *Journal of Clinical Investigation* **129**, 5092–5107 (2019).

208. Piras, A., Gianetto, D., Conte, D., Bosone, A. & Vercelli, A. Activation of Autophagy in a Rat Model of Retinal Ischemia following High Intraocular Pressure. *PLoS ONE* **6**, e22514 (2011).

209. Vlahos, C. J., Matter, W. F., Hui, K. Y. & Brown, R. F. A specific inhibitor of phosphatidylinositol 3-kinase, 2-(4-morpholinyl)- 8-phenyl-4H-1-benzopyran-4-one (LY294002). *Journal of Biological Chemistry* **269**, 5241–5248 (1994).

210. Murakami, Y. *et al.* Photoreceptor cell death and rescue in retinal detachment and degenerations. *Progress in Retinal and Eye Research* **37**, 114–140 (2013).

211. Zaninello, M. *et al.* Inhibition of autophagy curtails visual loss in a model of autosomal dominant optic atrophy. *Nature Communications* **11**, 1–12 (2020).

212. Kurihara, T. *et al.* Angiotensin II type 1 receptor signaling contributes to synaptophysin degradation and neuronal dysfunction in the diabetic retina. *Diabetes* **57**, 2191–2198 (2008).

213. Kempen, G. I. J. M., Ballemans, J., Ranchor, A. V., Van Rens, G. H. M. B. & Zijlstra, G. A. R. The impact of low vision on activities of daily living, symptoms of depression, feelings of anxiety and social support in community-living older adults seeking vision rehabilitation services. *Quality of Life Research* **21**, 1405–1411 (2012).

214. Ucuzian, A. A., Gassman, A. A., East, A. T. & Greisler, H. P. Molecular mediators of angiogenesis. *Journal of Burn Care and Research* **31**, 158–175 (2010).

215. Neve, A., Cantatore, F. P., Maruotti, N., Corrado, A. & Ribatti, D. Extracellular matrix modulates angiogenesis in physiological and pathological conditions. *BioMed Research International* **2014**, 756078 (2014).

216. Fine, H. F., Despotidis, G. D. & Prenner, J. L. Ocular inflammation associated with antivascular endothelial growth factor treatment. *Current Opinion in Ophthalmology* **26**, 184–187 (2015).

217. Carriero, M. V. *et al.* Structure-based design of an urokinase-type plasminogen activator receptor-derived peptide inhibiting cell migration and lung metastasis. *Molecular Cancer Therapeutics* **8**, 2708–2717 (2009).

218. Carriero, M. V. *et al.* UPARANT: A urokinase receptor-derived peptide inhibitor of VEGF-driven angiogenesis with enhanced stability and in vitro and in vivo potency. *Molecular Cancer Therapeutics* **13**, 1092–1104 (2014).

219. Dal Monte, M. *et al.* Antiangiogenic effectiveness of the urokinase receptor- derived peptide UPARANT in a model of oxygen-induced retinopathy. *Investigative Ophthalmology and Visual Science* **56**, 2392–2407 (2015).

220. Schnichels, S. *et al.* Comparative toxicity and proliferation testing of aflibercept, bevacizumab and ranibizumab on different ocular cells. *British Journal of Ophthalmology* **97**, 917–923 (2013).

221. Zudaire, E., Gambardella, L., Kurcz, C. & Vermeren, S. A computational tool for quantitative analysis of vascular networks. *PLoS ONE* **6**, e27385 (2011).

222. Leoni, G., Neumann, P. A., Sumagin, R., Denning, T. L. & Nusrat, A. Wound repair: Role of immune-epithelial interactions. *Mucosal Immunology* **8**, 959–968 (2015).

223. Carriero, M. V. *et al.* UPARANT: A urokinase receptor-derived peptide inhibitor of VEGF-driven angiogenesis with enhanced stability and in vitro and in vivo potency. *Molecular Cancer Therapeutics* **13**, 1092–1104 (2014).

224. Kotecha, A. *et al.* Intravitreal bevacizumab in refractory neovascular glaucoma: A prospective, observational case series. *Archives of Ophthalmology* **129**, 145–150 (2011).

225. Wong-Riley, M. Energy metabolism of the visual system. *Eye and Brain* **2**, 99 (2010).

226. Selvam, S., Kumar, T. & Fruttiger, M. Retinal vasculature development in health and disease. *Progress in Retinal and Eye Research* **63**, 1–19 (2018).

227. Dogra, M. R., Katoch, D. & Dogra, M. An Update on Retinopathy of Prematurity (ROP). *Indian Journal of Pediatrics* **84**, 930–936 (2017).

228. Higgins, R. D. Oxygen Saturation and Retinopathy of Prematurity. *Clinics in Perinatology* **46**, 593–599 (2019).

229. Hansen, R. M., Moskowitz, A., Akula, J. D. & Fulton, A. B. The neural retina in retinopathy of prematurity. *Progress in Retinal and Eye Research* **56**, 32–57 (2017).

230. Rivera, J. C. *et al.* Understanding retinopathy of prematurity: Update on pathogenesis. *Neonatology* **100**, 343–353 (2011).

231. Amirkavei, M. *et al.* Induction of heat shock protein 70 in mouse RPE as an in vivo model of transpupillary thermal stimulation. *International Journal of Molecular Sciences* **21**, (2020).

232. Stone, J. *et al.* Development of Retinal Vasculature Is Mediated by Hypoxia-Induced Vascular Endothelial Growth Factor (VEGF) Expression by Neuroglia. *The Journal of Neuroscience* **15**, 4738–4747 (1995).

233. Fulton, A. B., Hansen, R. M., Moskowitz, A. & Akula, J. D. The neurovascular retina in retinopathy of prematurity. *Progress in Retinal and Eye Research* **28**, 452–482 (2009).

234. Robson, J. G., Saszik, S. M., Ahmed, J. & Frishman, L. J. Rod and cone contributions to the a-wave of the electroretinogram of the macaque. *Journal of Physiology* **547**, 509–530 (2003).

235. Melincovici, C. S. *et al.* Vascular endothelial growth factor (VEGF) – key factor in normal and pathological angiogenesis. *Romanian Journal of Morphology and Embryology* **59**, 455–467 (2018).

236. Tanida, I. & Waguri, S. Measurement of autophagy in cells and tissues. *Methods in Molecular Biology* **648**, 193–214 (2010).

237. Tanida, I., Ueno, T. & Kominami, E. LC3 and autophagy. *Methods in Molecular Biology* **445**, 77–88 (2008).

238. Elizabeth Hartnett, M. The effects of oxygen stresses on the development of features of severe retinopathy of prematurity: Knowledge from the 50/10 OIR model. *Documenta Ophthalmologica* **120**, 25–39 (2010).

239. Chen, J. & Smith, L. E. H. Retinopathy of prematurity. *Angiogenesis* **10**, 133–140 (2007).

240. Mitter, S. K. & Boulton, M. E. Autophagy in Ocular Pathophysiology. *Autophagy in Current Trends in Cellular Physiology and Pathology* (2016) doi:10.5772/64667.

241. Cammalleri, M. *et al.* The beta adrenergic receptor blocker propranolol counteracts retinal dysfunction in a mouse model of oxygen induced retinopathy: Restoring the balance between apoptosis and autopha. *Frontiers in Cellular Neuroscience* **11**, (2017).

242. Amato, R. *et al.* Autophagy-mediated neuroprotection induced by octreotide in an ex vivo model of early diabetic retinopathy. *Pharmacological Research* **128**, 167–178 (2018).

References of Figures

Figure 1A: Adapted from: Anatomy of the Eye, Chapter: "*Essentials of Anatomy and Physiology: Senses*". brainkart.com/article/Anatomy-of-the-Eye_21840/.

Figure 1B: Adapted from: Anatomy & Physiology; connexions web site: cnx.org/content/col11496/1.6/. Jun 19, 2013.

Figure 1C: Adapted from: Newman EA. Functional hyperemia and mechanisms of neurovascular coupling in the retinal vasculature. J Cereb Blood Flow Metab. 2013 Nov;33(11):1685-95. doi: 10.1038/jcbfm.2013.145. Epub 2013 Aug 21. PMID: 23963372; PMCID: PMC3824187**.**

Figure 1D: Adapted from: Henry Vandyke Carter Henry Gray(1918) *Anatomy of the Human Body* (See "Book" section Bartleby.com:Gray's Anatomy,Plate 878).

Figure 2: Adapted from: Plastino F, Pesce NA, André H. MicroRNAs and the HIF/VEGF axis in ocular neovascular diseases. Acta Ophthalmol. 2021 Mar 17. doi: 10.1111/aos.14845. Epub ahead of print. PMID: 33729690.

Figure 3: Adapted from: Binder BR, Mihaly J, Prager GW. uPAR-uPA-PAI-1 interactions and signaling: a vascular biologist's view. Thromb Haemost. 2007 Mar;97(3):336-42. PMID: 17334498.

Figure 4: Adapted from: Hansen M, Rubinsztein DC, Walker DW. Autophagy as a promoter of longevity: insights from model organisms. Nat Rev Mol Cell Biol. 2018 Sep;19(9):579-593. doi: 10.1038/s41580-018-0033-y. Erratum in: Nat Rev Mol Cell Biol. 2018 Jul 25; PMID: 30006559.

PAPER I

UPARANT mitigates human iris angiogenesis through uPAR/LRP-1 interaction in an organotypic *ex vivo* model

Noemi A. Pesce[1,2], Filippo Locri[1], Flavia Plastino[1], Vincenzo Pavone[3], Anders Kvanta[1], Massimo Dal Monte[2], Helder André[1]*

[1]Department of Clinical Neuroscience, Division of Eye and Vision, St Erik Eye Hospital, Karolinska Institutet, Stockholm, Sweden.

[2]Department of Biology, University of Pisa, Pisa, Italy.

[3]Department of Chemical Sciences, University of Naples Federico II, Naples, Italy.

ABSTRACT

Rubeosis Iridis (RI) is characterized by an increase in neovascularization and inflammation factors in the iris. During angiogenesis, the urokinase plasminogen activator (uPA) and its receptor (uPAR) play a pivotal role in extracellular matrix remodeling, where uPAR regulates endothelial cell migration and proliferation through assembly with transmembrane receptors. Here, in a context of hypoxia-induced angiogenesis, the antagonist effects of UPARANT onto the uPA/uPAR system were investigated using a novel *ex vivo* human iris organotypic angiogenesis assay. UPARANT anti-angiogenic effects, in the new humanized model of ocular pathologic angiogenesis, was analyzed by transcript (quantitative PCR) and protein assays (western and dot blots, and co-immunoprecipitation). The effects of UPARANT in human *ex vivo* iris angiogenesis were focal to endothelial cells. Phospho-protein array illustrated an unidentified antagonism of UPARANT in the interaction of uPAR with the low-density lipoprotein receptor-related protein-1, resulting in inhibition of β-catenin–mediated angiogenesis in this model. Collectively, these findings broaden the understanding of the mechanisms of action of UPARANT, which could benefit the treatment of patients afflicted with multifactorial ocular neovascular diseases.

Keywords

Iris, neovascularization, hypoxia, interactome, UPARANT, cenupatide.

INTRODUCTION

Ocular vascular networks have an essential role in providing oxygen and nutrients to eye tissues. The uvea is the most vascularized tissue of the eye and comprises the choroid, ciliary body and iris. The iris is a vascular diaphragm with the main role of regulating the amount of light that enters through the pupil. In addition, the iris vasculature also plays a vital role to tissue's homeostasis, by supplying oxygen and nutrients to the anterior segment of the eye, thus contributing to the homeostasis of the cornea and lens [138]. Both during development and in adulthood, angiogenesis mechanisms have a fundamental importance in the formation of new blood vessels from the pre-existing vascular network. Angiogenic mechanisms are regulated by different cellular components, multiple soluble factors and are constituted

by multiple steps [214]. Angiogenesis can be physiologic or pathogenic, including wound healing, uterine cycling, tumor growth and several ophthalmic diseases that may lead to blindness. Pathologic events of angiogenesis occur in presence of an imbalance in pro- and anti-angiogenic factors [145].

The degradation of extracellular matrix (ECM) is one of the essential step in angiogenesis, which allows the migration and proliferation of endothelial cells, resulting in the formation of blood vessel tubes [215]. Vascular endothelial growth factors (VEGFs) and their receptors (VEGFRs) represent the most canonical promoters of angiogenesis. In addition, the urokinase plasminogen activator (uPA) and its receptor (uPAR) play a critical role in ECM remodeling. Within the uPAR interactome, the formyl peptide receptors (FPRs) have been shown to have a prevalent crosstalk in VEGF regulation [137], although through indirect mechanisms [139]. In the eye, albeit the neovascular mechanisms originating at the retina, some advanced stages of proliferative diabetic retinopathy (PDR) or neovascular glaucoma (nG) can lead to development of Rubeosis Iridis (RI), a clinical manifestation of PDR and nG characterized by iris angiogenesis. Little is known about iris neoangiogenesis, yet during PDR or nG it results from the increased vitreal proangiogenic factors, originating from the proliferative retina vasculature [47]. In therapeutics ophthalmology, anti-VEGF drugs have represented a critical step forward in the treatment of ocular neovascular diseases, but the effects can be somewhat limited [125,150,216]. Consequently, a pharmacologic strategy aimed at inhibiting several angiogenic pathways could be a more suitable therapeutic approach. Several molecules have been designed targeting the uPA/uPAR system [140,217,218]. In particular, the tetrapeptide Ac-L-Arg-Aib-L-Arg-L-α(Me)Phe-NH2, called UPARANT, is a FPR binding antagonist which has been demonstrated to reduce ocular angiogenesis in animal models [144,151,170,219]. Studies have shown that *in vitro* UPARANT displays a strong inhibition of VEGF-dependent tube formation of endothelial cells [218] and *in vivo* reduces ocular neovascularization, VEGF levels, and the expression of transcription factors associated with angiogenesis, inflammation and ECM remodeling in mouse models [14,18]. Moreover, qPCR and protein analysis demonstrated an increase of uPAR and inflammatory systems in association with neovascularization in a mouse model of iris angiogenesis [16,19–21]. Previously, a puncture induced mouse model of RI has demonstrated that iris neovascularization undergoes VEGF-independent angiogenesis [20,21]. In addition, similar animal studies have concluded that hypoxia-conditioning would increase the angiogenic responses in the mouse model of RI [19,20]. In the present study, in the context of hypoxia-induced angiogenic stimulus, UPARANT effects were investigated in an *ex vivo* human iris angiogenesis assay, and compared to the clinically used anti-VEGF, Aflibercept. Additionally, to further elucidate whether UPARANT acts on epithelial or endothelial cells, *in vitro* assays were performed on human iris epithelial versus human retinal endothelial cells, and corroborated by colocalization of immunofluorescence signals *ex vivo*. The mechanisms of VEGF-independent iris neovascularization were elaborated by analysis of uPAR co-receptor interactome.

MATERIAL AND METHODS

Ethical aspects

Human post-mortem research-consented donor eyes were obtained from the cornea bank at St. Erik Eye Hospital, Stockholm, Sweden. The use of human tissue was in accordance with the tenets of the Declaration of Helsinki and was approved by the Swedish legislative and ethical committee for the use of human donor material for research. Donors did not present any clinical diagnosis of ocular disease, and samples were anonymized and processed under the general data protection regulation.

Primary cell lines used were commercially available and do not present an ethical confinement.

Cell and organotypic cultures

Human iris epithelial cells (hIEC) and human retinal endothelial cells (hREC) were acquired from Innoprot (Derio, Spain). hIEC were maintained in Dulbecco's modified Eagle medium (DMEM) medium supplemented with 10% fetal bovine serum and 1% penicillin/streptomycin mix (medium and supplements ThermoFisher Scientific Inc., Waltham, MA, USA) and hREC in endothelial cell growth medium (ECGM; BioTechne Corp., Adingdon, UK).

Human irises were isolated and dissected from the eyes in MEM tissue culture medium (ThermoFisher Scientific Inc.). Human iris *ex vivo* organotypic cultures were prepared using segments of ¼ of the iris area and kept free-floating in ECGM, or using 3mm diameter tepan cutter fragments of whole-iris and mounted onto Matrigel (Sigma-Aldrich Corp., St. Louis, MO, USA).

All cell and tissue cultures were maintained in a standard cell culture incubator (humidified, 37°C, 5% CO_2).

Angiogenesis stimulus and pharmacological treatments

Human iris *ex vivo* organotypic, hIEC and hREC were kept in cell culture incubators (humidified, 37°C, 5% CO_2) in hypoxia (1% O_2) as angiogenesis stimulated condition. Normoxia (21% O_2), as unstimulated angiogenic condition, was used as control for untreated samples exposed to angiogenic stimulated condition (see supporting information).

Pharmacological treatments were 2 μg/μL of UPARANT or 8 μg/μL of Aflibercept, as determined based on extrapolation from previous *in vivo* and *in vitro* data [6,13,18,22], and non-treated controls were generated using phosphate buffer saline (PBS; ThermoFisher Scientific Inc.) as vehicle.

In vitro wound healing assay

hIEC were dissociated with TrypLE Express (ThermoFisher Scientific Inc.) into 6-well culture plates. At confluence, hIEC monolayers were scratched in two straight lines to create a "cross patch" with a p1000 pipet tip. Subsequently, the cells were kept in 1 mL of supplemented DMEM with pharmacological treatments and angiogenic stimulus for 24 h. Wound healing assay was monitored from images acquired with a PrimoVert phase-contrast microscope (Zeiss, Gottingen, Germany). The wound closure area was calculated in ImageJ (NIH freeware), where the length of two diagonals per each "cross patch" were measured.

In vitro spheroid sprouting assay

Confluent hREC cultures were dispersed with TrypLE Express and dispersed cells were collected by centrifugation (1200 g, 4°C, 10 min). The cleared cell pellet was resuspended in ECGM containing 0.4% methylcellulose (Sigma-Aldrich Corp.) and 1000 cells were transferred into ultra-low adherence round-bottom 96-well culture plates for an overnight (ON) in a standard cell culture incubator. hREC spheroids were transferred by centrifugation (100 g, 4°C, 3 min) into a new flat-bottom adherent 96-well culture plates with 25 µL Matrigel and kept for 30 min at 37°C, to allow ECM polymerization. Afterwards, 100 µL of ECGM was added, and exposed to angiogenic stimulus containing pharmacological treatments. The analysis of the 3D cultures was performed with the Angiotool software[221] by determining the average length of sprouts.

Ex vivo human iris organotypic sprouting assay

The tepan cut 3 mm diameter whole-iris fragments were rinsed in PBS, prior to mounting onto Matrigel-coated 24-well culture plates. Plates were incubated at 37°C in a humidified cell culture incubator for 1 h, to allow ECM polymerization and iris organotypic culture embedding. 500 µL of ECGM with pharmacological treatments was added to each organotypic culture. Iris explants were kept in a cell culture incubator for 48 h at 37°C with 5% CO_2, and 21% or 1% of O_2. Human *ex vivo* iris angiogenesis was determined by area of sprouting into the Matrigel matrix.

Immunofluorescence staining

For analysis of expression of endothelial cell markers, iris organoids were fixed for 30 min with 4% formaldehyde/PBS (FA; Solveco, Rosersberg, Sweden) at room temperature (RT), followed by permeabilization with PBS containing 0.5% Triton X-100 (PBS-T; Triton X-100 from Sigma-Aldrich Corp.) for 20 min at RT. Antigen retrieval was performed by microwave-heating for 3 min using Diva decloacker (Biocare Medical, Concorde, CA, USA). Blocking was performed in 0.1% PBS-T supplemented with 10% normal goat serum (ThermoFisher Scientific Inc.) for 1 h at RT. Primary antibodies (Table 1) were used in blocking solution, ON at 4°C. Secondary antibodies (Table 1) were used as fluorophore-conjugates, for 1 h at RT in blocking solution.

Finally, explants were mounted with fluorescent medium (Dako, Carpinteria, CA, USA). Fluorescence colocalization analysis was performed on dissected human irises fixed for 24 h in 4% PFA following the immunostaining protocol as described. Images were acquired using the LSM880 laser confocal microscope with the Zen software (Zeiss).

TABLE 1 List of antibodies and stains

Primary antibodies and stains	**Dilution**	**Company; Cat no**
Rat anti-PECAM-1	1:200 (IF)	Novus Biologicals; NB 6001475
Rabbit anti-VEGFR2	1:500 (IF)	Abcam; ab-10975
Mouse anti-uPAR	1:100 (IF)	Santa Cruz Biotech.; sc-37649
Isolectin-biotin	1:1000 (IF)	ThermoFisher; I21414
Goat anti-FPR1	1:100 (IF)	Santa Cruz Biotech.; sc-313198
Rabbit anti-FPR2	1:100 (IF)	Santa Cruz Biotech.; sc-66901
Rabbit anti-FPR3	1:100 (IF)	Santa Cruz Biotech.; sc-66899
Rabbit anti-LRP-1	1:200 (IF)	Cell Signaling Tech.; 64099S
Rabbit anti-HIF-1α	15:00 (WB)	Novus Biologicals; NB100479
Rabbit anti-AKT(p-Ser^{473})	1:500 (WB)	Cell Signaling Tech.; 9271
Rabbit anti-AKT	1:1000 (WB)	Cell Signaling Tech.; 9272
Goat anti-CREB (p-Ser^{133})	1:500 (WB)	Santa Cruz Biotech.; sc-7978
Rabbit anti-CREB	1:1000 (WB)	Santa Cruz Biotech.; sc-25785
Rabbit anti-actin	1:5000 (WB)	Sigma-Aldrich; SAB5600204
Rabbit anti-LRP-1	1:1000 (Co-IP)	Cell Signaling Tech.; 64099S
Mouse anti-uPAR	1:500 (Co-IP)	Santa Cruz Biotech.; 376494
Secondary antibodies and stains	**Dilution**	**Commercial information**
Anti-rat-Alexa546	1:500 (IF)	ThermoFisher; A11081
Anti-mouse-Alexa488	1:500 (IF)	ThermoFisher; A11001
Streptavidin-Alexa488	1:500 (IF)	ThermoFisher; S11223
Anti-rabbit-HRP	1:10000 (WB)	Dako; P044801-2
Anti-mouse-HRP	1:10000 (WB)	Dako; P016102-2
Anti-goat-Alexa647	1:1000 (IF)	Sigma Aldrich; SAB4600175
Anti-mouse-Alexa488	1:1000 (IF)	ThermoFisher; A11006
Anti-rabbit-Alexa647	1:1000 (IF)	ThermoFisher; A11010
Streptavidin-Alexa546	1:1000 (IF)	ThermoFisher; S11249

Abbreviations: IF, immunofluorescence; WB, western blot; Co-IP, co-immunoprecipitation; HRP, horseradish peroxidase.

Quantitative PCR (qPCR)

Total RNA was extracted from both hIEC and hREC with the single shot cell lysis kit. cDNA synthesis was performed from 1 µg RNA using iScript cDNA synthesis kit. Transcripts expression was determined using iQ SYBR green supermix and primers, in a CFX real-time thermal cycler. PrimePCR primers used: FPR1 (cat. no. qHsaCID00174321); FPR2 (cat. no. qHsaCED0037673); FPR3 (cat. no. qHsaCID0005919); uPA (cat. no. qHsaCID0019740); uPAR (cat. no. qHsaCID0017227); plasminogen activator inhibitor (PAI)-1 (cat. no. qHsaCID0006432). Threshold values were analyzed by the ΔΔCt method. Two housekeeping genes – ribosomal protein L13 A (RPL13; cat. no. qHsaCED0045063) and β-actin (ACTB; cat. no. qHsaCEP0036280) – were used for normalizing mRNA transcription. qPCR reagents, kits, PrimePCR paired oligos and equipment from BioRad Laboratories, Hercules, CA, USA.

Human phospho-kinase proteome array

Free-floating human iris *ex vivo* organotypic cultures were exposed to angiogenesis stimulation and pharmacological treatments for 24 hours. Total proteins were extracted using 200 µL of lysis buffer from the human phospho-kinase array (BioTechne Corp.) supplemented with protease and phosphatase inhibitor cocktails (Roche, Mannheim, Germany), following 3 cycles of sonication (Vibra Cell; Chemical Instruments AB, Lidingo, Sweden) and 10 donors were pooled into one sample to warrant high protein content. The human phospho-kinase array kit was used to detect the phosphorylation levels of 43 human kinases using 100 µL of pooled sample, according to the manufacturer's instructions. The blots were developed with the ECL max chemiluminescence reagent and the images were acquired by ChemiDoc XRS$^+$ (both BioRad Laboratories). The protein expression was determined by optical density (OD) of the dotblots, using Image Lab 3.0 software (BioRad Laboratories). The densitometric analysis was corrected with the three positive controls, as recommended by the manufacturer.

Immunoblotting assay

Human whole-iris protein extracts from *ex vivo* organotypic cultures from independent donors where prepared and quantified as described in "human phospho-kinase proteome array". 10 µg of whole-tissue protein extract was denatured for 10 min in boiling Laemmli buffer, separated by SDS-PAGE and transferred onto polyvinylidene difluoride (PVDF) membranes (all Bio-Rad Laboratories). Blots were blocked for 1 h at RT, using 5% of non-fat milk in Tris-buffered saline (nfm/TBS; Bio-Rad Laboratories) containing 0.05% Tween-20 (TBS-T; Sigma-Aldrich Corp.). PVDF membranes were incubated with primary antibodies (Table 1) over night at 4°C. Afterwards, secondary antibodies (Table 1) were used for 1 hour at RT. Both antibody solutions were performed in 1% nfm/TBS-T and each antibody step was followed by 3 washes with TBS-T. Finally, blots were developed, the images were acquired and OD evaluated as in "human phospho-kinase proteome array". Protein levels were corrected to the β-actin loading control or the equivalent non-phosphorylated proteins.

Co-immunoprecipitation assay

Human iris *ex vivo* organotypic cultures from independent donors were prepared into total protein extracts as described above. Whole-tissue protein extracts from 10 donors were pooled into one sample to warrant high protein content. 30 µl Dynabeads protein G (ThermoFisher Scientific Inc.) were prepared for antibody binding by washing with TBS, and blocked with 1% bovine serum albumin (BSA; Sigma-Aldrich Corp.) in TBS, for 30 min at RT under rotation. For precipitation of LRP1/uPAR complexes, 5 µL of rabbit monoclonal anti-LRP-1 antibody (Cell Signaling Technology, Danvers, MA, USA) was added and incubated for 1h at RT. Beads were magnetized and the solution removed. 1 mg of total protein from whole-tissue extract was added to the immunized beads, diluted to a final volume of 500 µL with TBS, and incubated ON at 4°C under rotation. Extensive washes with TBS-T followed, and cleared sample beads were eluted by boiling with 15 µL denaturing Laemmli buffer for 10 min. 10 µg of total proteins from the whole-tissue extract were used as input. Eluates and inputs were separated and analyzed by immunoblotting.

Statistical analysis

Statistical analyses were performed using GraphPad Prism software (San Diego, CA, USA), applying One-way ANOVA with Tukey's multiple comparisons posttest. Data was presented as mean ± standard error of mean (SEM) with n as disclosed in figure legends. Differences with $P < 0.05$ were considered statistically significant.

RESULTS

UPARANT does not affect human iris epithelium yet reduces sprouting angiogenesis in human retinal endothelial spheroids

Epithelial cell migration and proliferation represents a critical step in tissue recovery associated with angiogenesis.[222] To investigate the effects of UPARANT on iris epithelial cells, a wound healing assay was performed. Wounded hIEC cultures received a paralleled treatment with Aflibercept, a commonly used anti-angiogenic treatment in ophthalmology. As depicted in Figure 1A, no significant difference was observable between the treatments, UPARANT or Aflibercept, as compared to the vehicle-treated controls. To evaluate the role of UPARANT in ocular endothelial cell angiogenesis, spheroid cultures of hREC were established to analyze their ability to create angiogenic sprouts when embedded in ECM (Figure 1B). Both UPARANT and Aflibercept significantly reduced sprouting angiogenesis in ocular endothelial

cells. A more predominant decrease of number of sprouts was observed in spheroids exposed to UPARANT ($P < 0.001$ versus vehicle; $P < 0.05$ versus Aflibercept). These data indicate that UPARANT did not influence migration of human iris epithelium cells, while significantly reduced hypoxia-induced sprouting of ocular retinal endothelial sprouting *in vitro*.

Previous studies have characterized the anti-angiogenic role of UPARANT through the modulation of the three FPR orthologs' signaling, by co-receptor binding antagonism of uPAR [13,15,18]. To further elaborate on UPARANT's ineffectiveness on human iris epithelial cells, expression analysis of FPR genes was performed by qPCR in both hIEC and hREC. Notably, no FPR transcript were detectable in hIEC (Figure 1C), while in hREC both FPR2 and -3 were expressed at detectable levels (Figure 1C). These results corroborated that UPARANT would have limited activity on hIEC migration in vitro, due to lack of canonical uPAR/FPR expression in this cell line. We have demonstrated previously an association between iris neovascularization and ECM degradation markers [153], thus the qPCR analysis was extended to analyze the transcript level of uPA, uPAR, and PAI-1 genes (Figure 1C). A similar transcription activity of inflammation and ECM degradation markers was observed in both hIEC and hREC cells, indicating that canonical uPAR signaling is present in both iris epithelial and ocular endothelial cells.

To assess the expression of uPAR and FPRs in human iris, FPR1, -2, and -3 were co-immunostained with uPAR and the vascular marker isolectin (Figure 2). Irises displayed a strong colocalization of FPR1 and FPR2 with uPAR to the iris vasculature, while FPR3 showed a more diffuse signal in the tissue with undetectable colocalization with either uPAR or iris vasculature. These data are in agreement with our previous work [152], where we demonstrated a colocalization of FPR1 and FPR2 in mouse iris blood vessels.

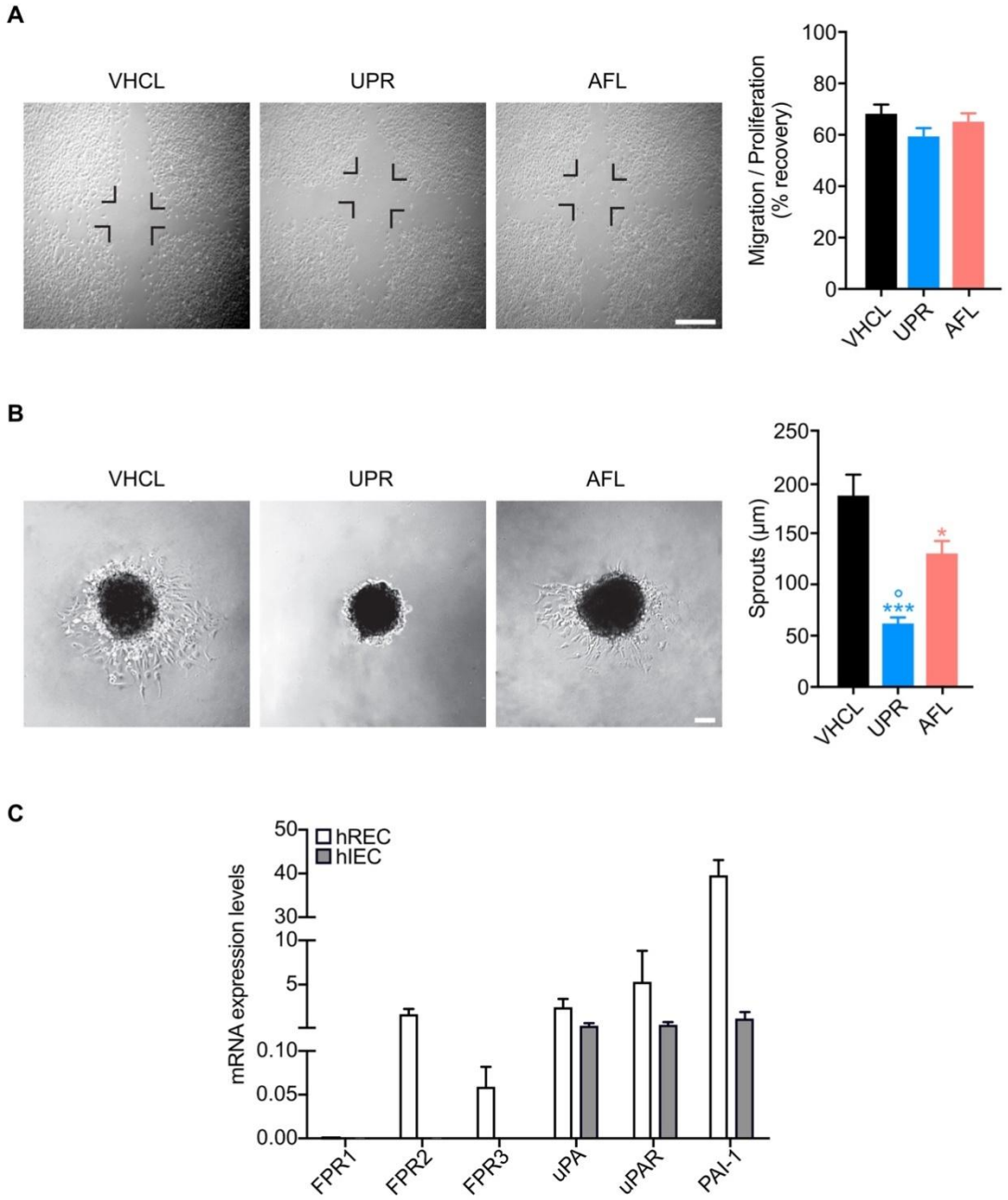

FIGURE 1 Evaluation of the effects of UPARANT on ocular cells migration. **(A)** *In vitro* wound healing assay was performed on hIECs treated with UPARANT (UPR) or Aflibercept (AFL), under hypoxia-stimulated angiogenesis. Quantitative analysis revealed no statistically different between treatments and untreated. Both UPR and AFL did not affect iris epithelial wound recovery. **(B)** Sprouting assay was performed in hREC spheroids exposed to hypoxia-stimulated angiogenesis. Quantitative analysis demonstrated a statistically significant reduction in average sprout length in spheroids exposed to either UPR and or AFL, compared to vehicle (VHCL)-treated controls; a significant reduction was determined in spheroids treated with UPR, compared to AFL. Data in **(A)** and **(B)** represented by: n = 9; * $P < 0.05$, *** $P < 0.001$ vs VHCL; ° $P < 0.05$ vs AFL; Scale bar = 100 µm. **(C)** Gene expression analysis was performed by qPCR in unstimulated hIEC and hREC cultures (n = 6). No transcript expression levels of FPRs were detected in hIEC, while in the expression of FPR 2 and 3 was confirmed in hREC. The transcription level of uPA, uPAR and PAI-1 genes was determined in both hIEC and hREC.

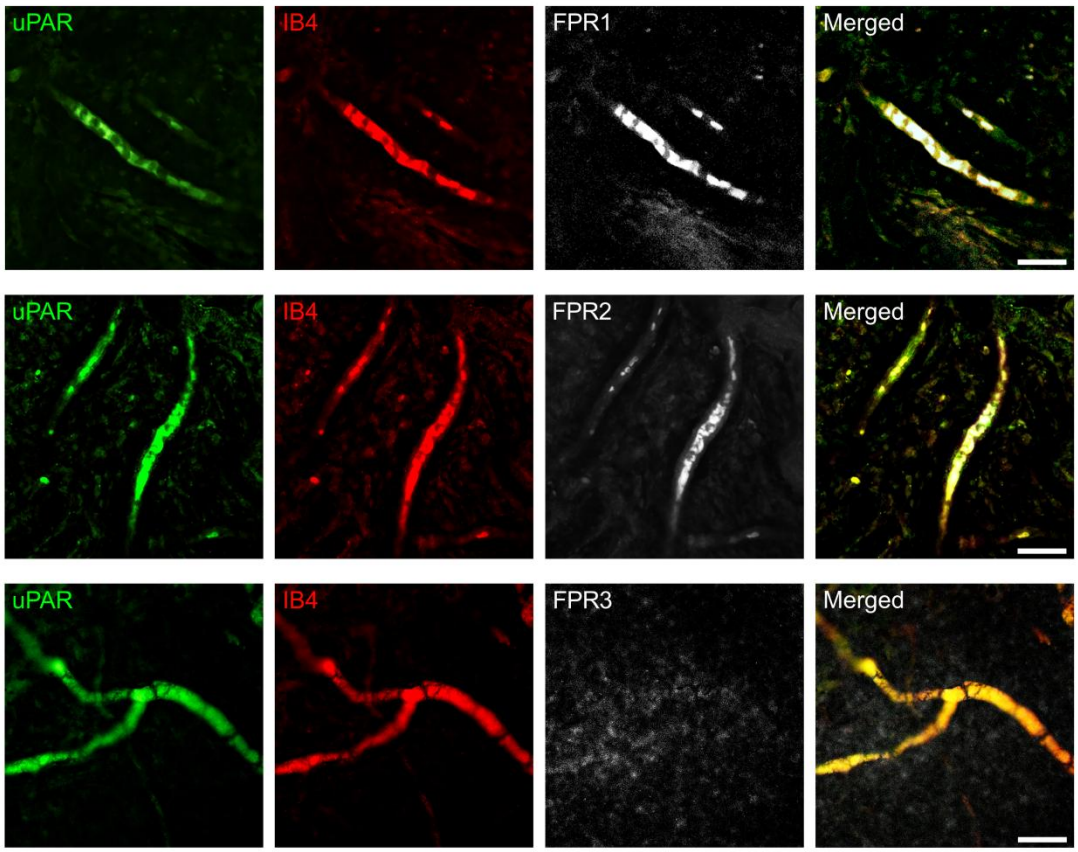

FIGURE 2. Expression analysis of the uPAR/FPR system in human iris. Human irises were co immunostained for uPAR (green), isolectin B4 (red) and FPR-1, -2 or-3 (white). FPR1, -2 and uPAR expression patterns are focally localized to human iris blood vessels, while FPR3 staining was more diffuse in the tissue. Scale bar = 200 μm.

UPARANT potently inhibits hypoxia-induced *ex vivo* iris angiogenesis

To investigate the ability of UPARANT to inhibit angiogenesis mechanism, iris organotypic cultures were established and analyzed for their ability to create angiogenic sprouts when embedded in ECM. Angiogenic sprouts were characterized by immunofluorescence analysis, through the expression of the endothelial-specific markers (Figure 3A). Staining for platelet endothelial cell adhesion molecule (PECAM)-1 and VEGFR2 was positive in areas of angiogenic sprouts. Furthermore, VEGFR2 staining suggests the formation of tip-cells associated with canonical sprouting angiogenesis. Subsequently, hypoxia-stimulated iris organotypic cultures were exposed to UPARANT or Aflibercept (Figure 3B). Both UPARANT and Aflibercept blocked sprouting angiogenesis in ocular endothelial cells ($P < 0.001$, $P < 0.01$ versus vehicle), yet UPARANT was more efficient as indicated by a statistically significant reduction as compared to Aflibercept treatment ($P < 0.05$).

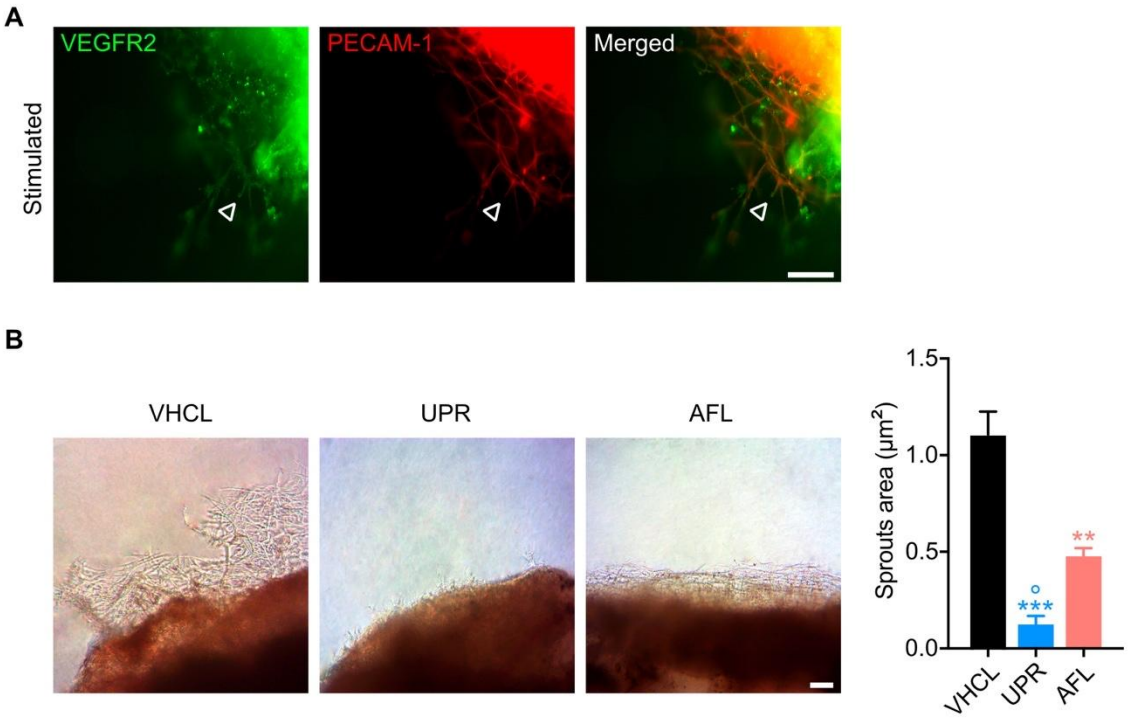

FIGURE 3 Effect of UPARANT in human *ex vivo* iris neoangiogenesis assay. (A) Representative pictures of sprouting angiogenesis evaluated by immunofluorescence on human iris organotypic cultures exposed to hypoxia-stimulated angiogenesis. The endothelial sprouts were characterized by positive staining of VEGFR2 and PECAM-1, as endothelial cell markers (arrow indicates a sprouting tip-cell). (B) Hypoxia-stimulated human *ex vivo* iris neoangiogenesis was mitigated by UPARANT (UPR) and Aflibercept (AFL). Analysis of sprouts area was compared with vehicle (VHCL)- treated controls, demonstrating a statistically significant reduction in sprouting angiogenesis, in explants treated with either UPR or AFL (n = 6; ** $P < 0.01$, *** $P < 0.001$ vs VHCL; ° $P < 0.05$ vs AFL). Scale bars = 100 µm.

UPARANT reduces phospho-transcription factors associated with angiogenesis in human iris

Hypoxia and inflammation responses play a central role in ocular neovascular diseases [25,26]. In this context, western blot analysis was performed to determine the effect of UPARANT on transcriptional activators mediating hypoxia and pro-inflammatory responses in human iris (Figure 4). In agreement with canonical uPAR/FPRs mediated mechanisms[7–9,17,27], densitometric analysis demonstrated that UPARANT leads to a decrease of hypoxia-inducible factor (HIF)-1α protein levels compared to both vehicle ($P < 0.001$) and Aflibercept treated ($P < 0.01$) irises, concomitantly with a decrease in phosphorylation levels of protein kinase B (AKT; $P < 0.001$) and cyclic AMP response element-binding protein (CREB; $P < 0.001$) when compared to vehicle treated.

To further elaborate on the mechanistic aspects of UPARANT-mediated uPAR antagonism in human iris, a phospho-proteome array was used to determine the phosphorylation status of factors involved in angiogenesis, cell survival, migration and chemotaxis (Figure 5). In general terms, treatment with UPARANT displayed lower phosphorylation levels as compared to Aflibercept. Particularly, UPARANT treatment decreased the phosphorylation of p38, epidermal growth factor receptor (EGFR),

mitogen- and stress-activated kinase (MSK) 1/2, CREB, β-catenin, and lysine-deficient protein kinase (WNK)1 when compared to vehicle treated irises. Collectively, this data suggests that in addition to the previously characterized uPAR/FPR interaction, UPARANT may displace additional co-receptor bindings to uPAR and modulate iris angiogenesis through non-canonical pathways.

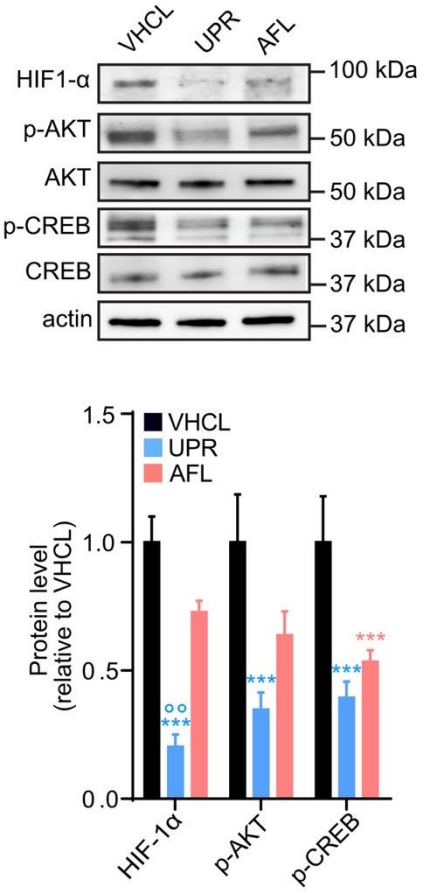

FIGURE 4 Effect of UPARANT on key factors involved in iris angiogenesis. Representative immunoblots of HIF-1α, AKT and CREB transcription factors and their relevant phosphorylated forms of hypoxia-stimulated human iris *ex vivo* organotypic cultures exposed to vehicle (VHCL), UPARANT (UPR) or Aflibercept (AFL). Densitometric analysis of protein levels corrected versus the actin loading control or the corresponding non-phosphorylated protein were normalized to VHCL controls (n = 4; *** $P < 0.001$ vs VHCL; °° $P < 0.01$ vs AFL).

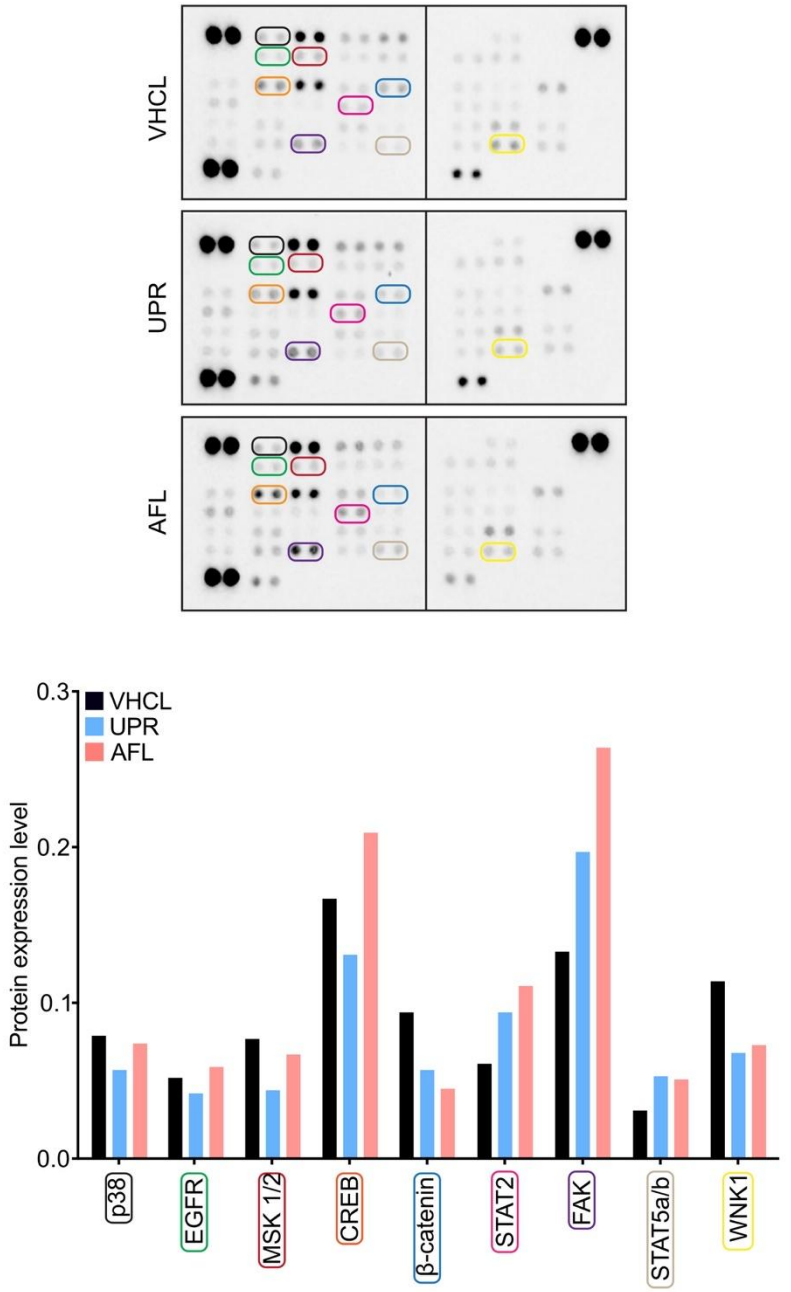

FIGURE 5 Analysis of the phosphoproteome in human iris. Phosphorylated protein levels of hypoxia-stimulated human iris organotypic cultures treated with vehicle (VHCL), UPARANT (UPR) or Aflibercept (AFL) were analyzed by a proteome array profiler. In general, densiometric analysis indicated a decrease of p38, EGFR, MSK 1/2, CREB, β-Catenin and WNK1 phosphorylation levels in human iris organotypic cultures treated with UPR as compared to VHCL controls. The analysis was performed in a pooled sample of 10 independent donors.

UPARANT interferes with the binding of uPAR to LRP-1

A previous study showed a correlation between uPAR and the low-density lipoprotein receptor-related protein (LRP)-1, with consequent activation of the β-catenin pathway with effects on angiogenesis.[159] Elaborating on the observation of β-catenin modulation in the presence of UPARANT (Figure 5), the expression of both uPAR and LRP-1 was determined in *ex vivo* hypoxia-stimulated human irises. Protein

levels of either uPAR and LRP-1 were unaffected by UPARANT or Aflibercept treatment (Figure 6A). Albeit, immunoprecipitation of the uPAR/LRP-1 complex demonstrated an interaction between LRP-1 and uPAR in human iris (Figure 6B), which could be impaired in the presence of UPARANT, but Aflibercept. Furthermore, LRP-1 is readily detectable in human iris vasculature, with clear co-localization with uPAR (Figure 6C), strengthening the role of UPARANT's anti-angiogenic mechanisms by inhibition of the uPAR/LRP-1–β-catenin activating complex, in addition to the previously identified uPAR/FPR interaction.

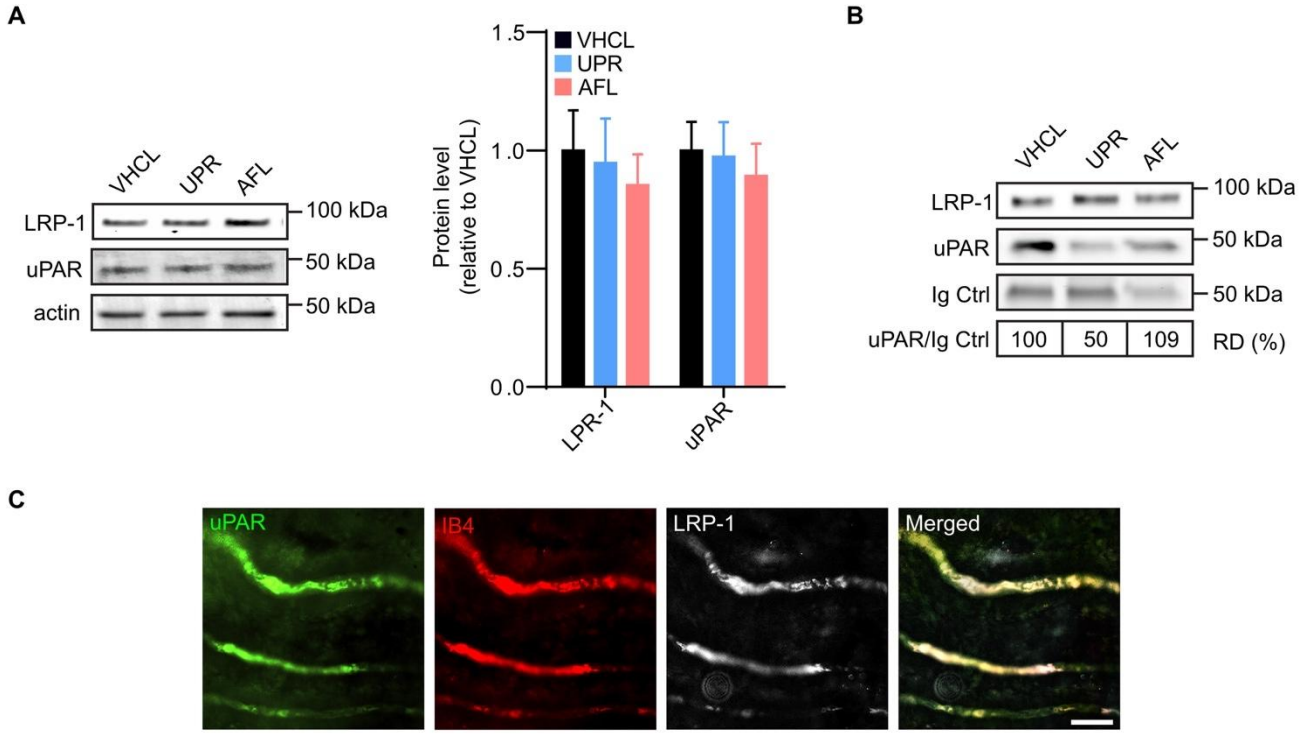

FIGURE 6 Effect of UPARANT on uPAR/LRP-1 interactome. **(A)** Illustrative western blots of LRP-1 and UPAR analysis. Densitometric analysis showed no significant differences in protein levels of LRP-1 and uPAR in hypoxia-stimulated human iris organotypic cultures (n = 4) exposed to vehicle (VHCL), UPARANT (UPR) or Aflibercept (AFL). **(B)** Co-immunoprecipitation of the uPAR/LRP-1 complex was performed with LRP-1 antibody and identified an interaction between LRP-1 and uPAR in hypoxia-stimulated human iris explants. The protein complex formation was reduced by 50% in organotypic cultures treated UPR but not AFL, as compared to VHCL and normalized to the IgG loading control. The co-immunoprecipitation was performed from a pooled sample of 10 independent donors. **(C)** Human irises were co-immunostained for uPAR (green), isolectin B4 (red) and LRP-1 (white). Data indicated that LRP-1 co-localizes with uPAR in human iris vasculature. Scale bar = 200 μm.

DISCUSSION

In advanced stage of retinopathies, iris neovascularization is due to an accumulation of several proangiogenic factors in the retina, among which VEGF.[29,30] Nowadays, anti-VEGF drugs represent the prime therapeutic

strategy to minimize neovascularization in ocular diseases, but the uses are limited.[31,32] Frequent intravitreal injections may lead to complications, including infectious endophthalmitis, acute rise of intraocular pressure, and even hematogenous retinal detachment.[131] UPARANT has been shown to have an antiangiogenic effect in many animal models of vascular diseases, by interfering with the interaction of uPAR and FPRs.[14,15,18] This study demonstrates the efficacy of UPARANT in a novel *ex vivo* model of human iris neovascularization, induced by hypoxia stimulus. In addition, the efficacy of UPARANT in human iris neovascularization *ex vivo* is compared to a clinically used anti-VEGF agent, Aflibercept.

The macrostructure of the iris includes epithelial and endothelial structures that both can contribute to the neovascular mechanisms.[138] Using *in vitro* assays to assess the effects of UPARANT in either epithelium or endothelium, antagonism of both UPARANT and Aflibercept on hypoxia-stimulated hIEC migration was indiscernible from vehicle-treated controls, while hREC 3D culture's sprouting was mitigated by Aflibercept and even further by UPARANT. These findings are further corroborated by gene expression where uPAR and its ligands, uPA and PAI-1, where expressed in both hIEC and hREC, yet the canonical uPAR co-receptors FPR2 and -3 where only detectable in hREC. Combined these data suggest that UPARANT does not influence iris epithelial cells but affects ocular endothelial cells. The current observation that UPARANT exerts a considerable antagonistic effect in hREC is in agreement with previous data, where UPARANT has been demonstrated to inhibit both FPR- and VEGFR-mediated uPAR signaling in endothelial cells.[139] On the contrary, the absence of expression of FPRs in hIEC is confounding, since expression of uPAR and FPR signaling has been shown in other epithelial cells.[11,27] Albeit, the expression of uPAR on epithelial cells has been performed in tumorigenic cell lines where the uPAR/FPR system has been demonstrated to be upregulated[142] and antagonism of uPAR binding to FPRs could interfere with lipid-raft partitioning, thus impairing epithelial cell migration.[143] The present data is limited to the *in vitro* nature of the study, where isolated iris epithelial cells lack their tissue cues and context, and also by the unavailability of iris endothelial cells, thus the use of retinal endothelium as an ocular model of vascular endothelial cells. Consequently, protein expression of FPRs and uPAR is analyzed in human iris with colocalization to the vasculature. Confocal imaging displays expression of uPAR predominantly in human iris blood vessels, with colocalization of FPR1 and -2 expression, a result substantiated with previous mouse iris analysis.[144] Collectively, the present data demonstrate that canonical FPR/uPAR signaling is focal to human iris vasculature, and may be associated with iris neovascular responses to angiogenic stimuli.

Iris neovascularization during RI has been associated with an increase in pro-angiogenic factors, particularly VEGF in PDR patients, as a result of an hypoxic stimulus to the diabetic retina.[3,7,29] Using ECM-embedded iris organotypic cultures, a novel model of human *ex vivo* neoangiogenesis is established in the present study. Under hypoxia stimulated angiogenic conditions, human iris explants form *ex vivo* capillary sprouts expressing both VEGFR2 and PECAM-1 endothelial markers, which confirms sprouting angiogenesis.[147] In this context, human iris *ex vivo* organotypic cultures treated with UPARANT demonstrate a reduction of angiogenic sprouts' area, concomitant with a downregulation of HIF-1α protein levels. In both experimental approaches, the antiangiogenic effects of UPARANT are more pronounced than Aflibercept, at the doses analyzed. Similar findings are demonstrated for p-AKT protein levels, while p-CREB protein levels are reduced by both UPARANT and Aflibercept. The role of uPAR/FPR signaling has been demonstrated previously in mouse models of RI.[16,19] In

parallel to the mouse models, UPARANT reduces hypoxia-, AKT- and CREB-mediated signaling in human iris *ex vivo* neoangiogenesis, while Aflibercept only modulates p-CREB levels as a downstream signaling from the VEGFR signaling pathway.[6,17] These results further confirm the role of uPAR and its interactome in regulating neoangiogenic processes in human iris vasculature.

The present data suggest that canonical uPAR/FPR and uPAR/VEGFR interactions can mediate human iris neoangiogenesis. Animal models of RI have demonstrated both VEGF-dependent and -independent neovascularization mechanisms in the iris.[16,19,20] Consequently, the current study assesses the hypoxia-stimulated phosphorylated protein level of p38, MSK 1/2, CREB, AKT, as well as auto-phosphorylation of EGFR, in human iris *ex vivo* organotypic cultures. Studies have suggested that uPAR activates directly EGFR, through lateral interaction with integrin α5β1, initiating an intracellular signaling that leads to tube formation and motility of cells.[20,38,39] Moreover, inflammation and migration regulating pathways, including p38, MSK 1/2 and CREB downstream responses of activation of EGFR.[156–158] The interference of UPARANT with the uPAR/uPA system decreased phosphorylation levels of all aforementioned proteins, which leads to the observed inhibition of migration and sprout formation in human iris *ex vivo* neovascularization. Interestingly, UPARANT decreased β-catenin phosphorylation levels in human iris. Considering that uPAR is linked to the cell surface solemnly by a glycosylphosphatidylinositol anchor, its signal is dependent on lateral interaction with neighboring receptors, such as integrins, EGFR and LRP-1, all implicated in β-catenin–mediated angiogenesis.[38,43–46]

Previous studies have demonstrated that PAI-1 interacts with LRP-1, inducing cellular migration.[159,160] PAI-1 has been described generically as a physiological inhibitor of uPA that can inhibit cell migration and adhesion.[161] Yet, protease cleaved PAI-1 can bind both uPA and LRP-1, and induce cell motility through the activation of β-catenin intracellular pathways[162] and the modulation of LRP-1 binding to the lipid-rafts.[50,51] In line with the observed decrease of β-catenin levels in human iris *ex vivo* organotypic cultures treated with UPARANT, the data suggest an unidentified antagonism of the uPAR/LRP-1 interaction, and downstream inhibition of the β-catenin cell motility pathway. In fact, UPARANT treatment of human iris does not alter protein expression of uPAR and LRP-1, but it interferes with the formation of the uPAR/LRP-1 interactome. In addition, both uPAR and LRP-1 protein colocalize in human iris, with focal expression to the vascular structures, and expression of the ligands uPA and PAI-1 is detected in iris epithelial cells. In this manner, UPARANT interferes with uPAR/LRP-1 complex and inhibits cell motility induced by β-catenin (Figure 7).

In sum, the present data provide a better understanding of the molecular mechanisms of action of UPARANT in iris, using a novel *ex vivo* human angiogenesis model. The study has the novelty of determining expression of FPR and uPAR in human iris vasculature. Moreover, the new human *ex vivo* iris angiogenesis model using organotypic cultures addresses molecular and cellular queries in a whole-tissue context, which heightens the molecular relevance of UPARANT antagonism of angiogenesis at a multicellular level. In line with the multileveled complexity of the organotypic cultures, the current study illustrated a yet uncharacterized mechanism of action of UPARANT, through inhibition of uPAR/LRP-1 interactome and its β-catenin downstream signaling. Collectively, the present data demonstrate the efficacy of UPARANT to mitigate both canonical and noncanonical vascular endothelial cell responses to angiogenic stimuli, thus illustrating a broader mechanism of inhibition of ocular pathological neovascularization when compared to the canonical VEGF-signaling inhibitor, Aflibercept. These

findings both deepen and corroborate the role of UPARANT as a bonafide multifactor inhibitor of ocular vascular endothelial cells, which could benefit the treatment of RI in patients afflicted with PDR or nG, as well as multiple other ocular neovascular diseases.

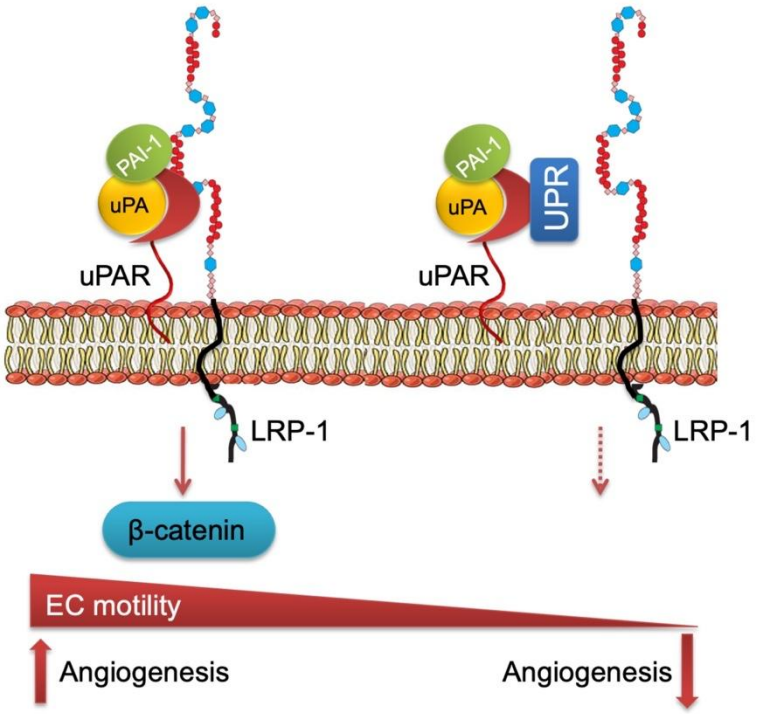

FIGURE 7 Mechanistic antagonism of UPARANT on uPAR/LRP-1 interactome. In the presence of PAI-1, uPAR interacts with LRP-1 and downstream activates β-catenin to mediate endothelial cell (EC) motility in association with pro-angiogenic stimuli. In the presence of UPARANT (UPR) the protein complex uPAR/LRP-1 is displaced, thus mitigating angiogenesis.

ACKNOWLEDGMENTS

This study was partly funded by a research grant from Kaleyde Pharmaceuticals AG (Lugano, Switzerland), the Karolinska Institutet Foundations and Funds, and The Swedish Eye Foundation. The authors would like to thank Maurizio Cammalleri, Mario De Rosa and Paola Bagnoli for critical discussion on UPARANT's mechanisms of action, the St Erik Eye Hospital cornea bank unit for assistance in collecting donor ocular tissues, and the Biomedicum Imaging Core facility at Karolinska Institutet for assistance with confocal imaging.

CONFLICT OF INTEREST

V.P. is a patent holder for UPARANT, assigned the international non-proprietary name Cenupatide (CAS number: 1006388-38-0) by the World Health Organization. All other authors declare no conflict of interest.

AUTHOR CONTRIBUTIONS

N.A.P. and H.A. designed research; N.A.P., F.L. and F.P. performed research and analyzed data; V.P. and A.K. contributed with resources; M.D.M. and H.A. obtained funding; N.A.P. and H.A. wrote the paper. All authors have read and agreed to the published version of the manuscript.

REFERENCES

1. Yang, H., Yu, P.K., Cringle, S.J., Sun, X., Yu, D.-Y. Iridal vasculature and the vital roles of the iris. *Journal of Nature and Science*. **1** (8), 157, at <www.jnsci.org/content/157> (2015).
2. Ucuzian, A.A., Gassman, A.A., East, A.T., Greisler, H.P. Molecular mediators of angiogenesis. *Journal of Burn Care and Research*. **31** (1), 158–175, doi: 10.1097/BCR.0b013e3181c7ed82 (2010).
3. Mohan, N., Monickaraj, F., Balasubramanyam, M., Rema, M., Mohan, V. Imbalanced levels of angiogenic and angiostatic factors in vitreous, plasma and postmortem retinal tissue of patients with proliferative diabetic retinopathy. *Journal of Diabetes and its Complications*. **26** (5), 435–441, doi: 10.1016/j.jdiacomp.2012.05.005 (2012).
4. Neve, A., Cantatore, F.P., Maruotti, N., Corrado, A., Ribatti, D. Extracellular matrix modulates angiogenesis in physiological and pathological conditions. *BioMed Research International*. **2014**, 756078, doi: 10.1155/2014/756078 (2014).
5. Breuss, J.M., Uhrin, P. VEGF-initiated angiogenesis and the uPA/uPAR system. *Cell Adhesion and Migration*. **6** (6), 535–540, doi: 10.4161/cam.22243 (2012).
6. Motta, C. *et al.* Molecular mechanisms mediating antiangiogenic action of the urokinase receptor-derived peptide UPARANT in human retinal endothelial cells. *Investigative Ophthalmology and Visual Science*. **57** (13), 5723–5735, doi: 10.1167/iovs.16-19909 (2016).
7. Jeong, Y.C., Hwang, Y.H. Etiology and features of eyes with rubeosis iridis among Korean patients: A population-based single center study. *PLoS ONE*. **11** (8), doi: 10.1371/journal.pone.0160662 (2016).
8. Fogli, S., Del Re, M., Rofi, E., Posarelli, C., Figus, M., Danesi, R. Clinical pharmacology of intravitreal anti-VEGF drugs. *Eye (Basingstoke)*. **32** (6), 1010–1020, doi: 10.1038/s41433-018-0021-7 (2018).
9. Xu, J.J., Li, Y.M., Hong, J.X. Progress of anti-vascular endothelial growth factor therapy for ocular neovascular disease: Benefits and challenges. *Chinese Medical Journal*. **127** (8), 1550–1557, doi: 10.3760/cma.j.issn.0366-6999.20140017 (2014).
10. Fine, H.F., Despotidis, G.D., Prenner, J.L. Ocular inflammation associated with antivascular endothelial growth factor treatment. *Current Opinion in Ophthalmology*. **26** (3), 184–187, doi: 10.1097/ICU.0000000000000154 (2015).
11. Bifulco, K. *et al.* An urokinase receptor antagonist that inhibits cell migration by blocking the formyl peptide receptor. *FEBS Letters*. **582** (7), 1141–1146, doi: 10.1016/j.febslet.2008.03.001 (2008).
12. Carriero, M.V. *et al.* Structure-based design of an urokinase-type plasminogen activator receptor-derived peptide inhibiting cell migration and lung metastasis. *Molecular Cancer Therapeutics*. **8** (9), 2708–2717, doi: 10.1158/1535-7163.MCT-09-0174 (2009).
13. Carriero, M.V. *et al.* UPARANT: A urokinase receptor-derived peptide inhibitor of VEGF-driven

angiogenesis with enhanced stability and in vitro and in vivo potency. *Molecular Cancer Therapeutics*. **13** (5), 1092–1104, doi: 10.1158/1535-7163.MCT-13-0949 (2014).
14. Dal Monte, M. *et al.* Antiangiogenic effectiveness of the urokinase receptor- derived peptide UPARANT in a model of oxygen-induced retinopathy. *Investigative Ophthalmology and Visual Science*. **56** (4), 2392–2407, doi: 10.1167/iovs.14-16323 (2015).
15. Cammalleri, M. *et al.* Diabetic Retinopathy in the Spontaneously Diabetic Torii Rat: Pathogenetic Mechanisms and Preventive Efficacy of Inhibiting the Urokinase-Type Plasminogen Activator Receptor System. *Journal of Diabetes Research*. **2017**, 2904150, doi: 10.1155/2017/2904150 (2017).
16. Locri, F. *et al.* UPARANT is an effective antiangiogenic agent in a mouse model of rubeosis iridis. *Journal of Molecular Medicine*. **97** (9), 1273–1283, doi: 10.1007/s00109-019-01794-w (2019).
17. Cammalleri, M., Dal Monte, M., Pavone, V., De Rosa, M., Rusciano, D., Bagnoli, P. The uPAR System as a Potential Therapeutic Target in the Diseased Eye. *Cells*. **8** (8), 925, doi: 10.3390/cells8080925 (2019).
18. Cammalleri, M. *et al.* The urokinase receptor-derived peptide UPARANT mitigates angiogenesis in a mouse model of laser-induced choroidal neovascularization. *Investigative Ophthalmology and Visual Science*. **57** (6), 2600–2611, doi: 10.1167/iovs.15-18758 (2016).
19. Locri, F. *et al.* Gaining insight on mitigation of rubeosis iridis by UPARANT in a mouse model associated with proliferative retinopathy. *Journal of Molecular Medicine*. **98** (11), 1629–1638, doi: 10.1007/s00109-020-01979-8 (2020).
20. Beaujean, O., Locri, F., Aronsson, M., Kvanta, A., André, H. A novel in vivo model of puncture-induced iris neovascularization. *PLoS ONE*. **12** (6), e0180235, doi: 10.1371/journal.pone.0180235 (2017).
21. Locri, F., Aronsson, M., Beaujean, O., Kvanta, A., André, H. Puncture-induced iris neovascularization as a mouse model of rubeosis iridis. *Journal of Visualized Experiments*. **2018** (133), doi: 10.3791/57398 (2018).
22. Schnichels, S. *et al.* Comparative toxicity and proliferation testing of aflibercept, bevacizumab and ranibizumab on different ocular cells. *British Journal of Ophthalmology*. **97** (7), 917–923, doi: 10.1136/bjophthalmol-2013-303130 (2013).
23. Zudaire, E., Gambardella, L., Kurcz, C., Vermeren, S. A computational tool for quantitative analysis of vascular networks. *PLoS ONE*. **6** (11), e27385, doi: 10.1371/journal.pone.0027385 (2011).
24. Leoni, G., Neumann, P.A., Sumagin, R., Denning, T.L., Nusrat, A. Wound repair: Role of immune-epithelial interactions. *Mucosal Immunology*. **8** (5), 959–968, doi: 10.1038/mi.2015.63 (2015).
25. Al-Kharashi, A.S. Role of oxidative stress, inflammation, hypoxia and angiogenesis in the development of diabetic retinopathy. *Saudi Journal of Ophthalmology*. **32** (4), 318–323, doi: 10.1016/j.sjopt.2018.05.002 (2018).
26. Li, Y., Zhou, Y. Interleukin-17: The role for pathological angiogenesis in ocular neovascular diseases. *Tohoku Journal of Experimental Medicine*. **247** (2), 87–98, doi: 10.1620/tjem.247.87 (2019).
27. Carriero, M.V. *et al.* Structure-based design of an urokinase-type plasminogen activator receptor-derived peptide inhibiting cell migration and lung metastasis. *Molecular Cancer Therapeutics*. **8** (9), 2708–2717, doi: 10.1158/1535-7163.MCT-09-0174 (2009).
28. Kozlova, N., Jensen, J.K., Chi, T.F., Samoylenko, A., Kietzmann, T. PAI-1 modulates cell migration in a LRP1-dependent manner via β-catenin and ERK1/2. *Thrombosis and Haemostasis*. **113** (5), 988–998, doi: 10.1160/TH14-08-0678 (2015).
29. Kovacs, K. *et al.* Angiogenic and inflammatory vitreous biomarkers associated with increasing levels of retinal ischemia. *Investigative Ophthalmology and Visual Science*. **56** (11), 6523–6530, doi: 10.1167/iovs.15-16793 (2015).
30. Gartner, S., Henkind, P. Neovascularization of the iris (rubeosis iridis). *Survey of Ophthalmology*.

22 (5), 291–312, doi: 10.1016/0039-6257(78)90175-3 (1978).
31. Gheith, M.E., Siam, G.A., Monteiro De Barros, D.S., Garg, S.J., Moster, M.R. Role of intravitreal bevacizumab in neovascular glaucoma. *Journal of Ocular Pharmacology and Therapeutics*. **23** (5), 487–491, doi: 10.1089/jop.2007.0036 (2007).
32. Kotecha, A. *et al.* Intravitreal bevacizumab in refractory neovascular glaucoma: A prospective, observational case series. *Archives of Ophthalmology*. **129** (2), 145–150, doi: 10.1001/archophthalmol.2010.350 (2011).
33. Falavarjani, K.G., Nguyen, Q.D. Adverse events and complications associated with intravitreal injection of anti-VEGF agents: A review of literature. *Eye (Basingstoke)*. **27** (7), 787–794, doi: 10.1038/eye.2013.107 (2013).
34. Yang, H., Yu, P.K., Cringle, S.J., Sun, X., Yu, D.-Y. *Iridal vasculature and the vital roles of the iris*. *Journal of Nature and Science*. **1** (8), at <www.jnsci.org/content/157>. (2015).
35. Noh, H., Hong, S., Huang, S. Role of urokinase receptor in tumor progression and development. *Theranostics*. **3** (7), 487–495, doi: 10.7150/thno.4218 (2013).
36. Gorrasi, A., Petrone, A.M., Li Santi, A., Alfieri, M., Montuori, N., Ragno, P. New Pieces in the Puzzle of uPAR Role in Cell Migration Mechanisms. *Cells*. **9** (12), 2531, doi: 10.3390/cells9122531 (2020).
37. Domigan, C.K., Ziyad, S., Luisa Iruela-Arispe, M. Canonical and noncanonical vascular endothelial growth factor pathways: New developments in biology and signal transduction. *Arteriosclerosis, Thrombosis, and Vascular Biology*. **35** (1), 30–39, doi: 10.1161/ATVBAHA.114.303215 (2015).
38. Van Cruijsen, H., Giaccone, G., Hoekman, K. Epidermal growth factor receptor and angiogenesis: Opportunities for combined anticancer strategies. *International Journal of Cancer*. **117** (6), 883–888, doi: 10.1002/ijc.21479 (2005).
39. Aguirre Ghiso, J.A. Inhibition of FAK signaling activated by urokinase receptor induces dormancy in human carcinoma cells in vivo. *Oncogene*. **21** (16), 2513–2524, doi: 10.1038/sj.onc.1205342 (2002).
40. Lakka, S.S., Gondi, C.S., Rao, J.S. Proteases and glioma angiogenesis. *Brain Pathology*. **15** (4), 327–341, doi: 10.1111/j.1750-3639.2005.tb00118.x (2005).
41. Cuenda, A., Rousseau, S. p38 MAP-Kinases pathway regulation, function and role in human diseases. *Biochimica et Biophysica Acta - Molecular Cell Research*. **1773** (8), 1358–1375, doi: 10.1016/j.bbamcr.2007.03.010 (2007).
42. Dodeller, F., Schulze-Koops, H. The p38 mitogen-activated protein kinase signaling cascade in CD4 T cells. *Arthritis Research and Therapy*. **8** (2), 205, doi: 10.1186/ar1905 (2006).
43. Smith, H.W., Marshall, C.J. Regulation of cell signalling by uPAR. *Nature Reviews Molecular Cell Biology*. **11** (1), 23–36, doi: 10.1038/nrm2821 (2010).
44. Eden, G., Archinti, M., Furlan, F., Murphy, R., Degryse, B. The Urokinase Receptor Interactome. *Current Pharmaceutical Design*. **17** (19), 1874–1889, doi: 10.2174/138161211796718215 (2011).
45. Gorrasi, A. *et al.* The urokinase receptor takes control of cell migration by recruiting integrins and FPR1 on the cell surface. *PLoS ONE*. **9** (1), 86352, doi: 10.1371/journal.pone.0086352 (2014).
46. Breuss, J.M., Uhrin, P. VEGF-initiated angiogenesis and the uPA/uPAR system. *Cell Adhesion and Migration*. **6** (6), 535–540, doi: 10.4161/cam.22243 (2012).
47. Palmieri, D., Lee, J.W., Juliano, R.L., Church, F.C. Plasminogen activator inhibitor-1 and -3 increase cell adhesion and motility of MDA-MB-435 breast cancer cells. *Journal of Biological Chemistry*. **277** (43), 40950–40957, doi: 10.1074/jbc.M202333200 (2002).
48. Uhrin, P., Breuss, J.M. uPAR: A modulator of VEGF-induced angiogenesis. *Cell Adhesion and Migration*. **7** (1), 23–26, doi: 10.4161/cam.22124 (2013).
49. Kamikubo, Y., Neels, J.G., Degryse, B. Vitronectin inhibits plasminogen activator inhibitor-1-induced signalling and chemotaxis by blocking plasminogen activator inhibitor-1 binding to the low-density lipoprotein receptor-related protein. *International Journal of Biochemistry and Cell Biology*. **41** (3), 578–585, doi: 10.1016/j.biocel.2008.07.006 (2009).
50. Wu, L., Gonias, S.L. The low-density lipoprotein receptor-related protein-1 associates transiently

with lipid rafts. *Journal of Cellular Biochemistry*. **96** (5), 1021–1033, doi: 10.1002/jcb.20596 (2005).
51. L. Gonias, S., Gaultier, A., Jo, M. Regulation of the Urokinase Receptor (uPAR) by LDL Receptor-related Protein-1 (LRP1). *Current Pharmaceutical Design*. **17** (19), 1962–1969, doi: 10.2174/138161211796718224 (2011).

PAPER II

Journal of Molecular Medicine https://doi.org/10.1007/s00109-020-01979-8

JMolMed

ORIGINAL ARTICLE

Gaining insight on mitigation of rubeosis iridis by UPARANT in a mouse model associated with proliferative retinopathy

Filippo Locri [1] Noemi A. Pesce[1,2] Monica Aronsson[1] Maurizio Cammalleri[2] Mario De Rosa [3] Vincenzo Pavone[4] Paola Bagnoli [2] Anders Kvanta[1] Massimo Dal Monte [2] Helder André[1]

Received: 16 July 2020 / Revised: 4 September 2020 / Accepted: 10 September 2020

Abstract

Proliferative retinopathies (PR) lead to an increase in neovascularization and inflammation factors, at times culminating in pathologic rubeosis iridis (RI). In mice, uveal puncture combined with injection of hypoxia-conditioned media mimics RI associated with proliferative retinopathies. Here, we investigated the effects of the urokinase plasminogen activator receptor (uPAR) antagonist—UPARANT—on the angiogenic and inflammatory processes that are dysregulated in this model. In addition, the effects of UPARANT were compared with those of anti-vascular endothelial growth factor (VEGF) therapies. Administration of UPARANT promptly decreased iris vasculature, while anti-VEGF effects were slower and less pronounced. Immunoblot and qPCR analysis suggested that UPARANT acts predominantly by reducing the upregulated inflammatory and extracellular matrix degradation responses. UPARANT appears to be more effective in comparison to anti-VEGF in the treatment of RI associated with PR in the murine model, by modulating multiple uPAR-associated signaling pathways. Furthermore, UPARANT effectiveness was maintained when systemically administered, which could open to novel improved therapies for proliferative ocular diseases, particularly those associated with PR.

Key messages

- Further evidence of UPARANT effectiveness in normalizing pathological iris neovascularization.
- Both systemic and local administration of UPARANT reduce iris neovascularization in a model associated with proliferative retinopathies.
- In the mouse models of rubeosis iridis associated with proliferative retinopathy, UPARANT displays stronger effects when compared with anti-vascular endothelial growth factor regimen.

Keywords Rubeosis iridis · Proliferative retinopathy · Inflammation · Antiangiogenic drug · UPARANT

Filippo Locri and Noemi A. Pesce contributed equally to this work.

Electronic supplementary material The online version of this article (https://doi.org/10.1007/s00109-020-01979-8) contains supplementary material, which is available to authorized users.

✉ Helder André
Helder.Andre@ki.se

[1] Department of Clinical Neuroscience, Division of Eye and Vision, St Erik Eye Hospital, Karolinska Institutet, Polhemsgatan 50, 112 82 Stockholm, Sweden

[2] Department of Biology, University of Pisa, Pisa, Italy

[3] Department of Experimental Medicine, Second University of Naples, Naples, Italy

[4] Department of Chemical Sciences, University of Naples Federico II, Naples, Italy

Introduction

In the eye, vascular networks are essential to provide oxygen and nutrients to the cells. The uvea, comprising the choroid, the ciliary body, and the iris, represents the most vascularized ocular tissue. The iris vasculature is characterized by abundant arterio-venous anastomoses, and supply nutrients to the anterior chamber of the eye, including the avascular trabecular meshwork, cornea, and lens. Furthermore, the iris vascular network represents a major source of oxygen in the aqueous humor [1]. During embryonic development and in adult life, angiogenesis processes lead to the formation of new blood vessels from pre-existing vasculature.

Angiogenesis is finely regulated by several angiogenic stimulators and inhibitors. The vascular endothelial growth

factor (VEGF) is the most canonical angiogenic mediator, yet other factors, such as the plasminogen-activator system and inflammatory factors, play an essential role in neoangiogenesis. A molecular imbalance between angiogenic inducers and inhibitors results in neoangiogenesis, a common denominator in several ophthalmic diseases that can lead to blindness [2]. In many proliferative ocular diseases, the neovascularization is located in the retina; however, some advanced stages of proliferative diabetic retinopathy (PDR) and central retinal venous occlusion (CRVO) can trigger pathologic iris neovascularization, clinically determined rubeosis iridis (RI) [3, 4]. In proliferative retinopathies (PR), the in- crease in vitreal neoangiogenic factors induces iris neovascularization [5]. The proliferation of new blood vessels, along the surface of the iris, can lead to obstruction of the aqueous humor flow, increased intraocular pressure, and finally neovascular glaucoma (NVG) [6].

Anti-VEGF agents are effective in reducing RI; neverthe- less, there are some concerns, since the effects are limited [7–10]. The small tetrapeptide UPARANT has been shown to reduce endothelial cell proliferation, motility and tube formation by interfering between the complex crosstalk interac- tion of plasmin activity, and the urokinase-type plasminogen activator receptor (uPAR) and formyl peptide receptors (FPRs) [11–14]. uPAR and its ligand, the urokinase-type plasminogen activator (uPA), have an important role in angiogenesis and inflammation. uPAR-uPA system regulates the degradation of specific components of the basement membrane and extracellular matrix, processes essential for the penetration of the capillary basement membrane by sprouting endothelial cells. UPARANT has been tested in several rodent models of PR [15–18]; the pharmacological administration of UPARANT has demonstrated effectiveness in reducing angiogenesis and ameliorating visual dysfunction. Previously, in a mouse model of induced RI [19, 20], we have demonstrated the effectiveness of UPARANT in mitigating RI [21]. In this model, the major drive of iris neovascularization is wound healing responses, with increased expression of the plasminogen-activator and inflammation systems, and has the advantage of allowing for direct, noninvasive quantification of the iris vasculature in vivo.

In the present study, we have extended the puncture-induced RI model and associated it with PR (RI-PR) by co-injection of hypoxia-conditioned medium to mimic the increase in proangiogenic pressure from the posterior compartment of the eye. UPARANT efficacy in counteracting the exacerbated iris neovascular response characteristic of the RI-PR model was assayed and com- pared with a mouse equivalent of aflibercept, an anti- VEGF drug in clinical use. Moreover, mitigation of iris vascular responses by UPARANT in the RI-PR was determined both by intravitreal and subcutaneous administrations.

Materials and methods

Pharmacological treatments

UPARANT (World Health Organization international non- proprietary name Cenupatide; CAS number: 1006388-38-0) [11, 22] was solubilized in sterile phosphate buffered saline (PBS; ThermoFisher Scientific Inc., Waltham, MA, USA) as a succinate salt at 10 mg/mL (intravitreal administration) and 20 mg/kg (subcutaneous administration). These concentrations correspond respectively to 7.6 mg/mL and 15.2 mg/kg of active pharmaceutical ingredient, as previously reported [16]. The mouse equivalent of aflibercept, a VEGF-receptor (VEGFR)1 ligand-binding domain/Ig Fc chimeric protein (referred to as VEGFR1 chimera), was purchased from R&D Systems (Minneapolis, MN, USA) and used as 1 mg/mL in sterile PBS solution.

Mouse model of RI-PR

All experiments were performed in accordance with the statement for the Use of Animals in Ophthalmologic and Vision Research and approved by Stockholm's Committee for Ethical Animal Research. A total of twenty-nine P12.5 BALB/c mice (Charles River, Cologne, Germany) of either sex were used in this study. Mice were kept in litters with their nursing mother on 12-h day/night cycle, with free access to food and water, and observed daily. Mice were anesthetized with a mix of 4% isoflurane in room-air (Baxter, Kista, Sweden) and euthanized by cervical dislocation.

To mimic PR (RI-PR model), three groups of six mice each, for a total of eighteen mice, were subjected to uveal punctures as described previously [19, 20] and co-injected in both eyes with 1 µL of hypoxia-conditioned medium from ARPE-19 cells (ATCC, Manassas, VA, USA). Six mice were kept as untreated controls. Intravitreal UPARANT or VEGFR1 chimera injections were executed on experimental days 4, 8, and 12.

For the systemic administration study, five mice underwent RI-PR induction in one eye while the contralateral eye was left as untreated control. Mouse pups received a 5-day loading dose of UPARANT by subcutaneous administration, through experimental days 4 to 8. The experimental paradigms are outlined in Fig. 1. Post- procedure care of the mouse pups included analgesia with topical tetracaine (1% ocular solution; Bausch & Lomb, Rochester, NY, USA) and hydration by subcutaneous administration of injectable 0.9% NaCl solution (B. Braun, Melsungen, Germany). Mice were euthanized on experimental day 15, eyes

enucleated, and immediate- ly processed for molecular analysis or fixed in a 4% formaldehyde (Solveco, Rosersberg, Sweden) for 6 h at room-temperature for immunostainings.

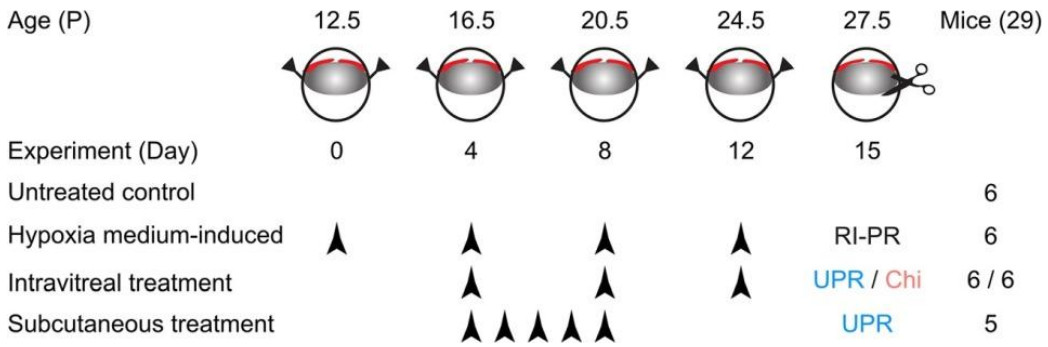

Fig. 1 Schematic representation of the study groups and treatment paradigms. Rubeosis iridis associated with proliferative retinopathy (RIPR) was induced in 12.5-day-old mouse pups by double puncture of the uvea in the eye, with co-injection of hypoxia-conditioned medium, repente at 4-day interval (experimental days 0 through 12). Pharmacological treatments were performed by intravitreal injection of UPARANT (UPR) or VEGFR1 chimera (Chi) on experimental days 4, 8, and 12. UPARANT systemic administration was performed as 5-dayly subcutaneous loading dose (experimental days 4 through 8).

In vivo iris vasculature analysis

Iris photos were acquired on experimental days, prior to any procedure and analyzed as previously reported [19–21]. Briefly, vascular density was determined as percentage of un- treated controls and corrected by total iris area.

Immunohistofluorescence

Fixed irises were dissected and processed for whole-mount immunofluorescence, as previously described [21, 23]. Irises were incubated with antibodies for platelet endothelial cell adhesion molecule (PECAM)-1 (Suppl. Table 1). Images of iris vasculature were acquired with an Axioscope 2 plus epifluorescence microscope and analyzed with the AngioTool freeware [24]. Microvasculature parameters (total vasculature, number of sprouts, and total branching index) were reported as percentage of untreated control.

Quantitative PCR

Total RNA was extracted from whole-eyes using a RNeasy mini plus kit (Qiagen, Hilden, Germany), retrotranscribed to cDNA, and gene expression levels were assayed by quantitative PCR (qPCR; all BioRad Laboratories, Hercules, CA, USA), as previously described [21, 23]. Relative transcript expression levels (corrected with two housekeep genes; Suppl. Table 2) were normalized to untreated controls (ΔΔCT method).

Quantitative western blot

Protein expression analysis was performed as previously report- ed [21]. Briefly, 15 µg of total protein, extracted from whole- eye, were separated by SDS-PAGE and transferred onto polyvinylidene difluoride (PVDF) membranes. Immunoblots were incubated with primary and secondary antibodies (Suppl. Table 1). Protein expression level was normalized against total non-phosphorylated corresponding protein (phosphorylated tar- gets) or actin (non-phosphorylated targets).

Statistical analysis

Densitometric analysis of in vivo iris blood vessels was per- formed by two-way ANOVA with Tukey posttest on six mice per group (n = 12 eyes). All other experiments were analyzed by one-way ANOVA with Tukey posttest on four eyes for intravitreal (n = 4) or five eyes for systemic paradigms (n = 5). $p < 0.05$ was considered significant.

Results

UPARANT reduces neovascularization in rubeosis iridis associated with proliferative retinopathy

Proliferative retinopathies, such as PDR and CRVO, have been associated with the development of pathological RI,

due to an increase of a myriad of pro-angiogenic factors, including VEGF, originating from the retinal tissue [3, 4]. An increase of similar angiogenic factors has been identified in hypoxia-exposed RPE cell media [19, 23]. We have established a murine model of puncture-induced RI in association with PR by co-injection of pro-angiogenic factors derived from hypoxia-exposed RPE culture media [19], with increased neovascularization when compared with the puncture-induced RI mouse model (Suppl. Fig. 1). To assess the effectiveness of UPARANT and anti-VEGF drugs in the RI-PR model, the effects of intravitreally administered UPARANT were compared with those of the VEGFR1 chimera protein. In vivo densitometric analysis demonstrated an increase of

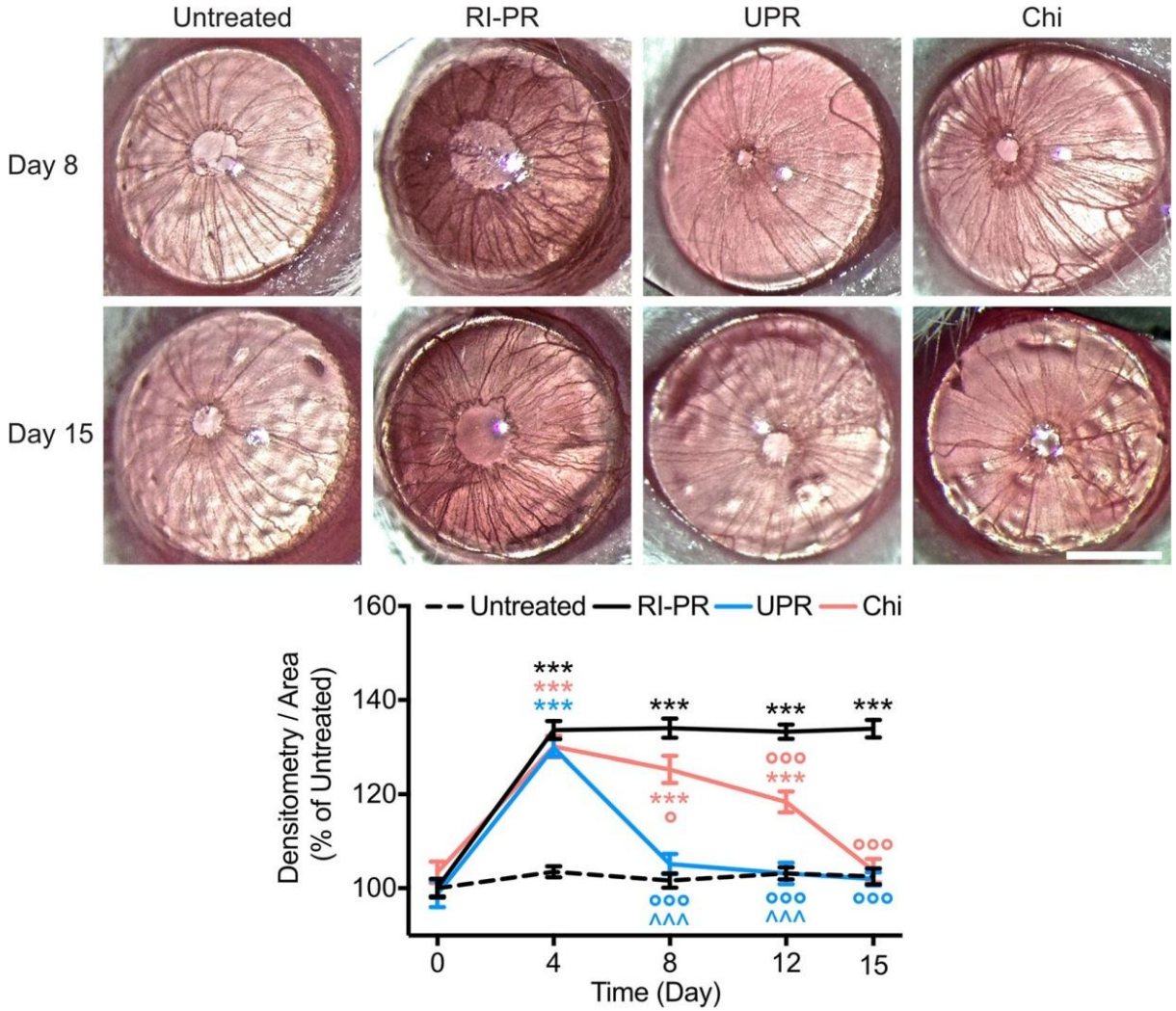

Fig. 2 UPARANT reduces neovascularization in rubeosis iridis associated with proliferative retinopathy (RI-PR). Illustrative pictures of mouse eyes at experimental days 8 and 15, upon treatment with UPARANT (UPR) or VEGFR1 chimera (Chi). Scale bar = 1 mm. Data of noninvasive densitometric analysis of iris vasculature were normalized as percentage of untreated controls, displayed as mean ± SEM (n = 12 eyes per group), and analyzed by two-way ANOVA with Tukey post-hoc tests (***p < 0.001 vs untreated; °p < 0.05 and °°°p < 0.001 vs RP-PR; ^^^p < 0.001 vs Chi).

approximately 35% of iris vasculature (p < 0.001 versus untreated controls) in RI-PR eyes (Fig. 2). On experimental day 8, UPARANT intravitreal injections restored the increased vessel density to untreated levels (p < 0.001 versus RI-PR) and yielded results statistically different from VEGFR1 chimera-treated eyes (p < 0.001). In contrast, the VEGFR1 chimera treatment was unable to restore iris vasculature to untreated levels (p = 0.018). Notably, the VEGFR1 chimera treatment did not regress iris blood vessel density to control levels in the RI-PR model until experimental day 15 (p < 0.001). The iris microvascular beds of the various experimental groups

(Fig. 3) were subsequently analyzed on day 15 by immunofluorescence assay with PECAM-1, an endothelial marker. We observed an increase of roughly 50% in the number of total vasculature in RI-PR eyes ($p < 0.001$) as compared with untreated controls. Intravitreal UPARANT reduced the total vasculature to control levels ($p < 0.001$ versus RI-PR), and UPARANT-treated irises were statistically different from VEGFR1 chimera-treated irises ($p < 0.001$). Additionally, VEGFR1 chimera treatment reduced iris vascular response, though not to untreated levels ($p = 0.017$). The analysis of vascular sprouting demonstrated an increase of approximately 50% in vessel sprouts of RI-PR irises compared with controls ($p < 0.001$). UPARANT treatment was effective in decreasing blood vessel sprouts to untreated levels, whereas VEGFR1 chimera did not decrease to control the levels of the number of sprouts in the RI-PR model. Additionally, we observed a 40% increase in vessel junctions, represented by vascular branches, respective to control ($p = 0.002$) in RI-PR irises. UPARANT significantly ($p = 0.008$) reduces the number of vascular branches.

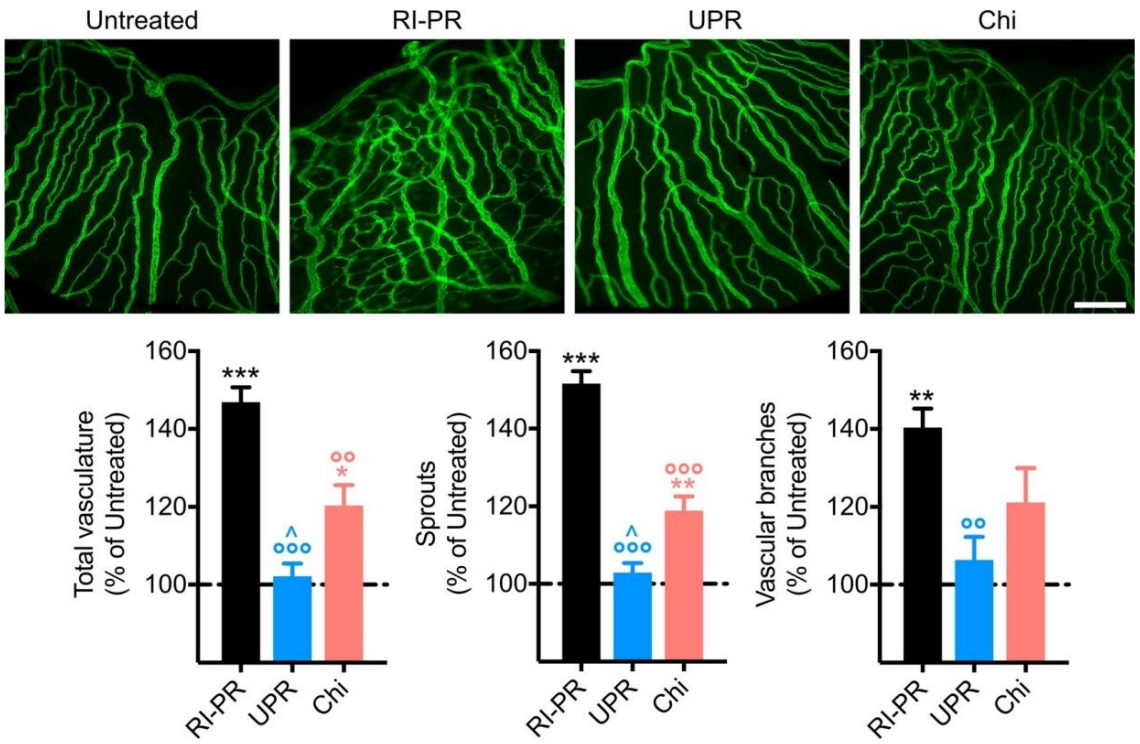

Fig. 3 UPARANT ameliorates pathological iris microvasculature. Iris microvasculature was immunolabeled with PECAM-1, a marker of endothelial cells on experimental day 15. Measurements of total vasculature, number of sprouts, and vascular branches of RI-PR, and UPARANT (UPR) or VEGFR1 chimera (Chi) treated eyes were normalized as percentage of untreated, represented as mean ± SEM ($n = 4$ irises per group), and analyzed by one-way ANOVA with Tukey posttest (**$p < 0.01$ and ***$p < 0.001$ vs untreated; °°$p < 0.01$ and °°°$p < 0.001$ vs RP-PR; ^$p < 0.05$ vs Chi). Scale bar = 200 µm.

UPARANT counteracts inflammation and ECM remodeling in the RI-PR model

Hypoxia and inflammation responses are major players in ocular neovascular diseases. Nuclear factor kappa-light-chain-enhancer of activated B cells (NFκB), hypoxia-inducible factor (HIF)-1α, cyclic AMP response element-binding protein (CREB), and their relevant phosphorylated forms play a prominent role in the regulation of hypoxia and pro-inflammatory processes [25], thus were assayed by western blotting (Fig. 4). We could not determine an increase in HIF-1α in the RI-PR model, while in RI-PR eyes phosphorylated NFκB was significantly increased compared with untreated (p = 0.003), and phosphorylated CREB was slightly increased yet not significantly. Intravitreal UPARANT treatment demonstrated a statistical de- crease in NFκB alone (p = 0.026), as well as VEGFR1 chimera treatment (p = 0.009), when compared with RI-PR eyes. We then evaluated genes associated with iris neovascularization by

qPCR to assess UPARANT effects and to compare them with the effects of VEGFR1 chimera in the RI-PR model (Fig. 5a). We could determine a significant upregulation in various inflammation markers, including interleukin (IL)1β, IL6, transforming growth factor (TGF) α, chemokine C-X-C motif receptor (CXCR)4, and chemokine C-C motif ligand (CCL)2 ($p < 0.001$, IL1β, IL6, CXCR4, $p = 0.002$ CCL2) in RI-PR eyes (Fig. 5a). Moreover, we detected a significant overexpression of extracellular matrix (ECM) remodeling and degradation markers, in the RI-PR eyes. In detail, transcript levels of metalloproteinase (MMP)2 and MMP9, uPAR and its ligands uPA, and plasminogen-activator inhibitor (PAI)-1 were upregulated.

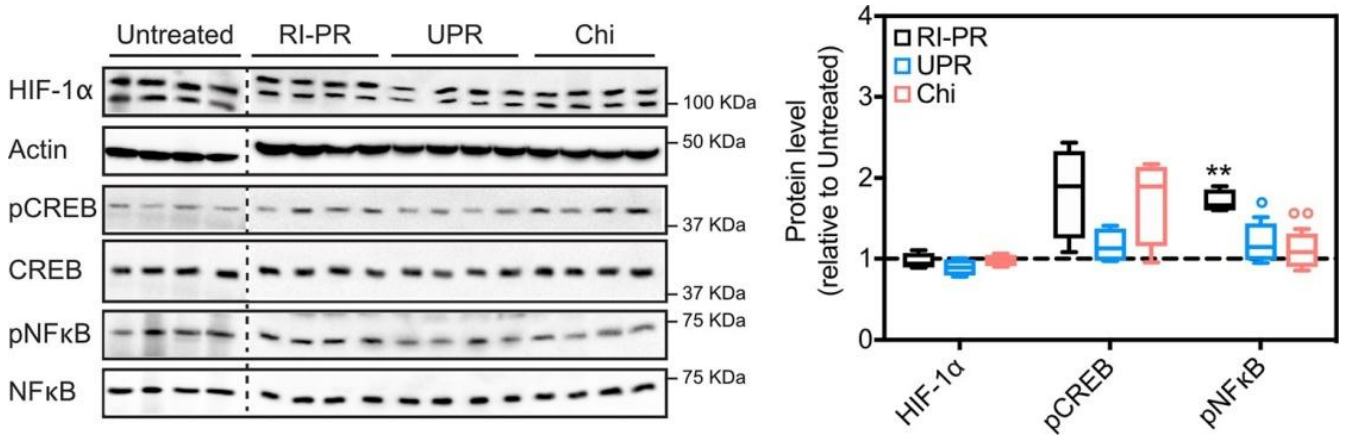

Fig. 4 UPARANT effects on transcriptional regulators during iris neovascularization. Paralleled exposure representative immunoblots of HIF-1α, CREB, and NFκB transcription factors and their relevant phosphorylated forms, of untreated controls, RP-PR, and eyes intravitreally administered with UPARANT (UPR) or VEGFR1 chimera (Chi) are presented for comparison. Quantitative densitometric analysis of protein levels corrected versus actin or non-phosphorylated protein was normalized to untreated controls, presented as box plots ($n = 4$ eyes per group), and analyzed by one-way ANOVA with Tukey post hoc tests (**$p < 0.01$ vs untreated; °$p < 0.05$ and °°$p < 0.01$ vs RP-PR).

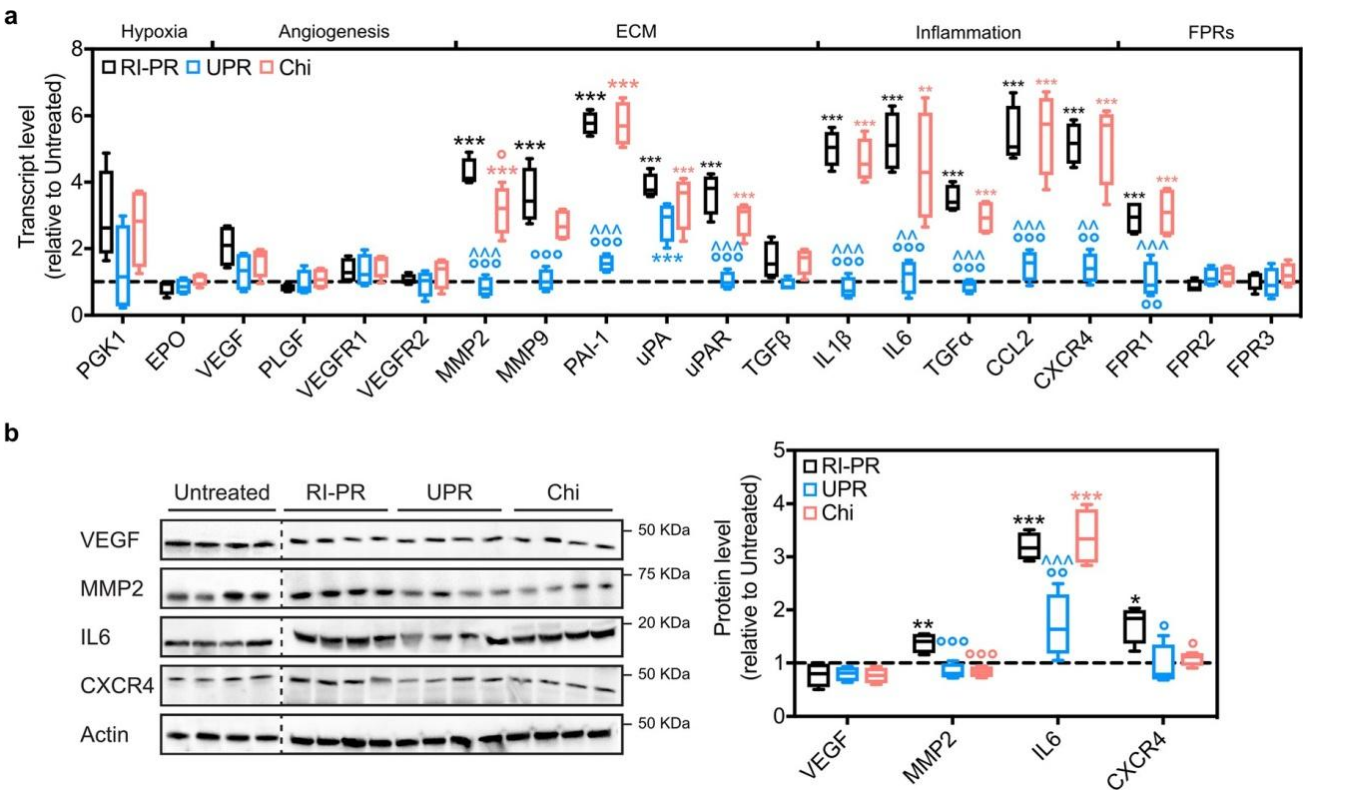

Fig. 5 UPARANT counteracts overexpression of markers associated with iris neovascularization. **a** Expression levels of transcript involved in hypoxia, angiogenesis, ECM remodeling, inflammation, and FPR pathways were analyzed by qPCR in untreated controls, RI-PR, eyes injected with UPARANT (UPR) or VEGFR1 chimera (Chi) intravitreally. Results are showed as box plots (n = 4 eyes per group) and normalized to untreated controls. Statistical evaluation was achieved by one-way ANOVA with Tukey post-hoc tests (**p < 0.01 and ***p < 0.001 vs untreated; °p < 0.05, °°p < 0.01, and °°°p < 0.001 vs RP-PR; ^^p < 0.01 and ^^^p < 0.001 vs Chi). **b** Representative immunoblots of key effectors of angiogenesis of untreated controls, RI-PR, and eyes treated by intravitreal administration of UPARANT (UPR) or VEGFR1 chimera (Chi). Densitometric analysis of protein levels corrected versus actin as loading control were normalized to untreated controls), displayed as box plots (n = 4 eyes per group), and analyzed by one-way ANOVA with Tukey posttest (*p < 0.05, **p < 0.01, and ***p < 0.001 vs untreated; °p < 0.05, °°p < 0.01, and °°°p < 0.001 vs RP-PR; ^^^p < 0.001 vs Chi).

significantly ($p < 0.001$ for all) compared with untreated controls. UPARANT treatment restored RI-PR upregulated markers to control levels, with the exception of uPA transcript level, which was significantly higher than the untreated controls ($p < 0.001$). VEGFR1 chimera treatment of RI-PR-induced eyes did not reduce these overexpressed markers (all markers $p < 0.01$ versus untreated controls), and yielded results statistically different from the UPARANT treatment ($p < 0.001$ MMP2, PAI-1, IL1β, IL6, CCL2, CXCR4, $p = 0.002$ uPAR, $p = 0.003$ TGFα).

As we had observed previously with the punctured-induced RI mouse model [21], genes associated with classical angiogenesis (VEGF, VEGFR1 and VEGFR2, and placental growth factor; PLGF) and genes regulated in response to hypoxia (phospho-glycerate kinase and erythropoietin) were not induced in the RI- PR model. Lastly, FPR1 transcript levels displayed a median increase of 3-fold ($p < 0.001$ versus untreated controls). No al- teration in gene expression level of FPR2 or FPR3 was detected. In agreement with our previous findings [21], UPARANT de-creased FPR1 overexpression to untreated level and differed statistically from RI-PR and VEGFR1 chimera-treated eyes ($p < 0.001$ for both). Notably, no effect on FPR1 expression was observed under VEGFR1 chimera treatment.

To illustrate and analyze protein levels of the major family of genes associated with angiogenesis, inflammation, and extracellular matrix remodeling, as identified by qPCR, we per- formed immunoblotting assays on untreated controls, RI-PR, and intravitreal UPARANT-and VEGFR1 chimera-treated eyes (Fig. 5b). We could not observe significant difference in VEGF expression in the RI-PR model. In RI-PR eyes, we determined a significant increase in MMP2 ($p = 0.008$), IL6 ($p < 0.001$), and CXCR4 ($p = 0.022$) when compared with untreated controls. UPARANT treatment decreased MMP2, IL6, and CXCR4 pro- tein to untreated levels, and these levels were significantly low- er than the levels observed for RI-PR eyes ($p < 0.001$ MMP2; $p = 0.002$ IL6; $p = 0.013$ CXCR4). Treatment with VEGFR1 chimera significantly reduced protein levels of MMP2 ($p < 0.001$) and CXCR4 ($p = 0.047$) compared with RI-PR eyes, with no effect on IL6 levels.

Systemic efficacy of UPARANT in mitigating RI associated with PR

We have demonstrated previously that UPARANT was effective in reducing iris neovascularization by systemic UPARANT each day from experimental day 4 to experimental day 8 for a loading time of 5 days. We determined an increase of more than 135% in blood vessel density in RI-PR eyes, respective to untreated controls ($p < 0.001$; Fig. 6a). Upon quantification of iris blood vessel density, UPARANT subcutaneous treatment proved to be effective as no significant difference was detected between the RI-PR and the untreated contralateral eyes. Moreover, this effect lasted through the duration of the entire study protocol. Gene expression analysis of RI-PR and UPARANT-treated eyes demonstrated paralleled findings as the intravitreal treatment. In the RI-PR model (Fig. 6b), the up- regulated markers of extracellular matrix remodeling, including MMP2 and MMP9, uPAR, uPA, PAI-1, and inflammation, including IL1β, IL6, CCL2, and CXCR4, were significantly reduced to untreated control levels (all $p < 0.001$) upon UPARANT systemic treatment. As before, we observed that canonical VEGF pathway was not upregulated in RI-PR mice, and the upregulation of FPR1 transcription was significantly decreased to the untreated group ($p < 0.001$ versus RI-PR) in UPARANT-treated animals.

Discussion

Here, we demonstrate further evidence of the tetrapeptide UPARANT efficacy in mitigating RI, in a mouse model associated with PR, in both local (intravitreal) and systemic (subcutaneous) regimens. In addition, since treatment of RI with anti-VEGF drugs is a current clinical

standard [7–10], we compare intravitreal treatment with UPARANT to an anti-VEGF regimen.

Patients with RI commonly express high VEGF levels as a consequence of the underlying PR [4, 9, 10]. Nonetheless, the puncture-induced RI mouse model previously established by us has been demonstrated to be independent of VEGF signaling [19, 21]. Hypoxia-conditioned medium from ARPE-19 cells contains increased levels of VEGF and multiple other pro-angiogenic factors and cytokines [19, 23]. Combination of the puncture-induced RI with co-injection of hypoxia- conditioned medium enhances the RI-PR mouse model to more closely parallel patients with iris neovascularization as a consequence of associated eye diseases. As indicated by an increase in iris vasculature in the RI-PR model as compared with RI (Suppl. Fig. 1), the RI-PR mouse model represents as an ideal candidate for comparison of UPARANT treatment to anti-VEGF.

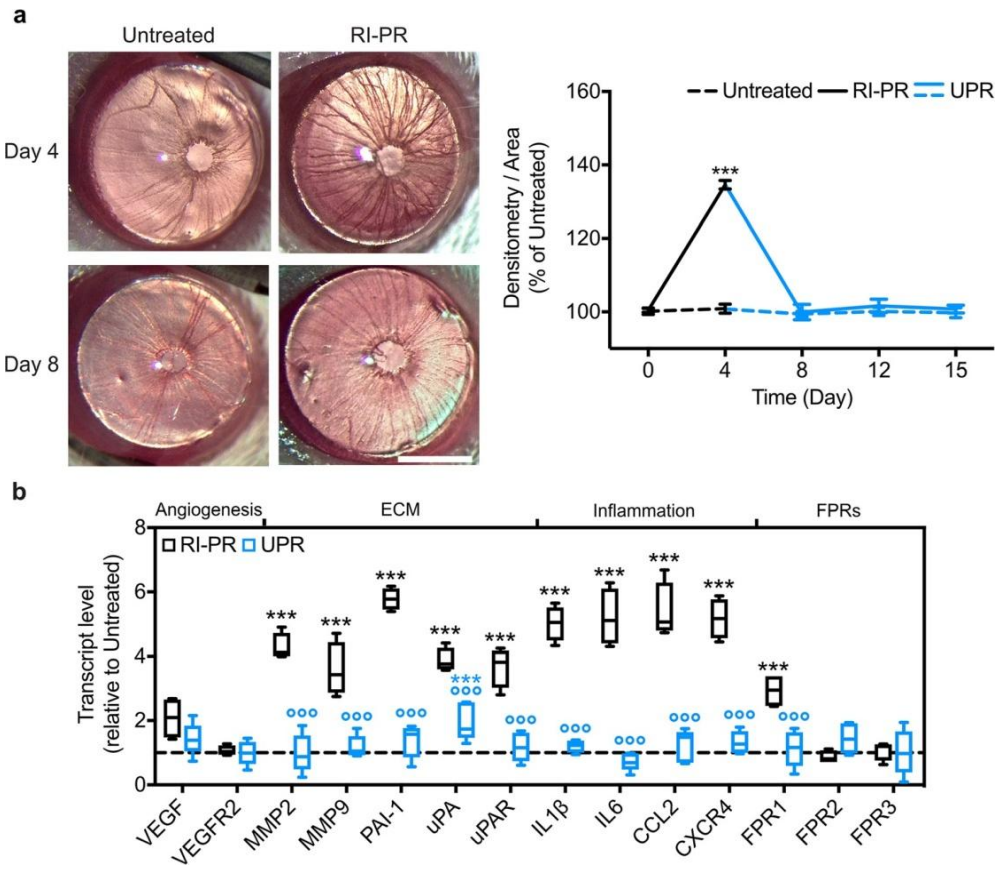

Fig. 6 Systemic delivery of UPARANT efficiently reduces RI-PR. **a** Pictures illustrate mouse iris vasculature at experimental days 4 and 8 of the untreated controls and RI-PR eyes with UPARANT delivered subcutaneously. Scale bar = 1 mm.

Densitometry of iris vasculature was normalized as percentage of untreated controls and presented as mean ± SEM of independent eyes (n = 5 per group). Statistical analysis was performed by two- way ANOVA with Tukey posttest (***p < 0.001 vs untreated). **b** Gene expression was analyzed by qPCR in RI-PR eyes treated subcutaneously with vehicle (n = 4) or with subcutaneous UPARANT (UPR; n = 5). Result were nor- malized to untreated controls and presented as box plots. Statistical analysis by one-way ANOVA with Tukey posttest (***p < 0.001 vs untreated; °°°p < 0.001 vs RP-PR)

Intravitreal administration of UPARANT promptly reduces RI-PR macrovasculature, as determined by noninvasive analysis of iris vasculature. Despite a considerable slower effect, anti-VEGF treatment produced similar outcomes within the study protocol. The mouse iris neovasculature develops through anastomosis [19], characterized by formation of vascular sprouts and branching. Analysis of irises microvasculature with PECAM-1 demonstrates that UPARANT- treated RI-PR eyes are indistinguishable from controls regarding number of blood vessels, sprouting, and branching, with a stronger reduction when compared with anti-VEGF. Overall, UPARANT demonstrates a faster mitigation and broader efficacy in decreasing microvascular events compared with anti- VEGF strategies in the RI-PR murine model. These data are in agreement with our previous studies demonstrating inflammation and ECM degradation as primary mechanisms of iris neovascularization in the mouse model [19, 21], even in the presence of increased hypoxia-mediated proangiogenic factors, including VEGF and many other factors as we demonstrate here. Our results corroborate that UPARANT acts on several angiogenic pathways, while anti-VEGF strategies are limited to VEGFR-driven angiogenesis. In fact, UPARANT reduces all analyzed iris microvascular parameters in the murine model of RI-PR to levels undistinguishable from untreated controls, while anti-VEGF treatment only significantly reduced vascular branching in RI-PR—a mechanism dependent on gradients of angiogenic factors, particularly VEGF [26]. As demonstrated in previous studies [14, 16–18, 21], UPARANT antagonizes uPAR/FPR signaling. In the iris, we have demonstrated FPR1 expression is localized on endothelial cells, and activation of FPR1 mediated hypoxia and inflammation cascades [21]. We analyzed the expression of the pivotal transcription factors for the hypoxia and pro-inflammatory signaling: HIF-1α, CREB, and NFκB. UPARANT antagonism of FPR1 in the mouse model of RI-PR downregulates inflammation-mediated transcription and is independent of the hypoxia pathways. In agreement with our previous findings [21], transcripts and proteins mediated by canonical hypoxia and angiogenesis were not modulated in the RI-PR model. Our data suggests that even in the presence of increased hypoxia- driven pro-angiogenic factors, the ECM and inflammation mechanisms of iris neovascularization appear predominant in the mouse models of induced RI.

Regulation of NFκB phosphorylation (pNFκB) by the plasminogen-activator and inflammation pathways is fundamental in angiogenesis [27–29]. We demonstrate reduced pNFκB levels in UPARANT-treated irises with concomitant downregulation of transcripts involved in ECM degradation and inflammation in the murine model of RI-PR, to levels comparable with untreated controls. Noticeable, a discreet non-significant increase in VEGF transcript levels is deter- mined in the RI-PR model, which could be the result of a crosstalk between the VEGFR- and FPR-mediated signaling, as previously suggested [30, 31]. Despite the fact, regulation of ECM degradation and inflammation transcripts in the RI- PR murine model is not affected by anti-VEGF treatment, which suggests a major role for FPR-mediated mechanisms over VEGFR-dependent pathways in iris neovascularization. Our findings on the effects of UPARANT and anti-VEGF treatment on gene expression are further evidenced by protein expression analysis in the RI-PR murine model. The cytokine IL6 is upregulated in the RI-PR model, and downregulated by UPARANT, but not by anti-VEGF treatment. In addition, in RI-PR eyes, the elevated protein levels of MMP2 and CXCR4 are reduced by both UPARANT and anti-VEGF treatment. Molecular dissection of MMP2 and CXCR4 protein upregulation in the RI-PR model might be influenced by the extensive increase of proangiogenic cytokines originating from hypoxia-conditioned ARPE-19 cell medium [19, 23]. Albeit, activation of VEGFRs independently of VEGF has been suggested through crosstalk with protein G-dependent signaling [31]. MMP2 increased protein levels could be a result of FPR-mediated VEGFR signaling, therefore being reduced by both UPARANT and anti-VEGF treatments in the RI-PR model. Interestingly, CXCR4 levels are significantly reduced in the RI-PR model, by both UPARANT and anti-VEGF. CXCR4 ligand, stromal-derived factor-1, has been implicated in the recruitment of circulating endothelial progenitor cells in the laser-induced choroidal neovascularization model [32]. Together with the previously demonstrated lack of vascular leakage in the induced iris neovascularization mouse model [21], upregulation of CXCR4 could be supporting the formation of anastomotic vessels, a mechanism associated mouse models of iris neovascularization [19, 33].

Systemic administration of UPARANT has been shown to distribute to the eye at pharmacological levels in multiple animal models [16–18], including models of iris neovascularization [21]. In similarity to the mouse model of puncture- induced RI, subcutaneous administration of UPARANT mitigates neovascularization and reduces upregulated transcripts to control levels in the RI-PR mouse model, much paralleled to the finding with local administration of UPARANT.

In the RI-PR model, mouse pups respond rapidly to the induction stimuli by increasing the anastomotic vessels of the iris. However, the stimuli must be repeated routinely to maintain the pathological stress, and warrant maturation of the anastomoses [19]. Interestingly, UPARANT treatment of RI-PR eyes suggests a protective effect on iris endothelial cell remodeling, thus sustaining the iris vasculature at control levels through the study period. On the contrary, anti-VEGF regimen can protect only endothelia from VEGF-specific signaling, resulting in the ob- served delay of iris vascular recovery. Our findings are in line with previous studies in rodent models, where UPARANT- mediated vascular recovery was associated with amelioration of vision loss [15, 17, 18]. Currently, treatment of RI associated with PR diseases relies on anti-VEGF intravitreal regimens [7]. The presence of various proangiogenic molecules and cytokines in PR patients [3, 4] has been associated with the limited effects of anti-VEGF treatment and the sustained need for pan-retinal photocoagulation [34], as neovascularization reoccurs in RI patients [8]. Our data demonstrates that local administration of UPARANT in the eye results in a stronger reduction in iris vascularization when compared with anti-VEGF regimen. Whereas anti-VEGF strategies focus exclusively on VEGF- driven signals, UPARANT modulates the upstream molecular mechanisms leading to angiogenesis and inflammation, and simultaneously downregulates multiple growth factors and cytokines involved in iris neovascularization. Together, our present study suggests a rational for UPARANT increased effectiveness when compared with anti-VEGF treatment in themouse model of RI-PR, indicating a gain of insight in the role of UPARANT in mitigating RI, as previously suggested by us [21]. Furthermore, the effectiveness of subcutaneous UPARANT administration is in line with systemic treatments of proliferative ocular pathologies, which could improve the treatment of patient afflicted by PDR and CRVO, or even NVG.Acknowledgments We thank Flavia Plastino for technical support and Diana Rydholm for animal husbandry.

Funding Open access funding provided by Karolinska Institute. This study was supported by research funding from Kaleyde Pharmaceuticals AG (Lugano, Switzerland) and the Karolinska Institutet Foundation

Data availability All study data is disclosed in the present work and its supplementary material. The materials used are available from the corre- sponding author on reasonable request.

Compliance with ethical standards

Conflict of interest M.D.R. and V.P. are patent holders for UPARANT with personal interest in Kaleyde Pharmaceuticals AG. All other authors declare no conflicts of interest.

References

1. network and its endothelial cells in the human iris. Curr Eye Res 43: 67–76
2. Dreyfuss JL, Giordano RJ, Regatieri CV (2015) Ocular Angiogenesis. J Ophthalmol 2015:2–4
3. Kovacs K, Marra KV, Yu G, Wagley S, Ma J, Teague GC, Nandakumar N, Lashkari K, Arroyo JG (2015) Angiogenic and inflammatory vitreous biomarkers associated with increasing levels of retinal ischemia. Investig Ophthalmol Vis Sci 56:6523–6530
4. Gartner S, Henkind P (1978) Neovascularization of the iris (rubeosis iridis). Surv Ophthalmol 22:291–312
5. Jeong YC, Hwang YH (2016) Etiology and features of eyes with rubeosis iridis among Korean patients: a population-based single center study. PLoS One 11:4–11
6. Rodrigues GB, Abe RY, Zangalli C, Sodre SL, Donini FA, Costa DC, Leite A, Felix JP, Torigoe M, Diniz-Filho A et al (2016) Neovascular glaucoma: A review. Int J Retin Vitr 2:1–10
7. Gheith ME, Siam GA, Monteiro de Barros DS, Garg SJ, Moster MR (2007) Role of intravitreal bevacizumab in neovascular glau- coma. J Ocul Pharmacol Ther 23:487–491
8. Kotecha A, Spratt A, Ogunbowale L, dell'Omo R, Kulkarni A, Bunce C, Franks WA (2011) Intravitreal bevacizumab in refractory neovascular glaucoma. Arch Ophthalmol 129:145–150
9. Slabaugh M, Salim S (2017) Use of anti-VEGF agents in glaucoma surgery. J Ophthalmol 2017:1645269–1645266
10. Simha A, Aziz K, Braganza A, Abraham L, Samuel P, Lindsley KB, Cochrane Eyes and Vision Group (2020) Anti-vascular endo- thelial growth factor for neovascular glaucoma. Cochrane Database Syst Rev 2:CD007920

11. Carriero MV, Longanesi-Cattani I, Bifulco K, Maglio O, Lista L, Barbieri A, Votta G, Masucci MT, Arra C, Franco R et al (2009) Structure-based design of an urokinase-type plasminogen activator receptor-derived peptide inhibiting cell migration and lung metas- tasis. Mol Cancer Ther 8:2708–2717
12. Carriero MV, Bifulco K, Minopoli M, Lista L, Maglio O, Mele L, di Carluccio G, de Rosa M, Pavone V (2014) UPARANT: a Urokinase receptor–derived peptide inhibitor of VEGF-driven an- giogenesis with enhanced stability and in vitro and in vivo potency. Mol Cancer Ther 13:1092–1104
13. Rezzola S, Corsini M, Chiodelli P, Cancarini A, Nawaz IM, Coltrini D, Mitola S, Ronca R, Belleri M, Lista L et al (2017) Inflammation and N-formyl peptide receptors mediate the angio- genic activity of human vitreous humour in proliferative diabetic retinopathy. Diabetologia 60:719–728
14. Cammalleri M, Dal Monte M, Pavone V, de Rosa M, Rusciano D, Bagnoli P (2019) The uPAR system as a potential therapeutic target in the diseased eye. Cells 8:925
15. Dal Monte M, Rezzola S, Cammalleri M, Belleri M, Locri F, Morbidelli L, Corsini M, Paganini G, Semeraro F, Cancarini A et al (2015) Antiangiogenic effectiveness of the urokinase receptor- derived peptide UPARANT in a model of oxygen- induced retinopathy. Investig Ophthalmol Vis Sci 56:2392–2407
16. Cammalleri M, Dal Monte M, Locri F, Lista L, Aronsson M, Kvanta A, Rusciano D, de Rosa M, Pavone V, André H et al (2016) The urokinase receptor-derived peptide UPARANT miti- gates angiogenesis in a mouse model of laser-induced choroidal neovascularization. Investig Ophthalmol Vis Sci 57:2600–2611
17. Cammalleri M, Locri F, Marsili S, Dal Monte M, Pisano C, Mancinelli A, Lista L, Rusciano D, de Rosa M, Pavone V et al (2017) The urokinase receptor-derived peptide UPARANT re- covers dysfunctional electroretinogram and blood-retinal barrier leakage in a rat model of diabetes. Investig Ophthalmol Vis Sci 58:3138–3148
18. Cammalleri M, Dal Monte M, Locri F, Marsili S, Lista L, de Rosa M, Pavone V, Rusciano D, Bagnoli P (2017) Diabetic retinopathy in the spontaneously diabetic Torii rat: pathogenetic mechanisms and preventive efficacy of inhibiting the urokinase-type plasmino- gen activator receptor system. J Diabetes Res 2017:1–18
19. Beaujean O, Locri F, Aronsson M, Kvanta A, André H (2017) A novel in vivo model of puncture-induced iris neovascularization. PLoS One 12:1–14
20. Locri F, Aronsson M, Beaujean O, Kvanta A, André H (2018) Puncture-induced iris neovascularization as a mouse model of rubeosis iridis. J Vis Exp 2018:1–6
21. Locri F, Dal Monte M, Aronsson M, Cammalleri M, de Rosa M, Pavone V, Kvanta A, Bagnoli P, André H (2019) UPARANT is an effective antiangiogenic agent in a mouse model of rubeosis iridis. J Mol Med 57:2600–2611
22. Boccella S, Panza E, Lista L, Belardo C, Ianaro A, de Rosa M, de Novellis V, Pavone V (2017) Preclinical evaluation of the uroki- nase receptor-derived peptide UPARANT as an anti-inflammatory drug. Inflamm Res 66:701–709
23. Takei A, Ekström M, Mammadzada P, Aronsson M, Yu M, Kvanta A, André H (2017) Gene transfer of prolyl hydroxylase domain 2 inhibits hypoxia-inducible angiogenesis in a model of choroidal neovascularization. Sci Rep 7:1–14
24. Zudaire E, Gambardella L, Kurcz C, Vermeren S (2011) A compu- tational tool for quantitative analysis of vascular networks. PLoS One 6:1–12
25. Nakayama K, Kataoka N (2019) Regulation of gene expression under hypoxic conditions. Int J Mol Sci 20:3278
26. Gerhardt H, Golding M, Fruttiger M, Ruhrberg C, Lundkvist A, Abramsson A, Jeltsch M, Mitchell C, Alitalo K, Shima D et al (2003) VEGF guides angiogenic sprouting utilizing endothelial tip cell filopodia. J Cell Biol 161:1163–1177
27. Prevete N, Liotti F, Marone G, Melillo RM, de Paulis A (2015) Formyl peptide receptors at the interface of inflammation, angio- genesis and tumor growth. Pharmacol Res 102:184–191
28. Tilborghs S, Corthouts J, Verhoeven Y, Arias D, Rolfo C, Trinh XB, van Dam PA (2017) The role of nuclear factor-kappa B signaling in human cervical cancer. Crit Rev Oncol Hematol 120: 141–150
29. Swamynathan S, Loughner CL, Swamynathan SK (2017) Inhibition of HUVEC tube formation via suppression of NFκB suggests an anti-angiogenic role for SLURP1 in the transparent cornea. Exp Eye Res 164:118–128
30. Motta C, Lupo G, Rusciano D, Olivieri M, Lista L, de Rosa M, Pavone V, Anfuso CD (2016) Molecular mechanisms mediating antiangiogenic action of the urokinase receptor-derived peptide UPARANT in human retinal endothelial cells. Investig Ophthalmol Vis Sci 57:5723–5735
31. Koch S, Claesson-Welsh L (2012) Signal transduction by vascular endothelial growth factor receptors. Cold Spring Harb Perspect Med 2:169–183
32. Zhang ZX, Wang YS, Shi YY, Hou HY, Zhang C, Cai Y, Dou GR, Yao LB, Li FY (2011) Hypoxia specific SDF-1 expression by ret- inal pigment epithelium initiates bone marrow-derived cells to par- ticipate in choroidal neovascularization in a laser-induced mouse model. Curr Eye Res 36:838–849
33. Ridiandries A, Tan JTM, Bursill CA (2016) The role of CC-chemokines in the regulation of angiogenesis. Int J Mol Sci 17:1– 16
34. Olmos LC, Sayed MS, Moraczewski AL, Gedde SJ, Rosenfeld PJ, Shi W, Feuer WJ, Lee RK (2016) Long-term outcomes of neovascular glaucoma treated with and without intravitreal bevacizumab. Eye 30:463–472

PAPER III

cells

MDPI

Article

Autophagy Involvement in the Postnatal Development of the Rat Retina

Noemi Anna Pesce [1,2], Alessio Canovai [2], Emma Lardner [1], Maurizio Cammalleri [2], Anders Kvanta [1], Helder André [1,*,†] and Massimo Dal Monte [2,†]

[1] Department of Clinical Neuroscience, Division of Eye and Vision, St. Erik Eye Hospital, Karolinska Institutet, Eugeniavägen 12, 17164 Solna, Sweden; n.pesce@student.unisi.it (N.A.P.); emma.lardner@sll.se (E.L.); anders.kvanta@ki.se (A.K.)

[2] Department of Biology, University of Pisa, Via San Zeno 31, 56127 Pisa, Italy; a.canovai@studenti.unipi.it (A.C.); maurizio.cammalleri@unipi.it (M.C.); massimo.dalmonte@unipi.it (M.D.M.)

* Correspondence: helder.andre@ki.se; Tel.: +46-700-923-479

† These authors contributed equally to the present work.

Abstract: During retinal development, a physiologic hypoxia stimulates endothelial cell proliferation. The hypoxic milieu warrants retina vascularization and promotes the activation of several mechanisms aimed to ensure homeostasis and energy balance of both endothelial and retinal cells. Autophagy is an evolutionarily conserved catabolic system that contributes to cellular adaptation to a variety of environmental changes and stresses. In association with the physiologic hypoxia, autophagy plays a crucial role during development. Autophagy expression profile was evaluated in the developing retina from birth to post-natal day 18 of rat pups, using qPCR, western blotting and immunostaining methodologies. The rat post-partum developing retina displayed increased active autophagy during the first postnatal days, correlating to the hypoxic phase. In latter stages of development, rat retinal autophagy decreases, reaching a normalization between post-natal days 14-18, when the retina is fully vascularized and mature. Collectively, the present study elaborates on the link between hypoxia and autophagy, and contributes to further elucidate the role of autophagy during retinal development.

Keywords: eye; retina; development; vascularization; hypoxia; autophagy

Citation: Pesce, N.A.; Canovai, A.; Lardner, E.; Cammalleri, M.; Kvanta, A.; André, H.; Dal Monte, M. Autophagy Involvement in the Postnatal Development of the Rat Retina. *Cells* **2021**, *10*, 177. https://doi.org/10.3390/cells10010177

Received: 18 December 2020

Accepted: 14 January 2021

Published: 17 January 2021

1. Introduction

The mature retina is considered one of the highest oxygen-demanding tissues in the body, with a considerable metabolic activity [1,2]. The heightened metabolic demand of the retina is supplied by a structured vascular systems, including retinal vessels and the choriocapillaris, which provide nutrients and oxygen to the inner and the outer layers of the retina respectively [3,4]. During development of the mammalian eye, the retinal vasculature undergoes considerable changes and reorganization [5]. In the early stages of embryogenesis, the interior of the eye is metabolically supplied by a transient embryonic circulatory network in the vitreous, referred to as the hyaloid system [6]. In the latter stages of development, the hyaloid vasculature regresses and concurrently is replaced by the retinal vasculature [7]. The physiologic hypoxia in uterus (O_2 levels < 5%) drives the proliferation of retinal blood vessels from the optic nerve to the periphery [8], through vascular endothelial growth factor (VEGF)-mediated angiogenesis [9,10].

At this level, the developing retinal vasculature lacks a functional barrier, necessary to maintain homeostasis into the retina and controlling vascular permeability [11,12]. Thus, the retinal capillary endothelial cells interact with each other to create a complex network, composed of tight junctions between transmembrane and peripheral membrane proteins. In this manner, the retinal endothelial cells form an inner blood retinal barrier (BRB),

which contributes to preserve neuronalenvironment regulating the entry of molecules from the blood into the retina [13,14]. At these critical times in developmental events, both retinal and endothelial cells (ECs) endure morphological changes and reorganization; as consequence, they require mechanisms for the degradation and recycling of obsolete cellular components [15].

Autophagy is an essential process in maintaining the normal cellular homeostasis under physiological conditions [16]; and it plays an important role in the turnover of damaged organelles, such as peroxisomes and endoplasmic reticulum, as well as in re- moving unnecessary aggregated or misfolded proteins [17,18]. Previous findings indicate that vascular remodeling in ocular development can be regulated by autophagy [19]; the blood vessels need autophagy to balance their bioenergetic dynamic mechanisms [20]. Moreover, autophagic mechanisms seem to have a critical role in anatomical involution of the hyaloid blood vessels [19]. Several studies have demonstrated that autophagy can be induced by physiological hypoxia, the key stimulus for retinal angiogenesis [21–23]. At the molecular level, hypoxia stimulates several molecules involved in different signaling path- ways, including hypoxia-inducible factors (HIFs) that induce angiogenesis through VEGF; and adenosine monophosphate-activated protein kinase (AMPK), a positive regulator of autophagy [24,25]. In conditions where nutrients are scarce, such as during development, AMPK is activated by a decreased ATP/AMP ratio and leads to phosphorylation of several molecules, including Unc-51-like autophagy activating kinase (ULK)1 [26,27]. Activated ULK1 is involved in the formation of multiple protein complexes that are responsible for the initiation of autophagic mechanisms that lead to the formation of autophagosome [28,29]. Elongation and maturation of the autophagosome involve the microtubule-associated protein I light chain 3 (LC3 I) system. LC3 I is conjugated to phosphatidylethanolamine, converted to LC3 II and inserted into the autophagosome membrane [30]. The synthesis and processing of LC3 II is increased during autophagy, thus acting as a key marker of lev- els of autophagy in cells [31]. The cargo is selected by targeted ubiquitination and carried to the autophagosome through the binding of LC3 II with sequestosome-1 (SQSTM-1), also known as ubiquitin-binding protein p62 [32,33]. The p62 is degraded by autophagy and a decrease in its protein levels correlates with an active autophagic flux [34]. Autophagy ends with the fusion of the autophagosome with the lysosome, where the inner cargo is degraded by lysosomal hydrolases.

Considering the myriad of autophagic mechanisms, the aim of the present study was to examine the changes of expression of autophagy markers in the developing retina in postnatal rats. Due to its postnatal development and accessibility, the rat retinal vasculature warrants a bonafide model to assess vascular developmental autophagy mechanisms from birth through postnatal day (P) 18 when retinal vasculature has attained its adult pattern.

2. Material and Methods

2.1. Animals and Ethics Statements

After birth, 84 Wistar rat pups were maintained with their nursing mothers through the experimental times P7, P14 and P18 in a regulated environment (24 1°C, 50 5% humidity), with a 12 h light/dark cycle and provided with food and water. Rat pups were euthanized with an intraperitoneal injection of 30 mg/kg of pentobarbital. All animal protocols were in accordance with the Statement for the Use of Animals in Ophthalmic and Vision Research (ARVO), the Italian regulation for animal care (DL 116/92), and the European Communities Council Directive (86/609/EEC). Animal procedures were authorized by the Ethical Committee in Animal Experiments of the University of Pisa (permit number: 133/2019-PR, 14 February 2019).

2.2. Vascular Labeling

A total of 24 rat pups of different ages (birth, P7, P14 and P18; six rats for each time point) were used to prepare whole-mount and retina sections. Isolated retinas were fixed in 4% paraformaldehyde in 0.1 M phosphate buffer, pH 7.4 (PB), at room temperature for

3 h. Subsequently, retinas were washed three times (5 min per wash) in PB and incubated for 1 h at room temperature (RT) in blocking buffer (PB containing 10% donkey serum and 0.5% Triton X-100; Sigma-Aldrich, St. Louis, MO, USA) to prevent non-specific labeling. Sequentially, retinas were incubated with fluorescein-labelled isolectin B4 (1:200; Vector Laboratories, Burlingame, CA, USA) in blocking solution, at 4 ˚C overnight (ON). Finally, after three washes with PB, retinas were placed onto a slide, mounted and covered with a coverslip. Immunostaining was observed by a digital fluorescence microscope (Ni-E; Nikon-Europe, Amsterdam, The Netherlands) and immunofluorescent images of the retinal vasculature were acquired using a digital camera (DS-Fi1c; Nikon-Europe). The vascular area and the total area were measured using ImageJ freeware. Vascular area was reported as percentage of the total area.

1.1. Western Blot Analysis

Proteins were extracted from retinas of 24 rat pups at different ages (birth, P7, P14 and P18; six rats for each time point) using RIPA lysis buffer (Santa Cruz Biotechnology, Dallas, TX, USA), supplemented with phosphatase inhibitor (Sigma-Aldrich) and protease inhibitor (Roche, Mannheim, Germany) cocktails. Protein extracts were quantified by the microBCA method (Thermo Fisher Scientific, Waltam, MA, USA) and 15 µg of total proteins were separated by SDS-PAGE and transferred onto polyvinylidene difluoride (PVDF) membranes (Bio-Rad Laboratories, Hercules, CA, United States). Membranes were blocked either with 5% of skim milk in Tris-buffered saline (TBS-T; Bio-Rad Laboratories, containing 0.05% Tween-20; Sigma-Aldrich) or with 4% of Bovine Serum Albumin (BSA; Sigma-Aldrich) in TBS-T, for 1 hour at RT. Subsequently, the membranes were incubated at 4 ˚C ON with primary antibodies: anti-HIF-1α (1:500, rabbit polyclonal, cat. no. NB100479; Novus Biologicals, Centennial, Colorado, USA); anti-pAMPKα (Thr172, 1:500, rabbit monoclonal, cat. no. 2535S; Cell Signaling Technology); anti-AMPKα (1:1000, rabbit monoclonal, cat. no. 5832S; Cell Signaling Technology); anti-pULK1 (Ser^{555}; 1:500, rabbit monoclonal, cat. no. 5869S; Cell Signaling Technology, Danvers, MA, USA); anti-ULK1 (1:1000, rabbit monoclonal, cat. no. 8054S; Cell Signaling Technology); anti-LC3 I and II (1:1000, rabbit polyclonal, cat. no. 4108S; Cell Signaling Technology); anti-p62 (1:1000, rabbit polyclonal, cat. no. ab-91526; Abcam, Cambridge, UK); and anti-β-actin (1:5000, rabbit monoclonal, cat. no. SAB5600204; Sigma-Aldrich). Secondary antibody anti-rabbit- IgG conjugated to horseradish peroxidase (1:10,000, cat. no. P044801-2; Dako, Carpinteria, CA, USA) was incubated for 1 h at RT. Following the incubation with both primary and secondary antibodies the membranes were washed with TBS-T, three times for 5 min. Finally, the protein of interest was visualized using the Clarity Western ECL substrate with a ChemiDoc XPS^{+} imaging system (Bio-Rad Laboratories, Hercules CA, USA). The optical density (OD) of the bands was determined with the Image Lab 3.0 software (Bio- Rad Laboratories). Protein levels were corrected to the β-actin loading control or non- phosphorylated proteins.

1.2. Quantitative PCR

Total RNA was extracted and purified from retinas of 24 rat pups at different ages (birth, P7, P14 and P18; six rats for each time point), using the Trizol® reagent (Invitrogen, Waltam MA, USA), resuspended in RNAse-free water, and quantified by spectrophotom- etry (BioSpectrometer basic; Eppendorf AG, Hamburg, Germany). First-strand cDNA was generated from 1 µg of total RNA (QuantiTect Reverse Transcription Kit; Qiagen, Hilden, Germany). Quantitative PCR was performed with a kit (SsoAdvanced Univer- sal SYBR Green Supermix; Bio-Rad Laboratories) on a CFX96 Real Time PCR Detection System (equipped with the CFX manager software (Bio-Rad Laboratories). Forward and reverse sequence of primers were chosen to hybridize to unique region of the appropriate gene sequence: occludin-1 (Forward: 5'-TTTCATGCCTTGGGGATTGAG-3'/Reverse: 5'-GACTTCCCAGAGTGCAGAGT-3'; Invitrogen); zonula-occludens-1 (ZO-1; Forward: 5'- AGTCTCGGAAAAGTGCCAGG-3'/Reverse: 5'-GGGCACCATACCAACCATCA-3^{J}; Invitrogen); VEGF-A (Forward: 5'-CAATGATGAAGCCCTGGAGTG-3'/Reverse: 5'-AGGTTTGATCCGCATGATCTG-3; Invitrogen) and Ribosomal Protein L13a (Rpl13a; Forward: 5^{J}- GGATCCCTCCACCCTATGACA-3^{J}/Reverse: 5^{J}-CTGGTACTTCCACCCGACCTC-3^{J}; Invitrogen). Samples were compared by the threshold cycle analysis (Ct) and absolute expression values were calculated using the $2^{-\Delta\Delta Ct}$ formula, with Rpl13a as the housekeeping gene.

2.3. Immunohistofluorescence

In total, 12 rat pups at different ages (birth, P7, P14 and P18; three rats for each time point) were fixed in 4% paraformaldehyde in PB at RT for 5 days prior to immunofluores- cence staining. Sections of 4 micrometers were processed for immunohistofluorescence in a Bond III robotic

system (Leica Biosystems, Newcastle, UK), as previously described [35]. According to the manufacturer's instructions, antigen retrieval was performed in 10 mM citrate buffer pH6 and sections were incubated with primary antibody step with anti-LC3 I and II (1:100) and isolectin-biotin (1:1000; cat. no. I21414; Thermo Fisher Scientific), while secondary antibody steps included Streptavidin-Alexa 488 (1:500; cat. no. S11223, Thermo Fisher Scientific), anti-rat-Alexa 546 (1:500; cat. no. A11081, Invitrogen) and anti-goat-Alexa 647 (1:500; cat. no. SAB4600175, Sigma-Aldrich). Sections were mounted by using a vector Vectashield with DAPI mounting medium (Vector Laboratories, CA, Burlingame, USA), and visualized with an Axioscope 2 plus with the AxioVision software (Zeiss, Gottingen, Germany).

2.4. Statistical Analysis

The statistical analyses were performed using Prism software (GraphPad software, Inc., San Diego, CA, USA), applying one-way ANOVA with Bonferroni's multiple com- parisons posttest. Data were presented as mean ± standard error of mean (SEM) of $n = 6$; p values < 0.05 were considered statistically significant.

3. Results

4.

4.1. The Rat Retina Is Partially Avascular at Birth

Fluorescein-labeled isolectin B4 was used to assess the progress of retinal vascular- ization in the rat. As previously described, rat retinal vascularization is almost completed around P13-P16 [36]. As depicted in Figure1A, at birth the hyaloid vasculature was still present and the retina remained partially avascular, as determined by measuring the vascular area as less than 50% of total area of the retina (Figure1B). Quantitative anal- ysis demonstrated a significant difference at P7, where the retina was 90% vascularized ($p < 0.001$) and in the late stages of ocular blood vessel development, P14-P18 ($p < 0.001$), where the retinas were fully vascularized (100%) as compared to birth.

4.2. Different Expression of Blood-Retina Barrier Genes during Rat Retina Development

In retinal blood vessels, ECs present tight junctions that function as a part of the BRB, fundamental to maintain retinal homeostasis and to mediate selective diffusion of molecules from the circulation to the retinal tissue [14,37]. Consequently, analysis of the expression of BRB genes in the rat retinas at birth, P7, P14 and P18 was performed by qPCR (Figure2). Transcript expression levels of occludin-1 and ZO-1 were upregulated at P14 and P18, compared to birth and P7 ($p < 0.01$ both). These results confirmed that at birth and P7 the rat retinal vasculature was still under development, presenting an incomplete vascular network.

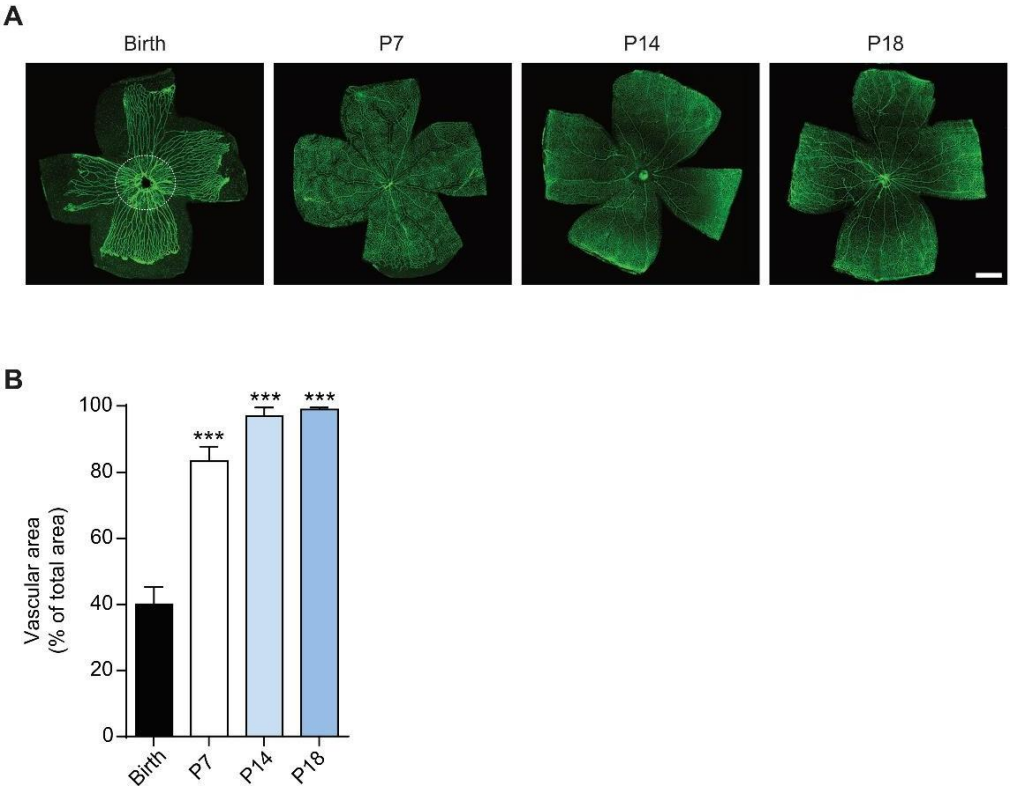

Figure 1. Development of the vascular network in rat retina. (**A**) Visualization of blood vessels by isolectin B4 staining of rat pup retinas at birth, postnatal day (P)7, P14 and P18. Dashed circle delineates the developing retinal vasculature (inner of the dashed circle) with the hyaloid vasculature (outer of the dashed circle). Scale bar = 500 μm. (**B**) Quantitative analysis of vascular area of the retina. Data is presented as mean ± SEM. One-way ANOVA was used as statistical analysis, followed by Bonferroni's multiple comparisons test ($n = 6$; *** $p < 0.001$ vs. birth).

1.1. At P7 the Rat Retina Is Hypoxic

During retinal development, physiologic hypoxia induces the activation of HIF-1α, which promotes the transcription of *VEGF-A* gene. This process is pivotal to induce endothelial cell proliferation and migration to form the vasculature network [38]. In this context, Western blotting was performed to analyze HIF-1α protein levels in the rat retina (Figure3A) at birth, P7, P14 and P18. Densitometric analysis showed an increase of HIF-1 α protein levels at P7 ($p < 0.001$) compared to birth, followed by a decrease at P14 ($p < 0.01$ vs. birth; $p < 0.01$ vs. P7) and at P18 ($p < 0.01$ vs. P7; Figure3B).

Since HIF-1α promotes the transcription of *VEGF-A* gene, expression analysis was performed by qPCR in rat retinas at birth, P7, P14 and P18. As depicted in Figure3C, VEGF-A was upregulated at P7, ($p < 0.001$ vs. birth) while at P14 and P18 its levels were comparable to those at birth, in agreement with the reduced levels of HIF-1α at the latter postnatal days.

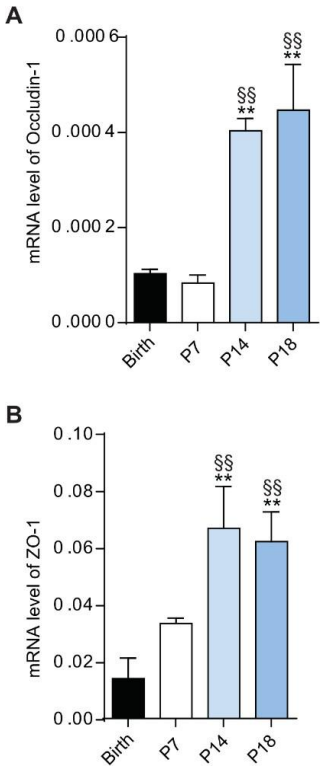

Figure 2. Expression of blood-retina barrier genes during retina rat development. mRNA expression of occludin-1 (**A**) and zonula occludens (ZO-1) (**B**) genes was evaluated by qPCR in rat retinas at birth, P7, P14 and P18. Data is presented as mean ± SEM. One-way ANOVA was used as statistical analysis, followed by Bonferroni's multiple comparisons test ($n = 6$; ** $p < 0.01$ vs. birth, §§ $p < 0.01$ vs. P7).

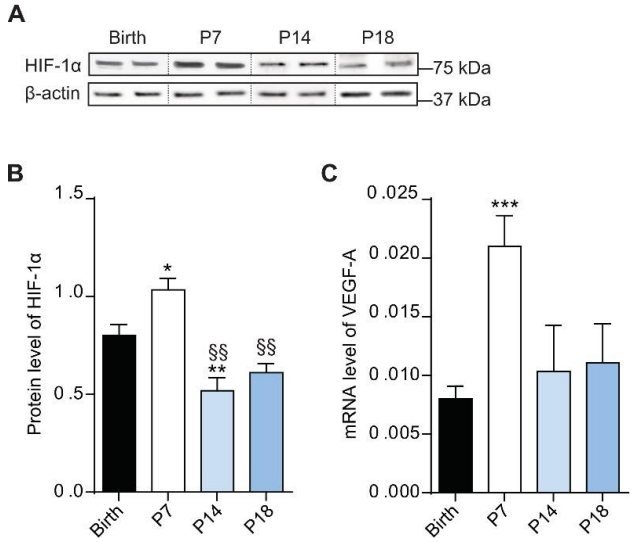

Figure 3. Protein levels of hypoxia-inducible factor (HIF) change during rat retina development. (**A**) Western blots illustrate representative immunoreactive bands of HIF-1α and β-actin (loading control) in the retina of rat pups from birth to P18. (**B**) Quantitative analysis of optical density of the immunoreactive bands of HIF-1α. (**C**) mRNA expression of vascular endothelial growth factor (*VEGF)-A* gene evaluated with qPCR in rat retinas at birth, P7, P14 and P18. One-way ANOVA followed by Bonferroni's multiple comparisons test was used as statistical analysis of mean ± SEM datasets ($n = 6$; * $p < 0.05$, ** $p < 0.01$, *** $p < 0.001$ vs. birth, §§ $p < 0.01$ vs. P7).

1.2. Autophagic Mechanisms Increased during the Hypoxic Phase

During development, autophagic mechanisms support cells to adapt and respond to several processes, including proliferation, differentiation and migration [39]. In this context, Western blotting analysis was performed to evaluate the levels of proteins involved in autophagy during retina development (Figure4A). Densitometric analysis demonstrated a significant increase of phosphorylated levels of AMPKα ($p < 0.001$ vs. birth; Figure4C) and ULK1 ($p < 0.01$ vs. birth; Figure4B) as well as LC3 II ($p < 0.01$ vs. birth; Figure4D) at P7. At P14 and P18, the levels of these

autophagic markers decreased then at levels comparable to those at birth.

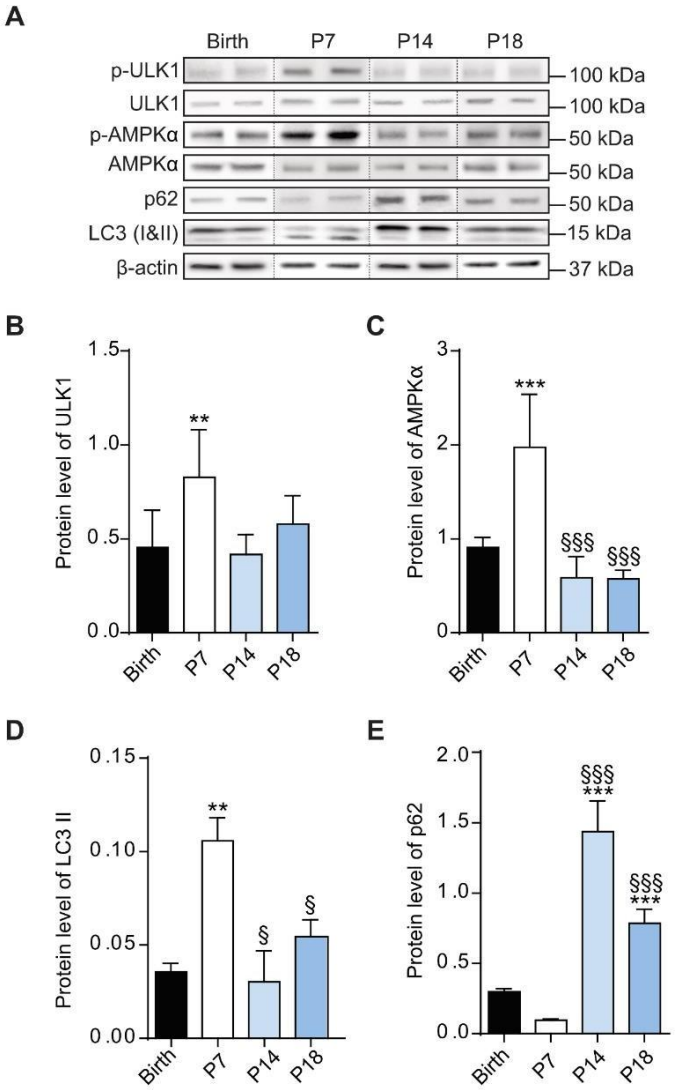

Figure 4. Protein levels of autophagic markers during rat retinal development. (**A**) Western blots depict representative immunoreactive bands of proteins involved in autophagic mechanisms in rat retinas, from birth to P18. Quantitative analysis of optical density of the ratio of immunoreactive bands between pSer^{555}Ulk1 / Ulk1 (**B**), *p*-AMPKα / AMPKα (**C**); LC3 II / β-actin (**D**) and p62/ β-actin (**E**). One-way ANOVA followed by Bonferroni's multiple comparisons test was used as statistical analysis of mean ± SEM datasets ($n = 6$; ** $p < 0.01$, *** $p < 0.001$ vs. birth, § $p < 0.05$, §§§ $p < 0.001$ vs. P7).

On the contrary, a trend to a decrease of SQSTM1/p62 protein levels, yet not statis- tically significative, was observed at P7, followed by a substantial increase at both P14 ($p < 0.001$ vs. birth; $p < 0.001$ vs. P7) and P18 ($p < 0.001$ vs. birth; $p < 0.001$ vs. p7).

1.1. High Expression of Autophagic Marker at P7 in Rat Retina

In rat, developing retinal cells are already organized into layers from P7, giving the tissue its stratified feature [40,41]. The variation of autophagic flux was evaluated relative to the retinal layers using immunostained retinal sections to visualize autophagy and vasculature, with LC3 as an autophagic marker and isolectin B4 as a marker of endothelial cells. The immunofluorescence demonstrated a clear variation of autophagy during retinal development, indicating a predominant expression of the autophagic marker LC3 at P7 (Figure5). At this specific time point, a substantial expression of LC3 was observed in both the inner plexiform and outer plexiform layers (IPL; OPL). At birth and on latter stages of retinal developmental, LC3 was predominantly expressed in the IPL and almost undetectable in the OPL. In addition, heightened colocalized expression of the autophagy and vascular markers was observed at P7, as compared to birth, P14 and P18, which could be related to the hypoxia associated with the involution of the hyaloid blood vessels. Albeit a positive staining for LC3 was detected in ganglion cell layer (GCL) and the photoreceptor outer

segments (OS), no changes were observed in the studied times of development.

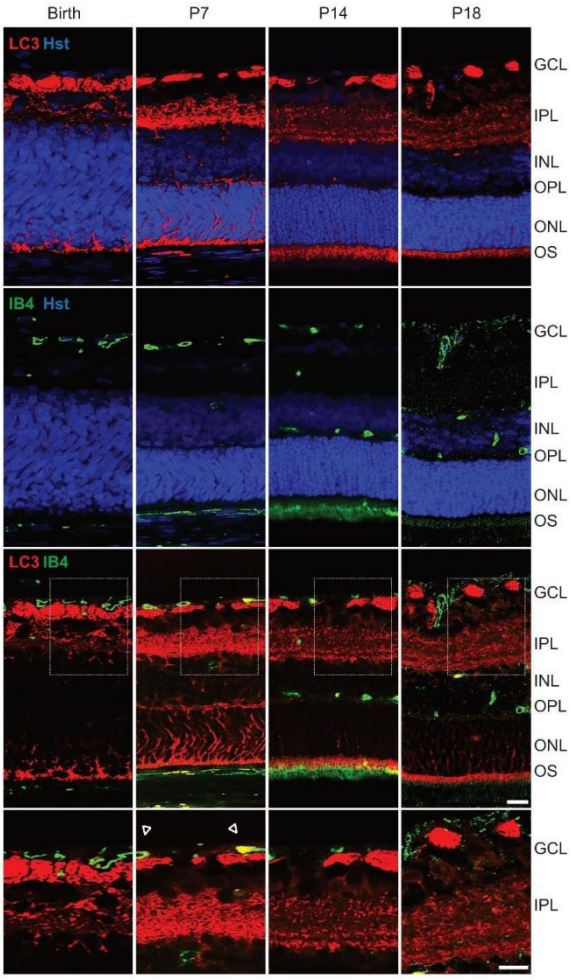

Figure 5. Expression pattern of LC3 in the developing rat retina. Representative immunohistofluo- rescence analysis of LC3 (red) and isolectin B4 (IB4; green) and Hoechst (Hst; blue) in retina sections of rat pups at birth, P7, P14 and P18. Dashed squares indicate the magnification area of GCL and IPL layers. Arrows represent colocalization of LC3 with IB4 in retinal vasculature. GCL, ganglion cell layer; IPL, inner plexiform layer; INL, inner nuclear layer; OPL, outer plexiform layer; ONL, outer nuclear layer; OS, outer segments of photoreceptors. Scale bar = 50 µm.

5. Discussion

During mammalian development, cells go through proliferation, cell death and differ- entiation, culminating in an adult organism formation. During these stages, autophagy assures cell adaptation, by promoting rapid changes in cytosolic composition and acceler- ating organelle and protein turnover [39,42]. The present study elaborates on the influence of autophagy mechanisms in the development of rat's retina from birth to P18.

In rats, the retinal vasculature develops postnatally. At birth, the retina surface is still covered by the hyaloid vessels, and the retinal vessels have merely begun to raise from the optic disc [43]. Previous studies have shown that the hyaloid network persists until P7, by which time the retinal vessels have almost propagated to the periphery of the retina [44,45]. Interestingly, in newborn rat retinas a large area lacking retinal capillary coverage is observed, indicating the presence of hyaloid vessels, while at P7 the rat retinas display nearly full vascularization. At this time point, the developing retina vascular network is still immature and the BRB is not formed [11]. To form the BRB, endothelial cells require tight junctions, essential to regulate the movement of solutes and nutrients from the outer to the inner retinal layers [46]. Tight junctions comprise several proteins, including occludin-1 and ZO-1, responsible for anchoring the junctional complex to the cytoskeleton [47]. As demonstrated here, at birth and P7 the retina of rat pups presents low transcript levels of both occludin-1 and ZO-1 genes. Reversely, mRNA levels of these genes are increased at P14 and P18, when the retinal vasculature is covering the total surface of retina. This suggests that retina vascularization is completed and mature around P14-P18, in alignment with the presence of tight junctions in retinal endothelial cells.

From embryonic stages to birth, a physiological hypoxia is paramount to drive retinal neovascularization, through the upregulation of HIF-1α and subsequently VEGF-A [9,48]. During

the early postpartum retinal developmental stage in rats, the involution of the hyaloid vasculature to the retinal vascular network results in a partially avascular and ischemic retina, correlating to increased oxygen demand and resulting in a hypoxic stim- ulus [10]. In the present study, a peak of HIF-1α and VEGF-A expression is determined at P7, which decreases during latter stages when the retina is fully vascularized. The hy- poxic environment contributes to activate essential mechanisms in adaptation and survival, ensuring cellular homeostasis during angiogenesis [49,50]. In fact, the developing retina exposed to changing environment and metabolic stress requires autophagy to adjust its bioenergetic and biosynthetic demands [20,49]. In this respect, both hypoxia and energy deprivation can promote AMPK activation, a known inducer of autophagy [22,25]. In agreement, an increase of p-AMPKα, p-ULK1 and LC3 II protein levels are demonstrated at P7, with a trend of decreased p62 protein levels, indicating an active autophagic flux at this developmental stage. At P14 and P18, with the presence of a fully vascularized retina, a decrease in p-ULK1 and LC3 II protein levels is determined concomitantly with an increase of p62. The observed accumulation of p62 with a decrease of LC3 II protein levels at P14 could be associated with a transition from autophagy-dependent to -independent mechanisms of retinal homeostasis, as previously suggested in retinal pigment epithelium cells [51,52].

To elaborate on the role of autophagy in the different cell layers during rat retinal development, a predominant expression of LC3 is confirmed in the GCL, IPL, OPL and OS, in agreement with previous studies in rodent retinas [53–55]. At P7, an increase of LC3 staining is denoted in the IPL and OPL, with a noticeable reduction in the autophagy marker at P14 and P18. During the early postpartum developmental stage, the rat retinal cells are affected by ischemia, which is correlated to the peak of expression of HIF-1α and VEGF-A, concomitantly with LC3. Moreover, an expression of LC3 is observed in endothelial cells at P7, suggesting that autophagy may contribute directly to the formation of the retinal vascular network. These findings indicate that during the physiologic hypoxia in the rat retina, HIF-mediated signaling induces the increase in VEGF-A to promote endothelial cell proliferation, and an upregulation of autophagy markers to sustain cellular homeostasis and cellular quality control in retinal cells.

6. Conclusions

The present study indicates that increased autophagy is intrinsically associated with the hypoxic phase of retinal development and critically contributes to the physiologic development of the different cell layers of the retina during the transition from the hyaloid to the retinal vasculature, thus allowing the normal development of the retina.

Author Contributions: Conceptualization, H.A. and M.D.M.; formal analysis, N.A.P.; investigation, N.A.P., A.C., H.A. and M.D.M.; methodology, N.A.P., A.C. and E.L.; resources, M.C. and A.K.; supervision, H.A. and M.D.M.; writing—original draft, N.A.P., H.A. and M.D.M.; writing—review and editing, N.A.P., H.A. and M.D.M. All authors have read and agreed to the published version of the manuscript.

Funding: This research was funded by the grants from the Karolinska Institutet Foundations and The Swedish Eye Foundation.

Institutional Review Board Statement: Animal protocols were conducted in accordance with the Statement for the Use of Animals in Ophthalmic and Vision Research (ARVO), the Italian regulation for animal care (DL 116/92), and the European Communities Council Directive (86/609/EEC). Ani- mal procedures were authorized by the Ethical Committee in Animal Experiments of the University of Pisa (permit number: 133/2019-PR, 14 February 2019).

Informed Consent Statement: Not applicable.

Data Availability Statement: The data presented in this study are available on request from the corresponding author.

Acknowledgments: The authors thank Flavia Plastino, Maria Grazia Rossino and Filippo Locri for technical support.

Conflicts of Interest: The authors declare no conflict of interest.

References

1. Wong-Riley, M. Energy metabolism of the visual system. *Eye Brain* **2010**, *2*, 99. [CrossRef]
2. Joyal, J.S.; Gantner, M.L.; Smith, L.E.H. Retinal energy demands control vascular supply of the retina in development and disease: The role of neuronal lipid and glucose metabolism. *Prog. Retin. Eye Res.* **2018**, *64*, 131–156. [CrossRef]
3. Archer, D.B.; Gardiner, T.A.; Stitt, A.W. Functional anatomy, fine structure and basic pathology of the retinal vasculature. In
4. *Retinal Vascular Disease*; Springer: Berlin/Heidelberg, Germany, 2007; pp. 3–23.
5. Sun, Y.; Smith, L.E.H. Notice of withdrawal: Retinal vasculature in development and diseases. *Annu. Rev. Vis. Sci.* **2020**. [CrossRef]
6. Rust, R.; Grönnert, L.; Dogançay, B.; Schwab, M.E. A revised view on growth and remodeling in the retinal vasculature. *Sci. Rep.*
7. **2019**, *9*, 3263. [CrossRef] [PubMed]

8. Fruttiger, M. Development of the retinal vasculature. *Angiogenesis* **2007**, *10*, 77–88. [CrossRef] [PubMed]
9. Liu, C.; Wang, Z.; Sun, Y.; Chen, J. Animal models of ocular angiogenesis: From development to pathologies. *FASEB J.* **2017**, *31*, 4665–4681. [CrossRef]
10. Selvam, S.; Kumar, T.; Fruttiger, M. Retinal vasculature development in health and disease. *Prog. Retin. Eye Res.* **2018**, *63*, 1–19. [CrossRef] [PubMed]
11. Krock, B.L.; Skuli, N.; Simon, M.C. Hypoxia-induced angiogenesis: Good and evil. *Genes Cancer* **2011**, *2*, 1117–1133. [CrossRef]
12. Stone, J.; Itin, A.; Alon, T.; Pe'er, J.; Gnessin, H.; Chan-Ling, T.; Keshet, E. Development of retinal vasculature is mediated by hypoxia-induced vascular endothelial growth factor (VEGF) expression by neuroglia. *J. Neurosci.* **1995**, *15*, 4738–4747. [CrossRef]
13. Díaz-Coránguez, M.; Ramos, C.; Antonetti, D.A. The inner blood-retinal barrier: Cellular basis and development. *Vision Res.* **2017**,
14. *139*, 123–137. [CrossRef]
15. Chow, B.W.; Gu, C. Gradual suppression of transcytosis governs functional blood-retinal barrier formation. *Neuron* **2017**, *93*, 1325–1333. [CrossRef] [PubMed]
16. van der Wijk, A.E.; Vogels, I.M.C.; van Veen, H.A.; van Noorden, C.J.F.; Schlingemann, R.O.; Klaassen, I. Spatial and temporal recruitment of the neurovascular unit during development of the mouse blood-retinal barrier. *Tissue Cell* **2018**, *52*, 42–50. [CrossRef] [PubMed]
17. Hosoya, K.I.; Tachikawa, M. The inner blood-retinal barrier molecular structure and transport biology. *Adv. Exp. Med. Biol.* **2013**,
18. *763*, 85–104. [CrossRef]
19. Dejana, E.; Hirschi, K.K.; Simons, M. The molecular basis of endothelial cell plasticity. *Nat. Commun.* **2017**, *8*, 1–11. [CrossRef] 16.Chun, Y.; Kim, J. Autophagy: An essential degradation program for cellular homeostasis and life. *Cells* **2018**, *7*, 278. [CrossRef]
20. 17.Glick, D.; Barth, S.; Macleod, K.F. Autophagy: Cellular and molecular mechanisms. *J. Pathol.* **2010**, *221*, 3–12. [CrossRef]
21. Levine, B.; Kroemer, G. Autophagy in the pathogenesis of disease. *Cell* **2008**, *132*, 27–42. [CrossRef]
22. Kim, J.H.; Kim, J.H.; Yu, Y.S.; Mun, J.Y.; Kim, K.W. Autophagy-induced regression of hyaloid vessels in early ocular development.
23. *Autophagy* **2010**, *6*, 922–928. [CrossRef]
24. Schaaf, M.B.; Houbaert, D.; Meçe, O.; Agostinis, P. Autophagy in endothelial cells and tumor angiogenesis. *Cell Death Differ.* **2019**,
25. *26*, 665–679. [CrossRef]
26. Bellot, G.; Garcia-Medina, R.; Gounon, P.; Chiche, J.; Roux, D.; Pouysségur, J.; Mazure, N.M. Hypoxia-induced autophagy is mediated through hypoxia-inducible factor induction of BNIP3 and BNIP3L via their BH3 domains. *Mol. Cell. Biol.* **2009**, *29*,
27. 2570–2581. [CrossRef]
28. Mazure, N.M.; Pouysségur, J. Hypoxia-induced autophagy: Cell death or cell survival? *Curr. Opin. Cell Biol.* **2010**, *22*, 177–180. [CrossRef] [PubMed]
29. Blagosklonny, M.V. Hypoxia, MTOR and autophagy. *Autophagy* **2013**, *9*, 260–262. [CrossRef] [PubMed]
30. Zhang, J.; Zhang, C.; Jiang, X.; Li, L.; Zhang, D.; Tang, D.; Yan, T.; Zhang, Q.; Yuan, H.; Jia, J.; et al. Involvement of autophagy in hypoxia-BNIP3 signaling to promote epidermal keratinocyte migration. *Cell Death Dis.* **2019**, *10*, 1–15. [CrossRef] [PubMed]
31. Dengler, F. Activation of ampk under hypoxia: Many roads leading to rome. *Int. J. Mol. Sci.* **2020**, *21*, 2428. [CrossRef] [PubMed]
32. Mihaylova, M.M.; Shaw, R.J. The AMPK signalling pathway coordinates cell growth, autophagy and metabolism. *Nat. Cell Biol.*
33. **2011**, *13*, 1016–1023. [CrossRef]
34. Egan, D.F.; Shackelford, D.B.; Mihaylova, M.M.; Gelino, S.; Kohnz, R.A.; Mair, W.; Vasquez, D.S.; Joshi, A.; Gwinn, D.M.; Taylor, R.; et al. Phosphorylation of ULK1 (hATG1) by AMP-activated protein kinase connects energy sensing to mitophagy. *Science* **2011**, *331*, 456–461. [CrossRef]
35. Grasso, D.; Renna, F.J.; Vaccaro, M.I. Initial steps in mammalian autophagosome biogenesis. *Front. Cell Dev. Biol.* **2018**, *6*, 146. [CrossRef]
36. Pyo, J.O.; Nah, J.; Jung, Y.K. Molecules and their functions in autophagy. *Exp. Mol. Med.* **2012**, *44*, 73–80. [CrossRef]
37. Metlagel, Z.; Otomo, C.; Takaesu, G.; Otomo, T. Structural basis of ATG3 recognition by the autophagic ubiquitin-like protein ATG12. *Proc. Natl. Acad. Sci. USA* **2013**, *110*, 18844–18849. [CrossRef]
38. Tanida, I.; Ueno, T.; Kominami, E. LC3 and autophagy. *Methods Mol. Biol.* **2008**, *445*, 77–88. [CrossRef]
39. Itakura, E.; Mizushima, N. p62 targeting to the autophagosome formation site requires self-oligomerization but not LC3 binding.
40. *J. Cell Biol.* **2011**, *192*, 17–27. [CrossRef] [PubMed]
41. Wurzer, B.; Zaffagnini, G.; Fracchiolla, D.; Turco, E.; Abert, C.; Romanov, J.; Martens, S. Oligomerization of p62 allows for selection of ubiquitinated cargo and isolation membrane during selective autophagy. *eLife* **2015**, *4*, e08941. [CrossRef] [PubMed]
42. Yoshii, S.R.; Mizushima, N. Monitoring and measuring autophagy. *Int. J. Mol. Sci.* **2017**, *18*, 1865. [CrossRef] [PubMed]
43. André, H.; Tunik, S.; Aronsson, M.; Kvanta, A. Hypoxia-inducible factor-1α Is associated with sprouting angiogenesis in the murine laser-induced Choroidal neovascularization model. *Investig. Ophthalmol. Vis. Sci.* **2015**, *56*, 6591–6604. [CrossRef]
44. Inagaki, K.; Koga, H.; Inoue, K.; Suzuki, K.; Suzuki, H. Spontaneous intraocular hemorrhage in rats during postnatal ocular development. *Comp. Med.* **2014**, *64*, 34–43.
45. Naylor, A.; Hopkins, A.; Hudson, N.; Campbell, M. Tight junctions of the outer blood retina barrier. *Int. J. Mol. Sci.* **2020**, *21*, 211. [CrossRef]
46. Oladipupo, S.; Hu, S.; Kovalski, J.; Yao, J.; Santeford, A.; Sohn, R.E.; Shohet, R.; Maslov, K.; Wang, L.V.; Arbeit, J.M. VEGF is essential for hypoxia-inducible factor-mediated neovascularization but dispensable for endothelial sprouting. *Proc. Natl. Acad. Sci. USA* **2011**, *108*, 13264–13269. [CrossRef]
47. Cecconi, F.; Levine, B. The role of autophagy in mammalian development: Cell makeover rather than cell death. *Dev. Cell* **2008**,
48. *15*, 344–357. [CrossRef]
49. Amini, R.; Rocha-Martins, M.; Norden, C. Neuronal migration and lamination in the vertebrate retina. *Front. Neurosci.* **2018**, *11*, 742. [CrossRef]

50. Kuwabara, T.; Weidman, T. Development of the prenatal rat retina. *Invest. Ophthalmol.* **1974**, *13*, 725–739.
51. Di Bartolomeo, S.; Nazio, F.; Cecconi, F. The role of autophagy during development in higher eukaryotes. *Traffic* **2010**, *11*, 1280–1289. [CrossRef] [PubMed]
52. Engerman, R.L.; Meyer, R.K. Development of retinal vasculature in rats. *Am. J. Ophthalmol.* **1965**, *60*, 628–641. [CrossRef]
53. Kim, Y.; Park, J.R.; Hong, H.K.; Han, M.; Lee, J.; Kim, P.; Woo, S.J.; Park, K.H.; Oh, W.Y. In vivo imaging of the hyaloid vascular regression and retinal and choroidal vascular development in rat eyes using optical coherence tomography angiography. *Sci. Rep.* **2020**, *10*, 12901. [CrossRef]
54. Cairns, J.E. Normal development of the hyaloid and retinal vessels in the rat. *Br. J. Ophthalmol.* **1959**, *43*, 385–393. [CrossRef] [PubMed]
55. Campbell, M.; Humphries, P. The blood-retina barrier tight junctions and barrier modulation. *Adv. Exp. Med. Biol.* **2013**, *763*, 70–84. [CrossRef]
56. Bazzoni, G.; Dejana, E. Endothelial cell-to-cell junctions: Molecular organization and role in vascular homeostasis. *Physiol. Rev.*
57. **2004**, *84*, 869–901. [CrossRef]
58. Rattner, A.; Williams, J.; Nathans, J. Roles of HIFs and VEGF in angiogenesis in the retina and brain. *J. Clin. Invest.* **2019**, *129*, 3807–3820. [CrossRef]
59. Nussenzweig, S.C.; Verma, S.; Finkel, T. The role of autophagy in vascular biology. *Circ. Res.* **2015**, *116*, 480–488. [CrossRef]
60. Oeste, C.L.; Seco, E.; Patton, W.F.; Boya, P.; Pérez-Sala, D. Interactions between autophagic and endo-lysosomal markers in endothelial cells. *Histochem. Cell Biol.* **2013**, *139*, 659–670. [CrossRef]
61. Ryhänen, T.; Hyttinen, J.M.T.; Kopitz, J.; Rilla, K.; Kuusisto, E.; Mannermaa, E.; Viiri, J.; Holmberg, C.I.; Immonen, I.; Meri, S.; et al. Crosstalk between Hsp70 molecular chaperone, lysosomes and proteasomes in autophagy-mediated proteolysis in human retinal pigment epithelial cells. *J. Cell. Mol. Med.* **2009**, *13*, 3616–3631. [CrossRef]
62. Viiri, J.; Hyttinen, J.M.T.; Ryhänen, T.; Rilla, K.; Paimela, T.; Kuusisto, E.; Siitonen, A.; Urtti, A.; Salminen, A.; Kaarniranta, K. p62/sequestosome 1 as a regulator of proteasome inhibitor-induced autophagy in human retinal pigment epithelial cells. *Mol. Vis.* **2010**, *16*, 1399–1414. [CrossRef] [PubMed]
63. Cammalleri, M.; Locri, F.; Catalani, E.; Filippi, L.; Cervia, D.; Dal Monte, M.; Bagnoli, P. The beta-adrenergic receptor blocker propranolol counteracts retinal dysfunction in a mouse model of oxygen induced retinopathy: Restoring the balance between apoptosis and autopha. *Front. Cell. Neurosci.* **2017**, *11*, 395. [CrossRef] [PubMed]
64. Boya, P.; Esteban-Martínez, L.; Serrano-Puebla, A.; Gómez-Sintes, R.; Villarejo-Zori, B. Autophagy in the eye: Development, degeneration, and aging. *Prog. Retin. Eye Res.* **2016**, *55*, 206–245. [CrossRef] [PubMed]
65. Boya, P. Why autophagy is good for retinal ganglion cells? *Eye* **2017**, *31*, 185–190. [CrossRef]

PAPER IV

An imbalance in the autophagy flux contributes to retinal dysfunction in the OIR rat model

Noemi Anna Pesce[1,2], Alessio Canovai[1], Flavia Plastino[2], Emma Lardner[2], Anders Kvanta[2], Maurizio Cammalleri[1], Helder André[2,*], Massimo Dal Monte[1,*]

[1]Department of Biology, University of Pisa, Pisa, Italy.

[2]Department of Clinical Neuroscience, Division of Eye and Vision, St Erik Eye Hospital, Karolinska Institutet, Solna, Sweden.

*Equal contributing senior authors

Abstract

In retinopathy of prematurity (ROP) the abnormal retinal neovascularization is often accompanied by retinal neuronal dysfunction. Here, a rat model of oxygen-induced retinopathy (OIR), which mimics the ROP disease, was used to investigate changes in the expression of key mediators of autophagy and markers of cell death in the rat retina. In addition, rats were treated from birth to post natal day 14 and 18 with 3-Methyladenine (3-MA), an inhibitor of autophagy. Immunoblot and immunohistofluorescence analysis demonstrated that autophagic mechanisms are dysregulated in the retina of OIR rats and indicated a possible correlation between autophagy and necroptosis. We found that 3-MA acts predominantly by reducing autophagy and necroptotic markers in the OIR retinas; however, it does not ameliorate retinal function, which results compromised in this model. Taken together, these results revealed the crucial role of autophagy in mechanisms of cell death present in retinal neurons of OIR rats. Thus autophagy could be a molecular target for ROP neuroprotective treatment strategies.

Keywords: retinopathy of prematurity, rat model, oxygen-induced retinopathy, autophagy, cell death, necroptosis.

INTRODUCTION

The retina is one of the highest oxygen demanding tissue in the body, and oxygen supply is guaranteed by a structured ocular vascular network [225]. In humans, the retinal vascularization begins development during the fourth month of gestation and is completed before birth, at nine months. In the uterus, the hypoxic environment (pO_2 of about 30 mmHg) allows retinal blood vessels to proliferate and migrate from the optic nerve to the retinal periphery, through vascular endothelial growth factor (VEGF)-mediated angiogenesis [226]. Infants born prematurely present an incompletely vascularized retina, characterized by a peripheral avascular zone; a hallmark of retinopathy of prematurity (ROP), a potentially blinding retinal vascular disease [227]. ROP is constituted by two typical oxygen-dependent phases. The first phase is induced by the hyperoxic extrauterine environment (pO_2 of 150 mmHg) and triggers immediately after the premature birth; the increase in

oxygen level initiates a decrease in VEGF, which causes the arresting of retinal vascular development. At this stage, the blood vessels are fragile and ineffective to reach the increasing demands of the developing retina, which becomes hypoxic. Consequently, the second phase starts with an increase in the levels of VEGF, which promotes an excessive growth of blood vessels that extend into the vitreous and, in worst cases, may lead to retinal detachment [228].

In ROP, the retinal vasculature is not the only component of the retina to be damaged [188]. Previous studies have demonstrated that multiple retinal cells in addition to the endothelial cells are compromised [229]. The rapid fluctuations in oxygen cause a substantial stress to the retina tissue, which can activate apoptotic pathways that lead to retinal cell death [230]. In line with these findings, an expansion of studies suggests that autophagy is involved in retinal diseases and, contributes to the progressive visual dysfunction [74,231].

Autophagy is an intracellular degradation system, essential to eliminate unnecessary cell components, including unfolded proteins and damaged organelles, through the intermediary formation of the autophagosome, a double membrane-bound vesicle that fuses with the lysosome to promote the degradation of its content by the cellular lysosomal system [73]. In healthy cells, autophagy is activated at low basal levels and has a crucial role to maintain cellular homeostasis, operating as a protective mechanism for adaptation to environmental stress, including oxidative stress, hypoxia and nutritional starvation. At the molecular level, autophagy is regulated by several factors, which are involved in specific steps of the mechanism. As a consequence of nutrient limitation, the major positive regulator of autophagic machinery is the adenosine monophosphate-activated protein kinase alpha (AMPKα), which phosphorylates the autophagic inducer, Unc-51 like autophagy activating kinase (Ulk)1 on Ser^{555}, promoting autophagy induction [106]. By contrast, autophagy can be inhibited by the mammalian target of rapamycin (mTOR) kinase, which is phosphorylated and activated by protein kinase B (Akt). mTOR inhibits autophagy by phosphorylating Ulk1 on Ser^{777} site and, activates other translational regulators, including the initiation factor 4E-binding protein (4E-BP1) and the ribosomal S6 protein (S6), which have a crucial role to regulate the initiation of mRNA translation [99].

However, in pathological conditions, an impairment of autophagy flux might be damaging and promote autophagic cell death, which is associated with an accumulation of autophagosomes in the cell [80]. Thus, certain cell death mechanisms have been classified as “autophagy-mediated,” when autophagy precedes and triggers the programmed cell death, which include necroptosis, a receptor-interacting protein kinases (RIPKs) dependent pathway; and apoptosis, a caspase-depended-mechanism [111,114]. Interestingly, several studies have suggested that the autophagy machinery might promote either apoptosis or necroptosis, based on the energetic state and ATP levels of the cells.

Crucially, a high level of intracellular of ATP promotes apoptosis, whereas a rapid drop in ATP, is implicated in necrotic cell death [119–122]. In both cases, autophagy flux is impaired and an accumulation of autophagosomes may compromise cell viability [81,113].

In the present study, we used a rat model of oxygen-induced retinopathy (OIR), an acknowledged model of ROP. In rats, the retinal vasculature develops postnatally, at around post-natal day (P) 13-P16 [232]. In the rat model of OIR developed by Penn [187], the exposure of the newborn rats to alternating daily cycles of oxygen (50% and 10%, respectively) for the first 14 days delays the development of retinal vessels, causing the appearance of an avascular periphery. Returning to room air until P18, causes the growth of aberrant retinal vessels that leads to the formation of neovascular tufts [189]. Neovascularization is further accompanied by a profound retinal dysfunction, all events seen in human ROP [233]. In the present study, the rat model of ROP was used to evaluate changes in the expression of key mediators implicated in autophagy. In addition, a possible correlation between autophagy and programmed cell death pathways was examined by assessing the expression of autophagic, apoptotic and necroptotic markers in retinal endothelial cells and in several retinal layers of rat pups. In addition, inhibitor of autophagy was valuated to analyze the possible effects of in mitigating autophagy-associated cell death and retinal function in the OIR rat model.

MATERIAL AND METHODS

Animals

Rat pup litters were maintained with their own nursing mothers in a regulated environment (24 ± 1°C, 50 ± 5% humidity), with a 12 hours light/dark cycle and provided with food and water ad libidum. Procedures involving animal experiments were performed in agreement with the Italian guidelines for animal care (DL 26/14) and the European Communities Council Directive (2010/63/UE). Experiment protocols were approved by the Ethical Committee in Animal Experiments of the University of Pisa.

Rat model of OIR and pharmacological treatment

Forty-six newborn rat pups with their nursing mothers were placed in an incubator and exposed to alternative daily hyperoxia and hypoxia cycles (respectively 50% ± 2% and 10% ± 2% O_2) for 14 days, and returned to room air (RA) until P18. Hyperoxia was obtained by increasing oxygen tension, while hypoxia by increasing nitrogen tension. Oxygen concentration was monitored with an

oxygen sensor connected to the chamber (Pro-Custom Elettronica, Milano, Italy). An equal number of rat pups were kept in RA as control.

Twelve OIR rat pups were treated with intraperitoneal injection of 3 mg/kg of 3-MA (cat. no. sc-205596; Santa Cruz Biotechnology; Dallas, TX, USA) dissolved in normal saline solution. The treatment was performed daily from birth to P14 (6 rats) or P18 (6 rats). As controls, 12 OIR rat pups were injected with an equal volume of vehicle until P14 (6 rats) or P18 (6 rats). Retinas were collected at P14 and P18 from both males and females, as there was no apparent gender difference. Rat pups were anesthetized with an intraperitoneal injection of 30 mg/kg of pentobarbital and the animals were sacrificed by cervical dislocation.

Whole-retina vascular area

A total of 12 rat pups at P14 and P18 exposed to RA or OIR (3 rats for each time point per oxygenation paradigm) were prepared as previously described [205]. Briefly, free-floating retinal whole-mounts were stained with fluorescein-labelled isolectin B4 (1:200; Vector Laboratories, Burlingame, CA, USA). Images were acquired by fluorescence microscopy (Ni-E; Nikon-Europe, Amsterdam, The Netherlands) and the percentual vascular area was determined with the ImageJ freeware.

Western blot analysis

Retinas, from both OIR and RA rat pups, were lysed with RIPA lysis buffer (Millipore Corporation, Burlington, MA, USA), containing phosphatase inhibitor (PhosStop, Roche, Mannheim, Germany) and protease inhibitor (Sigma-Aldrich, St. Louis, MO, USA) cocktails. Protein concentration was determined using a micro-BCA method (Thermo Fisher Scientific, Waltam MA, USA*)* and 15µg of total proteins were separated by SDS-PAGE and transferred to polyvinylidene fluoride (PVDF) membranes (Millipore Corporation).

PVDF membranes were blocked at room temperature (RT) for 1 hour, with 5% skimmed milk, except for membranes used to detect phosphorylated proteins, which were blocked with 4% bovine serum albumin (Sigma-Aldrich), both dissolved in Tris-buffered saline (Bio-Rad Laboratories Hercules, CA, United States). Membranes were incubated overnight (ON) at 4°C with primary antibodies (Table 1). Secondary antibodies anti-rabbit-IgG and anti-mouse-IgG conjugated to horseradish peroxidase (1:10,000; cat. no. P044801-2 and P016102-2 respectively; Dako, Carpinteria, CA, USA) were incubated for 1 h at RT. Finally, proteins bands were visualized using the Clarity Western ECL substrate with a ChemiDoc XP imaging system (Bio-Rad Laboratories), and normalized to β-actin or appropriate non-phosphorylated proteins.

Table1. List of primary antibodies

Antibody	Dilution ratio	Company; Cat No
Rabbit polyclonal anti-p-Ulk1 (Ser^{757})	1:500 (WB)	Cell Signaling Technology, Danvers, MA, USA; 6888
Rabbit monoclonal anti-p-Ulk1 (Ser^{555})	1:500 (WB)	Cell Signaling Tech.; 5869
Rabbit monoclonal anti-Ulk1	1:1000 (WB)	Cell Signaling Tech.; 8054
Rabbit monoclonal anti-p-AMPKα (Thr^{172})	1:500 (WB)	Cell Signaling Tech; 2535
Rabbit monoclonal anti-AMPKα	1:1000 (WB)	Cell Signaling Tech; 5832
Rabbit polyclonal anti- SQSTM1/p62	1:500 (WB)	Abcam; ab91526
Rabbit polyclonal anti-LC3	1:1000 (WB) 1:100 (IF)	Cell Signaling Tech.; 4108
Rabbit monoclonal anti-p-4E-BP1 ($Thr^{37/46}$)	1:500 (WB)	Cell Signaling Tech.; 2855
Rabbit monoclonal anti-4E-BP1	1:500 (WB)	Cell Signaling Tech.; 9644
Rabbit monoclonal anti-β-actin	1:5000 (WB)	Sigma-Aldr.; SAB5600204
Rabbit polyclonal anti-p-Akt (Ser^{473})	1:500 (WB)	Cell Signaling Tech.; 9271
Rabbit polyclonal anti-Akt	1:1000 (WB)	Cell Signaling Tech.; 9272
Rabbit polyclonal anti-p-S6 ($Ser^{240/244}$)	1:500 (WB)	Cell Signaling Tech.; 2215
Mouse monoclonal anti-S6	1:1000 (WB)	Cell Signaling Tech.; 2317
Rabbit polyclonal anti-Caspase-8	1:200 (IF)	Novus Biol., Centennial, Colorado, USA; 20086
Rabbit polyclonal anti-RIPK-1	1:100 (IF)	Novus Biol.; 77077
Isolectin-biotin	1:1000 (IF)	Thermo Fisher; I21414

WB, western blot; IF, immunofluorescence.

Tissue preparation for immunofluorescence

Both OIR and RA eyes, untreated or treated with 3-MA, were collected and used for retina sections. Eyeballs were fixed in 4% paraformaldehyde in 0.1 M phosphate buffer (PB), pH 7.4, at RT for 24 hours before processed for paraffin embedding. Four micrometer sections were subsequently deparaffinized in xylene. After rehydration into TBS, retinal sections were kept for 30 min in 10 mM citrate buffer (pH 6.0; Sigma-Aldrich) with Tween-20 (1:2,000; Sigma-Aldrich) at 96 °C. After rinsing in TBS, retina sections were incubated in a humidified chamber with 10% normal donkey serum (Abcam, Cambridge, UK) diluted in TBS containing 5% (w/v) IgG and protease-free

bovine serum albumin (Jackson Immunoresearch, Pennsylvania, USA.) for 30min. Primary antibodies (Table 1), were incubated ON at 4°C, while secondary antibodies, anti-rat-Alexa 546 (1:500; cat. no. A11081; Sigma-Aldrich) and anti-goat-Alexa 647 (1:500; cat. no. SAB4600175; Sigma-Aldrich) were incubated for 1 h at RT. Sections were mounted with Vectashield mounting with DAPI and images were acquired on an Axioskop 2 plus fluorescence microscope with the AxioVision software (Zeiss, Gottingen, Germany).

ERG recording

Retinal function was examined with scotopic full-field ERG recorded from P18 rat pups. Before ERG testing, rats were dark adapted for a minimum of 16 h and their manipulation was done under dim red light. Briefly, both RA and OIR rat pups, untreated or treated with 3-MA, were anesthetized by intraperitoneal injection of pentobarbital (30 mg/kg); pupils were dilated with 0.5% atropine and a heating pad was used to keep the body temperature at 38°C. The electrophysiological signals were recorded through silver/silver chloride ring electrodes inserted under the lower eyelids. The cornea was intermittently irrigated with saline solution to prevent clouding of the ocular media. Electrodes in each eye were referred to a needle electrode inserted subcutaneously at the level of the corresponding frontal region. The ground electrode was placed on the tail. The electrodes were connected to a two-channel amplifier and ERG responses were evoked at a 1 log cd-s/m^2 stimulus generated through a Ganzfeld stimulator (Biomedica Mangoni, Pisa, Italy), averaging 5 different ERG responses obtained with an interval of 20 seconds between light flashes. Responses were collected simultaneously from both eyes, amplified at 1,000 gain and filtered with a band pass of 0.2 to 500 Hz before digitized at 5 kHz rate with a data acquisition device (Biomedica Mangoni). ERG responses were first analyzed to evaluate the amplitude of a- and b-waves. The amplitude of the a-wave was measured at a fixed time of 8 ms after stimulus onset to minimize contamination from non-photoreceptor cell contributions [234]. The b-wave amplitude was measured from the trough of the a-wave to the peak of the b-wave.

Statistical analysis

Statistical analysis was evaluated applying one-way ANOVA followed by Bonferroni's multiple comparison posttest, with the GraphPad Prism software (San Diego, CA, USA). The results are expressed as mean ± standard error of the mean (SEM) of n = 6. Differences with $p < 0.05$ were considered statistically significant.

RESULTS

Increased VEGF modulates retinal vasculature in OIR rat

The exposure of the newborn rats to the OIR protocol delays the development of retinal vessels, causing peripheral retinal avascularity at P14, and at P18 the formation of neovascular tufts, as a consequence of the aberrant retinal vessels' growth [189]. Here, this vascular phenotype was confirmed by whole-retina vasculature analysis using Isolectin B4 (Fig. 1a), to visualize the retinal blood vessels' area (Fig. 1b).

In ROP, low oxygen levels play a crucial role in the development of the hypoxic phase of pathogenesis, through the transcription of hypoxia induced factor (HIF)-1-dependent VEGF [187,235]. As such, we assessed a western blot analysis to monitor protein levels of both HIF-1α (the oxygen-dependent subunit of HIF-1) and VEGF-A in the retina on P14 and P18 (Fig. 1c).

Densitometric analysis showed no significant difference in HIF-1α levels between OIR and RA-exposed rats on both P14 and P18. However, on P14 retinas showed a significant increase in VEGF-A level ($p < 0.05$) which increased in OIR rat retinas at P18 ($p < 0.01$ vs RA) (Fig. 1d).

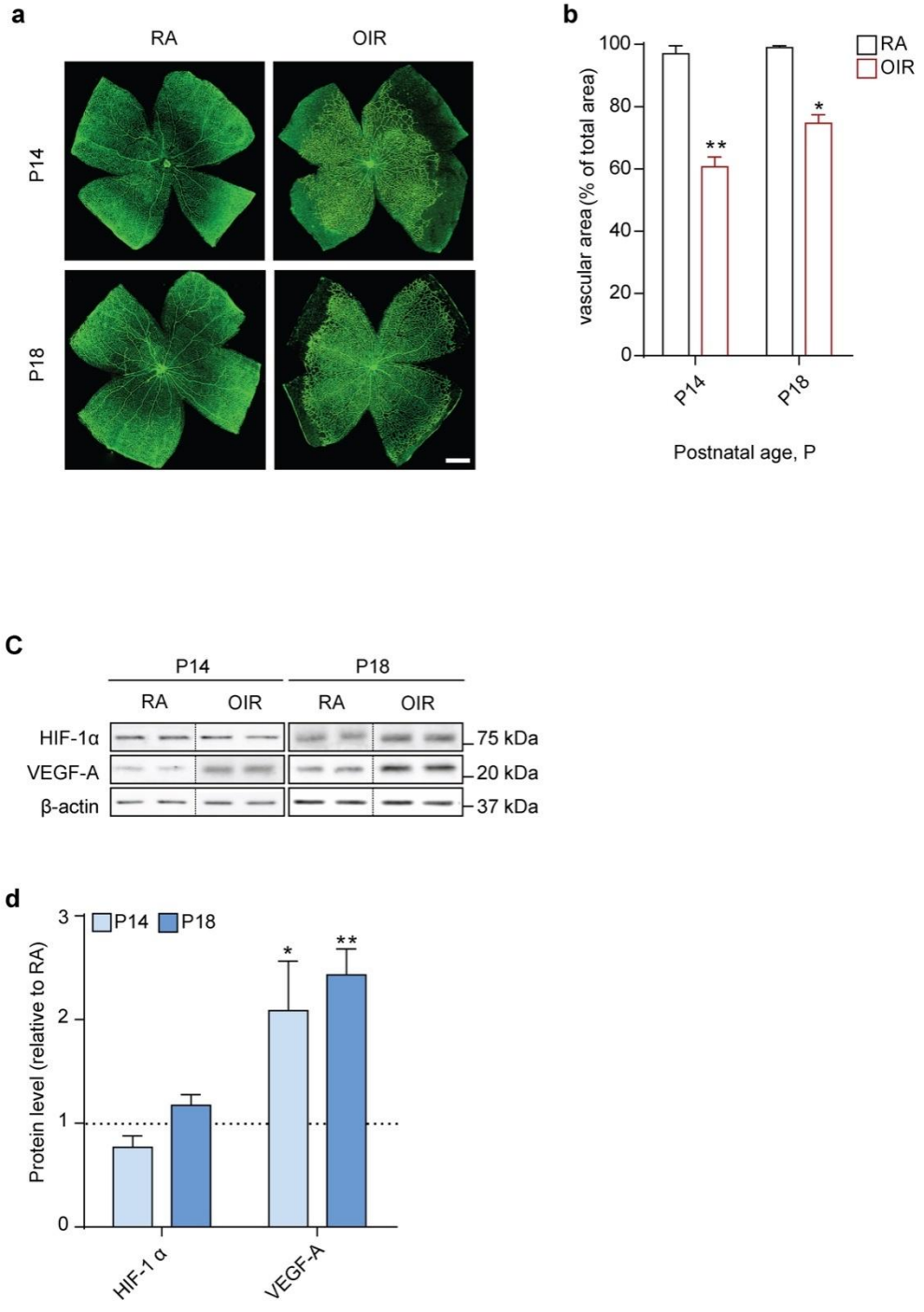

Fig. 1 Vascular network and angiogenic markers in OIR rat pups. **a** Visualization of blood vessels by isolectin B4 staining of both RA and OIR rat pup retinas, at P14 and P18. Scale bar = 500 µm. **b** The graph shows the mean ±SEM of vascular area of the retina (presented as % of total area). Statistical analysis performed using one-way ANOVA, followed by Bonferroni's multiple comparisons test (n = 6; * $p < 0.05$ ** $p < 0.01$ vs. RA). **c** Representative immunoblots of HIF-1α, VEGF-A and β-actin (loading control) of rat pups exposed to RA or OIR, at P14 and P18. **d** Quantitative densitometric analysis of protein levels was normalized to RA (n = 6 retinas per group) and analyzed by one-way ANOVA, followed by Bonferroni's multiple comparisons test. The error bars represent the Standard Error of the Mean; *$p<0.05$ and **$p<0.01$ vs respective P14 and P18 RA.

Autophagic flux is increased in the OIR rat retina

To evaluate the autophagic flux, we performed a western blot analysis on protein extracts from both RA and OIR rat retinas on P14 and P18 (Fig. 2a). We analyzed protein levels of microtubule-associated protein 1-light chain 3 (LC3) and sequestosome 1 (p62), acknowledged markers involved in autophagic mechanisms [236]. LC3 exists as a cytosolic protein, LC3-I, which can be lipidated to form LC3-phosphatidylethanolamine conjugate (LC3-II) that is recruited to autophagosomal membranes [237]; while, p62 is a cargo for degradation of ubiquitinated proteins via autophagy that decreases in presence of activated autophagy [199]. Densiometric analysis demonstrated a significant increase of LC3-II in OIR retinas on P14, when compared to RA ($p < 0.001$). A similar response of LC3-II was observed on P18 ($p < 0.01$). No significant difference in p62 protein levels was observed on both P14 and P18 (Fig. 2b).

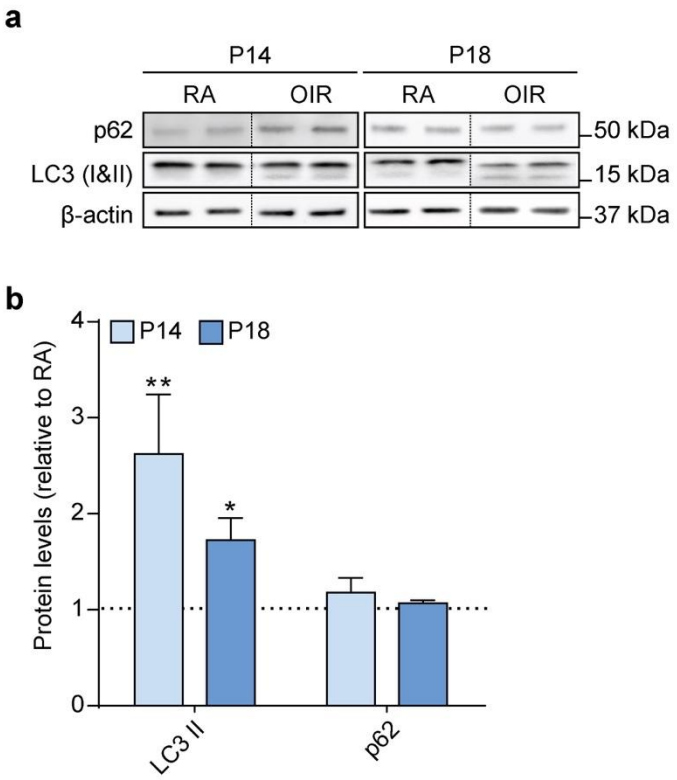

Fig. 2 Autophagic markers in retina of rat pups exposed to OIR protocol. **a** Protein levels of p62, LC3 A/B I, LC3 A/B II and β-actin (internal standard) in OIR retinas, at P14 and P18, were determined by western blotting. **b** Graphs show the Standard Error of the Mean of the experiments (n = 6 retinas per group), and significant **p<0.01 *p<0.05 and compared with respective P14 and P18 RA. For statistical analysis was used one-way ANOVA, followed by Bonferroni's multiple comparisons test.

OIR modulates autophagy in the rat retina by inactivating the Akt-mTOR anti-autophagic pathway, while activating the AMPK pro-autophagic pathway

To evaluate the role of the Akt-mTOR and the AMPKα pathways in the OIR-induced autophagic flux, western blot analysis was performed to analyze the phosphorylation status of both anti-autophagic molecules Akt, Ulk1 (phosphorylated at Ser^{757}), 4E-BP1 and S6, and pro-autophagic molecules AMPKα and Ulk1 (phosphorylated at Ser^{555}) (Fig. 3a). Densiometric analysis demonstrated that in OIR, p-Akt, p-Ulk1 (Ser^{757}), p-4E-BP1 ($p < 0.05$) and p-S6 ($p < 0.01$) were decreased at P14. In contrast, both p-AMPKα and p-Ulk1 (Ser^{555}) were increased at the same time point ($p < 0.01$). At P18, in the OIR rat retinas, we observed a decrease in p-4E-BP1 ($p < 0.05$), with no statistical difference in p-Akt, p-Ulk1 (Ser^{757}) and p-S6 levels, concomitant with an increase in the levels of both p-AMPKα and p-Ulk1 (Ser^{555}) ($p < 0.05$) (Fig. 3b).

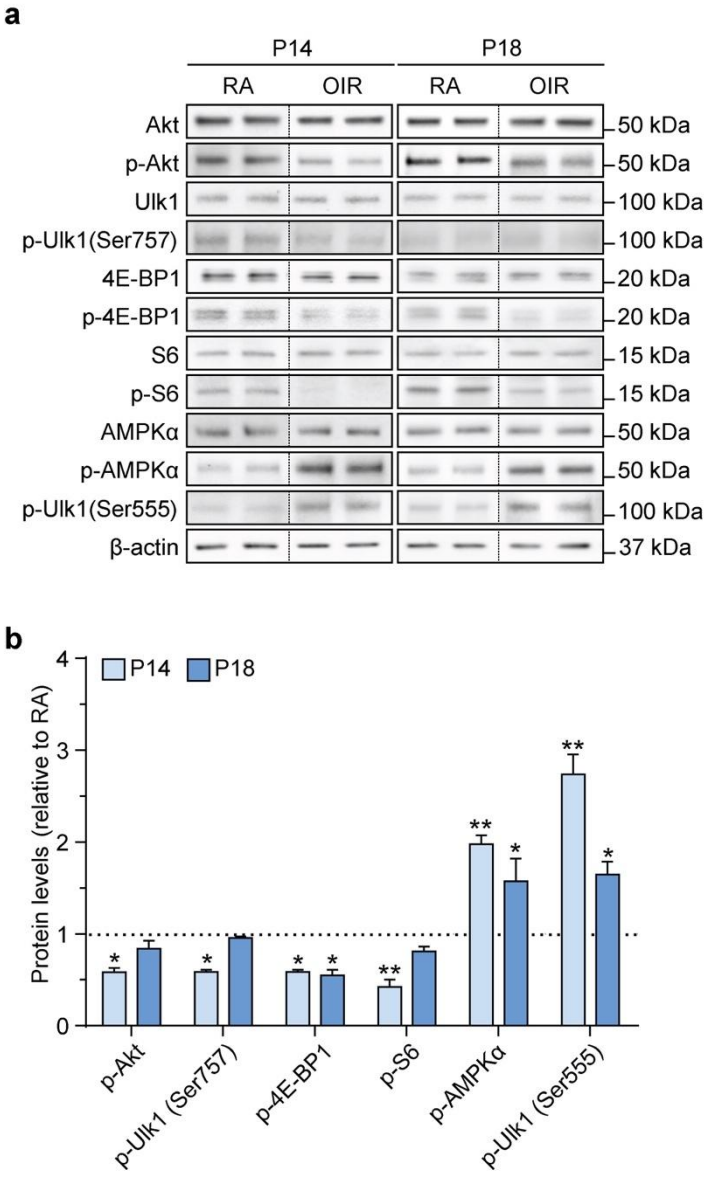

Fig. 3 Protein levels of anti- and pro-autophagic protein kinases in retinas of RA and OIR rat pups. **a** Levels of Akt, p-Ulk1 (Ser^{757}), p-4E-BP1, p-S6, AMPKα and Ulk1 (Ser^{555}) were evaluated in the retina of RA and OIR rats by western blot assay. **b** Graphs show the analysis of phosphorylated protein expression normalized to total protein; β-actin was used as loading control. One-way ANOVA was used as statistical analysis, followed by Bonferroni's multiple comparisons test; n=6. The error bars represent the Standard Error of the Mean; *p<0.05 and **p<0.01 vs respective P14 and P18 RA.

3-methyladenine reduces autophagic and necroptosis markers in the OIR rat retina

To visualize the variation of autophagic flux into the retina, immunostained retina sections of RA, OIR and 3-MA-treated OIR rats were assessed at both P14 and P18, using LC3 as an autophagic marker and Isolectin B4, as a marker of endothelial cells. Moreover, to better understand a possible correlation between autophagy and mechanisms of cells death, the sections were also stained for Casp-8 as an apoptotic marker, and RIPK-1 as a necroptotic marker. Immunohistofluorescence signals demonstrated a clear variation of autophagic, apoptotic and necroptotic markers in the OIR retina (Fig. 4). In particular, a predominant expression of LC3 and RIPK-1 was visualized in the inner plexiform layer (IPL), the outer segment (OS) and the outer nuclear layer (ONL), while a colocalized expression of Casp-8 and IB4 was observed in OIR retinas. As depicted in Figure 4, 3-MA treatment reduced the expression of both LC3 and RIPK-1 on both P14 and P18; in contrast, no detectable reduction of Casp-8 was observed in both the vasculature and retinal layers.

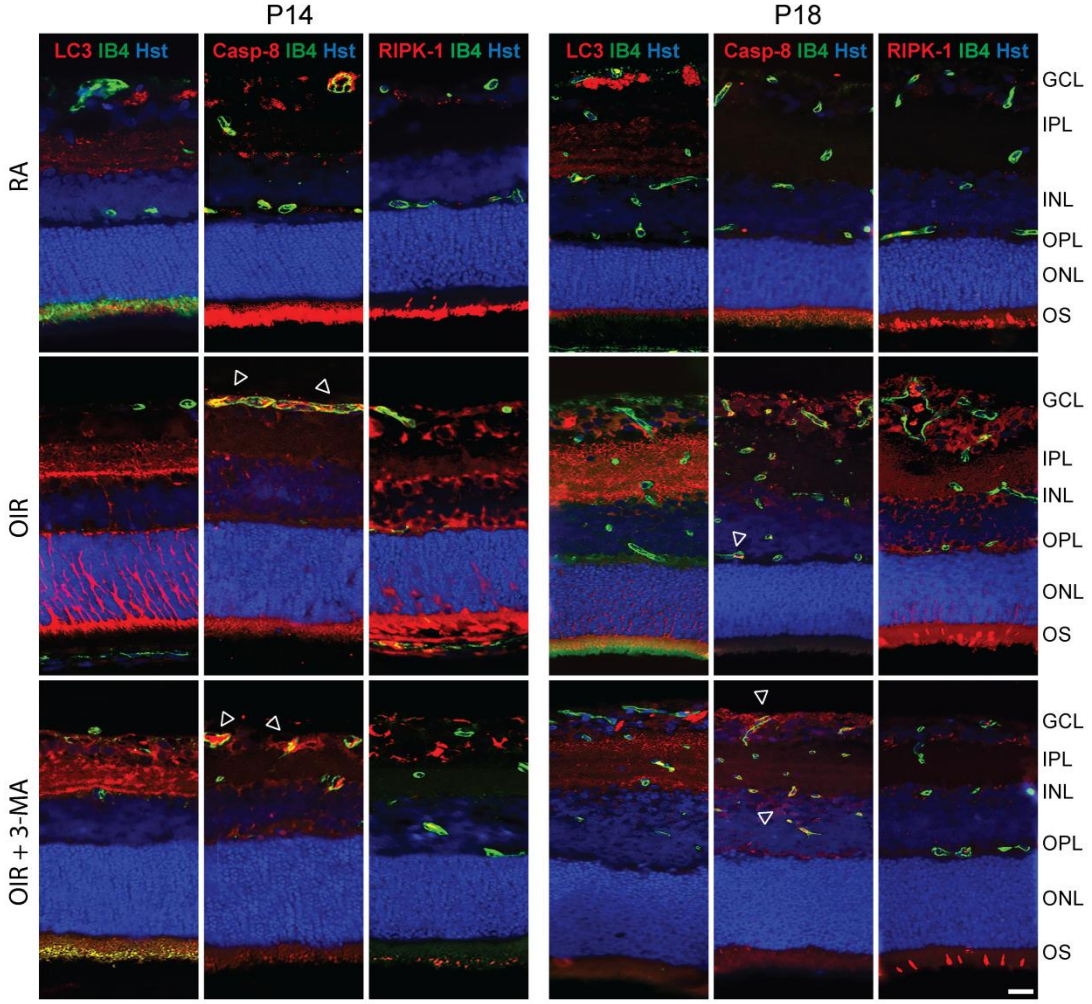

Fig. 4 Expression pattern of LC3, Casp-8 and RIPK-1 in the RA and OIR rat retinas at P14 and P18. Representative immunohistofluorescence analysis of LC3, Casp-8, RIPK-1 (red) and isolectin B4 (IB4; green) and Hoechst (Hst; blue) in retina sections of RA, OIR and OIR + 3-MA rats at P14 and P18. Arrows represent colocalization of Casp-8 with IB4

in retinal vasculature. GCL, ganglion cell layer; IPL, inner plexiform layer; INL, inner nuclear layer; OPL, outer plexiform layer; ONL, outer nuclear layer; OS, outer segments of photoreceptors. Scale bar = 50 µm.

3-Methyladenine does not affect retinal function

As previously described, newborn rats exposed to the OIR protocol are characterized by visual dysfunction [238]. By recording ERG, we measured retinal function at P18 in order to determine whether the effects of 3-MA on autophagy were accompanied by recovered visual function.

Representative mixed a-, b-waves recorded from RA and OIR rats either untreated or 3-MA-treated are shown in Fig. 5a. In Fig. 5b-c, a- and b-wave amplitudes of OIR rat pups recorded significantly reduced a- and b-wave amplitudes ($p < 0.001$). Nevertheless, when compared to untreated OIR rats, treatment with 3-MA did not ameliorate visual dysfunction.

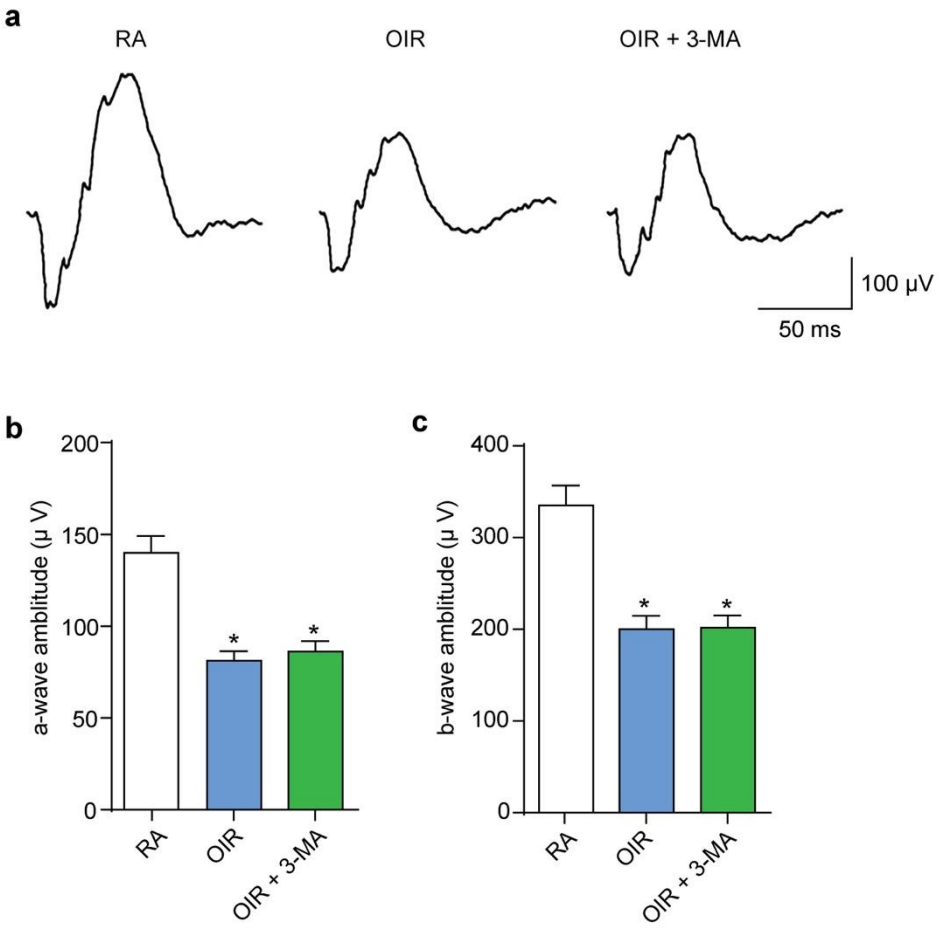

Fig. 5 3-MA effects on retinal function. **a** Representative ERG waveforms recorded at a light intensity of 1 log cd-s/m^2 in RA, OIR rat pups untreated and treated with 3 mg/Kg of 3-MA, at P18. **b** Scotopic a-wave amplitude and **c** scotopic b-wave amplitude. Each column represents the mean ± SEM of data from 6 rats for each experimental condition. $^*p < 0.001$ vs RA.

DISCUSSION

ROP is a vascular disorder, characterized by abnormal proliferation of retinal blood vessels [12]. Simultaneously, ROP is often accompanied by other events, such as inflammation and neurodegeneration, which might further compromise the visual function of preterm babies [42]. Increasing evidences have suggested that autophagic mechanisms of cell death are involved in ocular diseases [240]. Canonically, autophagy operates as a cytoprotective process, degrading toxic organelles or proteins through a recycle system. Albeit, in stress conditions, prolonged activation of autophagy contributes to the execution of programmed cell death, which is closely associated to the development of diseases [83].

Due to its high metabolic demand, the retina is characterized by a strong expression of autophagy proteins, and their imbalance might compromise the function of the neuroretina [74]. In a rat model of retinal ischemia and in an *in vivo* model of glaucoma, a prolonged activation of autophagy promotes cell death in retinal neurons; and its inhibition through 3-MA, suppresses autophagosome formation and reduces cell death [124,208]. On the other hand, in an *ex vivo* model of diabetic retinopathy and in a mouse model of OIR, an induction of autophagy mediates neuroprotection, by reducing cell death events in retinal cells [241,242]. Thus autophagic mechanism, if not balanced, could represent a double edged sword in retinal cells.

In the present study, we investigated the involvement of autophagy in a rat model of OIR, and we found evidence that the autophagy flux is activated in several retinal layers of OIR rats. In addition, we found that autophagy could involve the activation of necroptotic mechanisms, leading to retinal cell death. In conformity, we observed a reduction of retinal cell death by using the inhibitor of autophagy, 3-MA.

Initially, before exploring changes in the autophagy flux in the retina of OIR rats, we monitored protein levels of HIF-1α and VEGF-A, the main factors involved in neovascularization both in the OIR animal models and in ROP afflicted babies [190]. In the rat model, a previous study has reported a significant increase in VEGF levels in pup rats exposed to the OIR protocol, when compared with rats kept in RA [191]. This is in agreement with our data that showed a peak of VEGF in OIR rats at both P14 and P18. As demonstrated, the increase of VEGF-A levels is due to an adaption to supplements deficiency, which can be developed by the hypoxic stimulus from retinal cells [192]. In fact, as a consequence of the oxygen fluctuations induced in this model, the retinal blood vessels are fragile, structurally deficient and poorly organized; thus, they are not able to fully nourish oxygen and nutrients to retinal cells [193]. Nevertheless, no significant difference in HIF-1α levels has been detected in OIR retinas at P14 and P18. This data would suggest that VEGF-mediated angiogenesis in our OIR rat model might be induced also through HIF-1–independent signaling pathways, as

previously demonstrated in human retinal pigment epithelial cells [194,195]. A known sensor of energy status, AMPKα, has been reported to contribute to VEGF upregulation [196,197]. It is putative that the oxygen fluctuations in the rat OIR model could result to a low-grade, HIF-independent cellular hypoxia with elevated intracellular reactive oxygen species [136,198]that lead to starvation signals and AMPKα-mediated VEGF-A expression.

In addition, energy deprivation promoted AMPKα activation induces autophagic mechanisms by inhibition of mTOR and a direct phosphorylation of autophagy modulators [106]. Interestingly, here in OIR rats we observed an increase of p-AMPKα and p-Ulk1 (Ser^{555}) protein levels, with a significant upregulation of LC3-II on both P14 and P18 retinas. Concomitantly, a critical reduction was observed on Akt-mTOR pathway protein levels, including p-Akt, p-4E-BP-1 and p-S6. Altogether, these findings indicate that the 50/10 OIR protocol leads to an overall increased autophagic flux in the retina.

As reported, p62 protein is degraded upon induction of the autophagic when the autophagosomes fuse with the lysosomes [199]. Consequently, to monitor the autophagic flux, we investigate p62 protein levels. Here, a significant increase of LC3-II was not accompanied by a decrease of p62 protein levels in the OIR retina. Collectively, these results would suggest that in OIR rat retinas autophagy is induced, through AMPKα/Ulk1 pathway, proceeds with the elongation and nucleation of autophagosomes. Albeit, in this model the autophagolysosome formation is limited by the availability of the terminal lysosomal system, ultimately resulting in an autophagic flux blockade. This hypothesis was confirmed by recent findings, which reported that prolonged stresses induce an increase in autophagosome synthesis and a compromised autolysosomal activity. As a consequence, the increase in autophagophore nucleation into autophagosomes with limited fusion with the lysosomes might be a futile process for autophagy, and thus contribute to cell damage and autophagy-associated cell death mechanisms [200]. In this respect, an accumulation of autophagosomes has been related with several cell death mechanisms, including necroptotic RIPK-1-mediated mechanism, which can be induced directly by the autophagy machinery [201].

Necroptotic mechanisms have been reported to promote neuronal cell death in neurodegeneration and eye disease [202]. The crosstalk between autophagy and necroptosis has been the focus of multiple studies, although the mechanism is not fully elucidated. Necroptotic mechanisms can be induced upon a block of autophagy flux, through a crosstalk between p62, LC3-II and necroptosis markers, such as RIPK-1 [203]. Moreover, autophagy may occur in association with necroptosis when triggered by apoptotic caspase-mediated inhibition. At a molecular level, upon the activation of apoptosis, the RIPK-1 activity is subject to a tight repression, through Casp-8-mediated cleavage [204]. Interesting, our results demonstrated an increase of expression of both LC3 and RIPK-1 in GCL, IPL, OPL and

OS retinal layers of the OIR retina, in agreement with previous studies in rodent retinas [205]. These findings are accompanied by a predominant expression of Casp-8 in retinal endothelial cells. Unlike to RIPK-1, which was only detected in OIR retinas, the expression of Casp-8 was detected also in retinal endothelial cells of RA rats. It is important to highlight that at these time points the retinal vasculature in rat pups is still developing [206]. The expression of Casp-8 has been reported essential for the proper postnatal retinal vascularization, contributing to the physiological vascular remodeling process, as demonstrated in developing rodent retinas [207].

In a rat model of retinal ischemia, an inhibition of autophagy-associated with retinal cell death has been shown to prevent neuronal death following injury [208]. Following the observation that LC3 and RIPK-1 co-expressed in the same retinal layers, we evaluated if inhibition of autophagosomes nucleation with 3-MA [209], could decrease necroptosis in OIR retinas. Interestingly, we observed a notable decrease of both autophagic and necroptotic markers in GCL, IPL, OPL and OS retinal layers in OIR retinas treated with 3-MA, yet no reduction of apoptotic marker was observed in retinal endothelial cells. Taken together, these results suggest that the OIR protocol in rats leads to an induction of autophagy-dependent necroptotic mechanisms in retinal neurons, concomitantly with an increase of apoptotic-autophagy-independent mechanisms in retinal endothelial cells.

In retinal diseases, mechanisms of retinal cell death have been correlated with retinal dysfunction and visual loss [210]. Concomitantly with reducing retinal cell death, the inhibition of autophagy has been shown to have a neuroprotective effect and result in a partial recovery of visual impairment [211]. By recording ERG responses to full-field light flashed retinas, our data show that, although the treatment with 3-MA reduces necroptosis in retinal cells, visual function is not ameliorated in OIR rats treated with autophagy inhibitor. This controversial result could be associated with the fact that, in OIR retinas, the retinal endothelial cells are still branded by a strong activation of apoptosis. On the other hand, alterative mechanisms of autophagy-independent cell death might be affecting the neurons' functions, as demonstrated in the neuroretina of diabetic rats [212].Therefore, despite a reduction of necroptosis in retinal cells, retinal function still remains compromised due, for instance, to a dysfunction of retinal neurons involved in the generation of ERG traces.

Collectively, the present study demonstrates an activation of the autophagic pathway correlated with necroptosis in retinal cells of OIR rat pups. In this model, the stress induced by oxygen fluctuations from birth to P14, leads to a retinal energetic starvation, which results in the induction of the autophagic flux, through an activation of the AMPKα/Ulk1 pathway. Thus, the autophagy induction initially may act as a survival attempt to restore cellular energy in the retina, yet fails due to a putative impairment of the lysosomal system. This failure leads to an accumulation of

autophagosomes, which culminate in the activation of mechanisms of cell death, such as necroptosis, that further affect the retina of OIR rats.

In conclusion, the present findings contribute to deepen the understanding of the role of autophagic processes in vasculature and the neuroretina of rats exposed to the OIR protocol. Moreover, the present study supports the possibility that negative pharmacological regulation of the autophagy flux may contribute to reduce the mechanisms of cells death that occur in retinal cells exposed to prolonged stress, a condition paralleled in ROP-afflicted preterm babies.

REFERENCES

[1] **Wong-Riley M**. Energy metabolism of the visual system. *Eye and Brain* 2010; 2; 99.

[2] **Selvam S, Kumar T, Fruttiger M**. Retinal vasculature development in health and disease. *Progress in Retinal and Eye Research* 2018; 63; 1–19.

[3] **Dogra MR, Katoch D, Dogra M**. An Update on Retinopathy of Prematurity (ROP). *Indian Journal of Pediatrics* 2017; 84; 930–6.

[4] **Higgins RD**. Oxygen Saturation and Retinopathy of Prematurity. *Clinics in Perinatology* 2019; 46; 593–9.

[5] **Wilson A, Sapieha P**. Neurons and guidance cues in retinal vascular diseases. *Oncotarget* 2016; 7; 9618–9.

[6] **Hansen RM, Moskowitz A, Akula JD, et al.** The neural retina in retinopathy of prematurity. *Progress in Retinal and Eye Research* 2017; 56; 32–57.

[7] **Rivera JC, Sapieha P, Joyal JS, et al.** Understanding retinopathy of prematurity: Update on pathogenesis. *Neonatology* 2011; 100; 343–53.

[8] **Lin W, Xu G**. Autophagy: A Role in the Apoptosis, Survival, Inflammation, and Development of the Retina. *Ophthalmic Research* 2019; 61; 65–72.

[9] **Amirkavei M, Pitkänen M, Kaikkonen O, et al.** Induction of heat shock protein 70 in mouse RPE as an in vivo model of transpupillary thermal stimulation. *International Journal of Molecular Sciences* 2020; 21.

[10] **Glick D, Barth S, Macleod KF**. Autophagy: Cellular and molecular mechanisms. *Journal of Pathology* 2010; 221; 3–12.

[11] **Kim J, Kundu M, Viollet B, et al.** AMPK and mTOR regulate autophagy through direct phosphorylation of Ulk1. *Nature Cell Biology* 2011; 13; 132–41.

[12] **Jung CH, Ro SH, Cao J, et al.** MTOR regulation of autophagy. *FEBS Letters* 2010; 584; 1287–95.

[13] **Denton D, Nicolson S, Kumar S**. Cell death by autophagy: Facts and apparent artefacts. *Cell Death and Differentiation* 2012; 19; 87–95.

[14] **Jung S, Jeong H, Yu SW**. Autophagy as a decisive process for cell death. *Experimental and Molecular Medicine* 2020; 52; 921–30.

[15] **Galluzzi L, Vitale I, Aaronson SA, et al.** Molecular mechanisms of cell death: Recommendations of the Nomenclature Committee on Cell Death 2018. *Cell Death and Differentiation* 2018; 25; 486–541.

[16] **Goodall ML, Fitzwalter BE, Zahedi S, et al.** The Autophagy Machinery Controls Cell Death Switching between Apoptosis and Necroptosis. *Developmental Cell* 2016; 37; 337–49.

[17] **Loos B, Engelbrecht AM, Lockshin RA, et al.** The variability of autophagy and cell death susceptibility: Unanswered questions. *Autophagy* 2013; 9; 1270–85.
[18] **Nikoletopoulou V, Markaki M, Palikaras K, et al.** Crosstalk between apoptosis, necrosis and autophagy. *Biochimica et Biophysica Acta* 2013; 1833; 3448–59.
[19] **Chen Q, Kang J, Fu C**. The independence of and associations among apoptosis, autophagy, and necrosis. *Signal Transduction and Targeted Therapy* 2018; 3.
[20] **Oberst A**. Autophagic cell death RIPs into tumors. *Cell Death and Differentiation* 2013; 20; 1131–2.
[21] **Button RW, Roberts SL, Willis TL, et al.** Accumulation of autophagosomes confers cytotoxicity. *Journal of Biological Chemistry* 2017; 292; 13599–614.
[22] **Stone J, Itin A, Alon T, et al.** Development of Retinal Vasculature Is Mediated by Hypoxia-Induced Vascular Endothelial Growth Factor (VEGF) Expression by Neuroglia. *The Journal of Neuroscience* 1995; 15; 4738–47.
[23] **Penn JS, Henry MM, Wall PT, et al.** The range of PaO2 variation determines the severity of oxygen-induced retinopathy in newborn rats. *Investigative Ophthalmology and Visual Science* 1995; 36; 2063–70.
[24] **Li R, Yang X, Wang Y, et al.** Effect(s) of Preterm Birth on Normal Retinal Vascular Development and Oxygen-Induced Retinopathy in the Neonatal Rat. *Current Eye Research* 2013; 38; 1266–73.
[25] **Fulton AB, Hansen RM, Moskowitz A, et al.** The neurovascular retina in retinopathy of prematurity. *Progress in Retinal and Eye Research* 2009; 28; 452–82.
[26] **Pesce NA, Canovai A, Lardner E, et al.** Autophagy Involvement in the Postnatal Development of the Rat Retina. *Cells* 2021; 10; 177.
[27] **Robson JG, Saszik SM, Ahmed J, et al.** Rod and cone contributions to the a-wave of the electroretinogram of the macaque. *Journal of Physiology* 2003; 547; 509–30.
[28] **Melincovici CS, Boşca AB, Şuşman S, et al.** Vascular endothelial growth factor (VEGF) – key factor in normal and pathological angiogenesis. *Romanian Journal of Morphology and Embryology* 2018; 59; 455–67.
[29] **Tanida I, Waguri S**. Measurement of autophagy in cells and tissues. *Methods in Molecular Biology* 2010; 648; 193–214.
[30] **Tanida I, Ueno T, Kominami E**. LC3 and autophagy. *Methods in Molecular Biology* 2008; 445; 77–88.
[31] **Liu WJ, Ye L, Huang WF, et al.** p62 links the autophagy pathway and the ubiqutin-proteasome system upon ubiquitinated protein degradation. *Cellular and Molecular Biology Letters* 2016; 21; 29.
[32] **Elizabeth Hartnett M**. The effects of oxygen stresses on the development of features of severe retinopathy of prematurity: Knowledge from the 50/10 OIR model. *Documenta Ophthalmologica* 2010; 120; 25–39.
[33] **Chen J, Smith LEH**. Retinopathy of prematurity. *Angiogenesis* 2007; 10; 133–40.
[34] **Mitter SK, Boulton ME**. Autophagy in Ocular Pathophysiology. *Autophagy in Current Trends in Cellular Physiology and Pathology* 2016; DOI: 10.5772/64667.
[35] **Frost LS, Mitchell CH, Boesze-Battaglia K**. Autophagy in the eye: Implications for ocular cell health. *Experimental Eye Research* 2014; 124; 56–66.
[36] **Piras A, Gianetto D, Conte D, et al.** Activation of Autophagy in a Rat Model of Retinal Ischemia following High Intraocular Pressure. *PLoS ONE* 2011; 6; e22514.
[37] **Park HYL, Kim JH, Park CK**. Activation of autophagy induces retinal ganglion cell death in a chronic hypertensive glaucoma model. *Cell Death and Disease* 2012; 3; e290.
[38] **Cammalleri M, Locri F, Catalani E, et al.** The beta adrenergic receptor blocker propranolol counteracts retinal dysfunction in a mouse model of oxygen induced retinopathy: Restoring the balance between apoptosis and autopha. *Frontiers in Cellular Neuroscience* 2017; 11.

[39] **Amato R, Catalani E, Dal Monte M, et al.** Autophagy-mediated neuroprotection induced by octreotide in an ex vivo model of early diabetic retinopathy. *Pharmacological Research* 2018; 128; 167–78.
[40] **Higgins RD**. Oxygen Saturation and Retinopathy of Prematurity. *Clinics in Perinatology* 2019; 46; 593–9.
[41] **Hartmann JS, Thompson H, Wang H, et al.** Expression of vascular endothelial growth factor and pigment epithelial-derived factor in a rat model of retinopathy of prematurity. *Molecular Vision* 2011; 17; 1577–87.
[42] **Chung AS, Ferrara N**. Developmental and Pathological Angiogenesis. *Annual Review of Cell and Developmental Biology* 2011; 27; 563–84.
[43] **Soetikno BT, Yi J, Shah R, et al.** Inner retinal oxygen metabolism in the 50/10 oxygen-induced retinopathy model. *Scientific Reports* 2015; 5.
[44] **Kuroki M, Voest EE, Amano S, et al.** Reactive Oxygen Intermediates Increase VEGF Expression Reactive Oxygen Intermediates Increase Vascular Endothelial Growth Factor Expression In Vitro and In Vivo. *J. Clin. Invest* 1996; 98; 1667–75.
[45] **Berra E, Pagès G, Pouysségur J**. MAP kinases and hypoxia in the control of VEGF expression. *Cancer and Metastasis Reviews* 2000; 19; 139–45.
[46] **Nagata D, Mogi M, Walsh K**. AMP-activated protein kinase (AMPK) signaling in endothelial cells is essential for angiogenesis in response to hypoxic stress. *Journal of Biological Chemistry* 2003; 278; 31000–6.
[47] **Reihill JA, Ewart MA, Salt IP**. The role of AMP-activated protein kinase in the functional effects of vascular endothelial growth factor-A and -B in human aortic endothelial cells. *Vascular Cell* 2011; 3; 9.
[48] **Chinskey ND, Besirli CG, Zacks DN**. Retinal cell death and current strategies in retinal neuroprotection. *Current Opinion in Ophthalmology* 2014; 25; 228–33.
[49] **Moreno M-L, Mérida S, Bosch-Morell F, et al.** Autophagy Dysfunction and Oxidative Stress, Two Related Mechanisms Implicated in Retinitis Pigmentosa. *Frontiers in Physiology* 2018; 9; 1008.
[50] **Settembre C, Fraldi A, Jahreiss L, et al.** A block of autophagy in lysosomal storage disorders. *Human Molecular Genetics* 2008; 17; 119–29.
[51] **Chaabane W, User SD, El-Gazzah M, et al.** Autophagy, apoptosis, mitoptosis and necrosis: Interdependence between those pathways and effects on cancer. *Archivum Immunologiae et Therapiae Experimentalis* 2013; 61; 43–58.
[52] **Zhang S, Tang MB, Luo HY, et al.** Necroptosis in neurodegenerative diseases: a potential therapeutic target. *Cell Death & Disease* 2017; 8; e2905.
[53] **Sanz L, Sanchez P, Lallena MJ, et al.** The interaction of p62 with RIP links the atypical PKCs to NF-κB activation. *EMBO Journal* 1999; 18; 3044–53.
[54] **Liccardi G, Ramos Garcia L, Tenev T, et al.** RIPK1 and Caspase-8 Ensure Chromosome Stability Independently of Their Role in Cell Death and Inflammation. *Molecular Cell* 2019; 73; 413-428.e7.
[55] **Engerman RL, Meyer RK**. Development of retinal vasculature in rats. *American Journal of Ophthalmology* 1965; 60; 628–41.
[56] **Tisch N, Freire-Valls A, Yerbes R, et al.** Caspase-8 modulates physiological and pathological angiogenesis during retina development. *Journal of Clinical Investigation* 2019; 129; 5092–107.
[57] **Vlahos CJ, Matter WF, Hui KY, et al.** A specific inhibitor of phosphatidylinositol 3-kinase, 2-(4-morpholinyl)- 8-phenyl-4H-1-benzopyran-4-one (LY294002). *Journal of Biological Chemistry* 1994; 269; 5241–8.
[58] **Murakami Y, Notomi S, Hisatomi T, et al.** Photoreceptor cell death and rescue in retinal detachment and degenerations. *Progress in Retinal and Eye Research* 2013; 37; 114–40.
[59] **Zaninello M, Palikaras K, Naon D, et al.** Inhibition of autophagy curtails visual loss in a

model of autosomal dominant optic atrophy. *Nature Communications* 2020; 11; 1–12.

[60] **Kurihara T, Ozawa Y, Nagai N, et al.** Angiotensin II type 1 receptor signaling contributes to synaptophysin degradation and neuronal dysfunction in the diabetic retina. *Diabetes* 2008; 57; 2191–8.